



Republic of Iraq
Ministry of Higher Education and Scientific Research
University of Misan/College of Engineering
Civil Engineering Department



EXPERIMENTAL STUDY OF HOLLOW SLENDER REINFORCED CONCRETE COLUMN

By

Alaa Mohammed Sahi

B.Sc. in Civil Engineering, 2017

A thesis submitted in partial fulfillment
of the requirements for the Master of Science
degree in Civil Engineering
The University of Misan

February 2021

Thesis Supervisor: Prof. Dr. Mohammed Salih Abd-Ali

بِسْمِ اللَّهِ الرَّحْمَنِ الرَّحِيمِ

يَا أَيُّهَا الَّذِينَ آمَنُوا إِذَا قِيلَ لَكُمْ تَفَسَّحُوا فِي الْمَجَالِسِ فَافْسَحُوا

بِفَسْحِ اللَّهِ لَكُمْ ۖ وَإِذَا قِيلَ انشُزُوا فَانشُزُوا يَرْفَعِ اللَّهُ الَّذِينَ

آمَنُوا مِنْكُمْ وَالَّذِينَ أُوتُوا الْعِلْمَ حُرُجَاتٍ ۗ وَاللَّهُ بِمَا تَعْمَلُونَ خَبِيرٌ

مصداق الله العلي العظيم

المجالسة (11)

DEDICATION

- To the dedication and sincerity instance, my role model, and my ideal in life..... my beloved father.
- To the purest heart in my life..... dear mother.
- To my aunty ask God to extend her life.
- To my pleasures in life my sisters and brother Fatima, Amnah, Yaqeen and Ahmad for their support.
- For my cousin who put a lot of effort into helping me with this work Jawad Daram.
- To my cousin Murtdha Daram.

ACKNOWLEDGEMENTS

In the beginning, I thank my God, thank Allah for the grace with which I have been able to complete this work.

First, I would like to express my appreciation and deepest gratitude to my supervisor Prof. Dr. Mohammed Salih Abd-Ali for his remarkable suggestions, encouragement and guidance throughout the research. I am really indebted to him.

I would like to express my appreciation gratitude to Prof. Dr. Abbas Oda Dawood Dean of the College of Engineering, Prof. Dr. Ahmed Khadhim Al-Shara, Ali Al-lami, Assist Prof. Dr. Samir Mohamed Chassib, the Head of Civil Engineering Department.

I do not know how can I reach my big respect and thank to my family especially my father and mother, I thank my sisters and my brother. Special appreciation to my cousin (Jawad Daram) for his help in this work.

I would like to thank my cousins especially Mohammed Abbas, my friends in the master's and my closer friends. Also, I would like to thank Mustafa Kareem for his assistance, and my friend Zahraa. I would like to thank Mustafa Oda who helped me some of the time in the laboratory.

ABSTRACT

Transverse openings and longitudinal holes are often provided in reinforced concrete columns to allow arrival for services such as pipes for plumbing and electric wiring and when the cost of concrete is comparatively high, or in cases where the weight of concrete members is to be kept to a minimum. This study aimed to conduct an experimental investigation on the behavior of hollow slender reinforced concrete columns applied on it axial and eccentricity loaded. The experimental part of the research included testing of 15 hollow slender RC columns with dimensions of (140×80×2000) mm and slenderness ratio of (80.54). The 15 columns were divided into nine groups to study important parameters. These parameters were the strengthening by lateral reinforcement (ties), strengthening by carbon fiber reinforced polymer (CFRP), presence of eccentricity and the shape of the longitudinal hole. General observations concerning the ultimate load, lateral displacement, ultimate moment, ductility, energy absorption and failure mode of the column specimens are presented.

The strengthening reinforced concrete columns from the ends of columns by lateral reinforcement (ties) and (CFRP) make the column behaves at full capacity where the buckling occurs with in the middle third of the column instead of early failure at the edges. Also when comparing the strengthening by CFRP only or together with the lateral reinforcement (ties) gave a better performance in terms of ultimate load, ultimate moment, maximum lateral displacement, ductility and energy absorption than the strengthening by ties at the same distance of strengthening .

The experimental results indicated that the use of lateral reinforcement (ties) in different lengths at both ends of columns caused an increase in ultimate load by (2.7, 8.3, and 61.1)% when changed the distance of strengthening by ties from

(140, 333 to 500) mm, respectively. The strengthening by CFRP sheet from the end of ties up 50% at both ends of the column having the same opening shape (rectangular hole) caused an increasing in the ultimate about (16.4-37.9)%.

Eccentricity of load was one of the important factors on load carrying capacity of columns especially slender columns. Increasing eccentricity means that the moment is increased. Two eccentricity values ($e/h= 25\%$) and ($e/h= 50\%$) caused a decrease in the ultimate load for hollow slender columns. For eccentricities of 20 mm and 40 mm, it was found that the columns having a rectangular opening results in a decrease in the load-carrying capacity of about (10.26 and 17.95)% when compared with slender columns subjected to axial load.

Reinforced concrete columns having circular holes, either with or without CFRP sheets, have better performance in terms of ultimate load, ultimate moment, maximum lateral displacement, ductility and energy absorption compared to those having rectangular holes. The test results proved that the columns with circular hole have good performance compared to the columns have a rectangular hole (the area of circular hole equivalent to the area of the rectangular hole), under the same load and the eccentricity equal of 20 mm. The increase in ultimate load was 14.29% in a column having a circular hole compared to a column having a rectangular hole.

Also, a column subjected to load with an eccentricity of 120 mm ($e/h=150\%$) and the whole column was strengthened by CFRP sheet that had been tested. It was found that the ultimate load decreased compared to other columns and it scored an early failure.

LIST OF CONTENT

ACNOWLEDGEMENT.....	i
ABSTRACT.....	ii
LIST OF CONTENT.....	iv
LIST OF TABLES.....	x
LIST OF FIGURES.....	xi
LIST ABBREVIATIONS.....	xv
LIST OF SYMBOLES.....	xvi
CHAPTER ONE.....	1
1.1 General.....	1
1.2 Classification of columns.....	1
1.3 Slender column.....	4
1.4 Eccentricity.....	7
1.5 Hollow reinforced concrete columns.....	7
1.6 Fiber Reinforced Polymer (FRP).....	8
1.7 Objectives of research.....	10
1.8 Thesis layouts.....	11
CHAPTER TWO.....	12
LITERATURE REVIEW.....	12
2.1 General.....	12
2.2 Experimental work on slender reinforced concrete columns.....	12
2.3 Experimental work on hollow reinforced concrete columns.....	17

2.4 Summary.....	23
CHAPTER THREE.....	24
EXPERIMENTAL WORK.....	24
3.1 General.....	24
3.2 Material properties.....	24
3.2.1 Cement.....	24
3.2.2 Fine Aggregate.....	25
3.2.3 Coarse Aggregate.....	26
3.2.4 Mixing water.....	27
3.2.5 Carbon fiber reinforced polymer (CFRP).....	27
3.2.6 Bonding materials.....	28
3.2.7 Steel reinforcement.....	28
3.3 Models description.....	29
3.3.1 Effect of lateral reinforcement.....	33
3.3.2 Effect of lateral reinforcement and CFRP sheet.....	34
3.3.3 Effect of eccentricity (e= 20, 40) mm.....	35
3.3.4 Effect of opening shape with eccentricity (e=20 mm).....	36
3.3.5 Effect of opening shape with eccentricity (e=40 mm).....	37
3.3.6 Effect of eccentricity with CFRP sheet.....	38
3.3.7 Effect of opening with CFRP sheet.....	39
3.3.8 Effect of high eccentricity.....	41
3.3.9 Effect of CFRP sheet with the same eccentricity.....	41
3.4 Formwork and reinforcement cages.....	43

3.5 Mix proportion.....	46
3.6 Mixing procedure.....	46
3.7 Casting and curing procedure.....	46
3.8 Tests of Hardened Concrete.....	49
3.9 Important factors before starting works.....	54
3.9.1 End Column Cap.....	54
3.9.2 Number of specimen.....	54
3.10 Application of CFRP sheet.....	56
3.11 Measurement of lateral deflection.....	59
3.12 Testing machine.....	59
CHAPTER FOUR.....	61
RESULTS AND DISSCUSION.....	61
4.1 General.....	61
4.2 The factors concluded from the results.....	61
4.2.1 Ductility of column specimens.....	61
4.2.2 Energy absorption.....	63
4.2.3 First and second order moment.....	63
4.3 Test Results of columns specimens.....	65
4.3.1 Results of the effect of lateral reinforcement.....	66
4.3.1.1 Ultimate load and maximum lateral displacement.....	66
4.3.1.2 Ultimate moment.....	67
4.3.1.3 Ductility index.....	67
4.3.1.4 Energy absorption.....	68

4.3.1.5 Mode of failure.....	68
4.3.2 Results of. Effect of lateral reinforcement and CFRP sheet.....	69
4.3.2.1 Ultimate load and maximum lateral displacement.....	69
4.3.2.2 Ultimate moment.....	71
4.3.2.3 Ductility index.....	71
4.3.2.4 Energy absorption.....	72
4.3.2.5 Mode of failure.....	72
4.3.3 Results of the Effect of eccentricity (e= 20, 40) mm.....	74
4.3.3.1 Ultimate load and maximum lateral displacement.....	74
4.3.3.2 Ultimate moment.....	75
4.3.3.3 Ductility index.....	75
4.3.3.4 Energy absorption.....	76
4.3.3.5 Mode of failure.....	76
4.3.4 Result of the effect of opening shape with eccentricity (e=20 mm).....	78
4.3.4.1 Ultimate load and maximum displacement.....	78
4.3.4.2 Ultimate moment.....	79
4.3.4.3 Ductility index.....	79
4.3.4.4 Energy absorption.....	80
4.3.4.5 Mode of failure.....	81
4.3.5 Result of the effect of opening shape with eccentricity (e=40 mm).....	82
4.3.5.1 Ultimate load and maximum lateral displacement.....	82
4.3.5.2 Ultimate moment.....	82
4.3.5.3 Ductility index.....	83

4.3.5.4	Energy absorption.....	83
4.3.5.5	Mode of failure.....	84
4.3.6	Result of the effect of eccentricity with CFRP sheet.....	86
4.3.6.1	Ultimate load and maximum lateral displacement.....	86
4.3.6.2	Ultimate moment.....	86
4.3.6.3	Ductility index.....	87
4.3.6.4	Energy absorption.....	87
4.3.6.5	Mode of failure.....	88
4.3.7	Result of the effect of opening with CFRP sheet.....	90
4.3.7.1	Ultimate load and maximum lateral displacement.....	90
4.3.7.2	Ultimate moment.....	91
4.3.7.3	Ductility index.....	91
4.3.7.4	Energy absorption.....	92
4.3.2.5	Mode of failure.....	92
4.3.8	Result of the effect of high eccentricity.....	93
4.3.9	Result of the effect of CFRP sheet with same eccentricity.....	95
4.3.9.1	Ultimate load and maximum lateral displacement.....	95
4.3.9.2	Ultimate moment.....	96
4.3.9.3	Ductility index.....	96
4.3.9.4	Energy absorption.....	96
4.3.9.5	Mode of failure.....	97
CHAPTER FIVE.....		100
CONCLUSIONS AND RECOMMENDATIONS.....		100

5.1 Conclusion.....	100
5.1.1 Behavior of columns under axial loading.....	100
5.2.2 Behavior of columns under eccentric loading.....	101
5.2 Recommendation for future works.....	102
REFERENCES.....	104

LIST OF TABLES

Table 1.1 Summary of code procedures to determine Effective length factors and Column classification.....	6
Table 1.2 Typical mechanical properties of FRP composites.....	9
Table 3.1 Physical properties of the cement.....	24
Table 3.2 Chemical composition of the cement.....	25
Table 3.3 Grading of the fine aggregate.....	25
Table 3.4 Physical properties of the fine aggregate.....	26
Table 3.5 Grading of coarse aggregate.....	26
Table 3.6 Properties of coarse aggregate.....	26
Table 3.7 Technical properties of CFRP sheet.....	27
Table 3.8 Properties of reinforcing bars.....	29
Table 3.9 Details of groups of columns subjected to axial load.....	32
Table 3.10 Details of groups of columns subjected to eccentric load.....	32
Table 3.11 Results of mechanical properties of concrete.....	53
Table 4.1 Experimental test results of column specimens.....	65
Table 4.2 Mode failure of columns.....	99

LIST OF FIGURES

Fig. 1.1 Types of reinforced concrete columns.....	2
Fig. 1.2 Columns subjected to different types of loading.....	3
Fig. 1.3 Short columns failed.....	4
Fig. 1.4 Buckling failure.....	4
Fig. 1.5 Effective length of factor.....	5
Fig. 1.6 Strengthening of reinforced concrete columns by CFRP.....	10
Fig. 2.1 Final failure modes.....	16
Fig. 2.2 Detailing of hollow columns (Lignola et al., 2007).....	18
Fig. 2.3 Column elevation and cross section.....	22
Fig. 3.1 CFRP sheet.....	27
Fig. 3.2 Adhesive (Sikadur-330).....	28
Fig. 3.3 Stress-Strain relationship for steel.....	29
Fig. 3.4 column details without corbel.....	30
Fig. 3.5 Details of column with corbel.....	31
Fig. 3.6 First group details.....	33
Fig. 3.7 Second group details.....	35
Fig. 3.8 Third group details.....	36
Fig. 3.9 Fourth group details.....	37
Fig. 3.10 Fifth group details.....	38
Fig. 3.11 Sixth group details.....	39
Fig. 3.12 Seventh group details.....	40
Fig. 3.13 Eighth group detail.....	41

Fig. 3.14 Ninth group details.....	42
Fig. 3.15a Cage of steel reinforcement for columns (C1-C7).....	43
Fig. 3.15b Cage of steel reinforcement with corbels for columns.....	44
Fig. 3.16 Steel Reinforcement cage and molds without corbel.....	44
Fig. 3.17 Steel Reinforcement cage and mold with corbel.....	44
Fig. 3.18 The reinforcement of corbels.....	45
Fig. 3.19a Rectangular hole.....	45
Fig. 3.19b Circular hole.....	45
Fig. 3.20 Concrete mixer used in the present work.....	47
Fig. 3.21 using the vibrator during casting of column specimens.....	47
Fig. 3.22 Finishing casting of column specimens.....	48
Fig. 3.23 Curing of column specimens.....	48
Fig. 3.24 Painting of the column specimens by white emulsion.....	48
Fig. 3.25 Concrete compressive strength test.....	50
Fig. 3.26 Splitting tensile strength test.....	51
Fig. 3.27 Flexural strength test.....	52
Fig. 3.28 Plate cap jacket.....	53
Fig. 3.29a Column cap (side view).....	54
Fig. 3.29b End column cap (top view).....	54
Fig. 3.30 Plate cap of eccentric load.....	54
Fig. 3.31 The failure of experimental work of an experimental column.....	55
Fig. 3.32 Surface grinding.....	56
Fig. 3.33 Steps of installation CFRP sheet.....	57
Fig. 3.34 Dial gauges used in tests.....	59
Fig. 3.35 Test arrangement.....	60

Fig. 4.1 a Determination of the displacement ductility.....	62
Fig. 4.1 b Determination of the displacement ductility.....	63
Fig. 4.2 Axial and eccentric loading in the column.....	64
Fig. 4.3 Load-displacement curves for first group.....	66
Fig. 4.4 Effect of lateral reinforcement on ductility index.....	67
Fig. 4.5 Effect of lateral reinforcement on energy absorption.....	68
Fig. 4.6 Mode failure of first group.....	69
Fig. 4.7 Load-displacement curves for second group.....	70
Fig. 4.8 Effect of strengthening on ductility index.....	71
Fig. 4.9 Effect of strengthening on energy absorption.....	72
Fig. 4.10 Columns before testing (second group).....	73
Fig. 4.11 Failure mode of second group (after testing).....	73
Fig. 4.12 Load-displacement curves for third group.....	75
Fig. 4.13 Effect of eccentricity on ductility index.....	76
Fig. 4.14 Effect of eccentricity on energy absorption.....	76
Fig. 4.15 Mode failure of columns during the test for third group.....	77
Fig. 4.16 Mode failure of columns after the test for third group.....	78
Fig. 4.17 Load-displacement curve for fourth group.....	79
Fig. 4.18 Effect of shape opening on ductility index.....	80
Fig. 4.19 Effect of shape opening on energy absorption.....	80
Fig. 4.20 Mode failure of forth group.....	81
Fig. 4.21 Load-displacement curve for fifth group.....	82
Fig. 4.22 Effect of shape opening on ductility index.....	83
Fig. 4.23 Effect of shape opening on energy absorption.....	84
Fig. 4.24 Mode failure for fifth group before testing.....	85

Fig. 4.25 Load-displacement curve for sixth group.....	86
Fig. 4.26 Ductility index for sixth group.....	87
Fig. 4.27 Energy absorption for sixth group.....	88
Fig. 4.28 Mode failure of sixth group (during the test).....	89
Fig. 4.29 Mode failure of sixth group (after the test).....	89
Fig. 4.30 Load-displacement curve for seventh group.....	90
Fig. 4.31 Effect of CFRP with different opening on ductility.....	91
Fig. 4.32 Effect of CFRP with different opening on energy absorption.....	92
Fig. 4.33 Mode failure of sixth group.....	93
Fig. 4.34 Load-displacement curve for C14.....	94
Fig. 4.35 Mode failure of column C14.....	94
Fig. 4.36 Load-displacement curve for ninth group.....	95
Fig. 4.37 Effect of CFRP with circular hole on ductility.....	96
Fig. 4.38 Effect of CFRP with circular hole on energy absorption.....	97
Fig. 4.39 Mode failure of ninth group.....	98

ABBREVIATIONS

ACI	American concrete institute
AFRP	Aramid fiber reinforced polymer
ASTM	American Society for Testing and Materials
BS	British Standards Institution
CFRP	Carbon Fiber Reinforced Polymer
EC	Euro code Institution
FRP	Fiber Reinforced Polymer
GFRP	Glass Fiber Reinforced Polymer
HCRPC	Hollow Core Reactive Powder Concrete
HSC	High Strength Concrete
Kg	Kilogram
m	Meter
max	Maximum
mm	Millimeter
MPa	Mega Pascal
NSM	Near surface mounted
PVC	Polyvinyl Chloride
RPC	Reactive Powder Concrete
SFR	Steel Fiber Reinforced

LIST OF SYMBOLES

A_g	Gross area of column cross section
A_{st}	Area of steel bars
e	Eccentricity
e_{min}	Minimum eccentricity
f_c'	Cylinder concrete compressive strength
f_{cu}	Cube compressive strength
f_{ct}	Splitting tensile strength
f_r	Flexural strength
f_u	Tensile strength of reinforcement
f_y	Yield stress of reinforcement
Δ	Lateral mid height displacement
μ	Ductility index

CHAPTER ONE INTRODUCTION

1.1 General

A column is any member that has a ratio of length to a minimum lateral dimension equal to or greater than three and used primarily to support axial compressive load (ACI 318-19, 2014). Usually columns carry bending moments as well, about one or both axes of the cross section, and the bending action may produce tensile forces over a part of the cross section. Even in such cases, columns are generally referred to as compression members, because the compression forces dominate their behavior (David et al, 1997).

Columns intend to support the load-carrying beams and convey loads from the upper floors to the lower levels and from there onto the ground (David et al, 1997). Crush or failure in the most important building elements like column can cause the total collapse of the whole building as it is the only structural portion that transmits the dead and live loads to the ground. Happening the damages in these members cause a loss in the strength and stiffness of the entire structure (Mander et al., 1988 : Campione et al., 2007).

1.2 Classification of columns

Concrete columns are usually reinforced with longitudinal and transverse steel reinforcement and it can be classified into three kinds according to the reinforcement (Ferguson et al, 1981).

1- A tied column is one, usually of rectangular, square or circular shape, in which the longitudinal reinforcement is seized in position by discrete lateral ties, Fig. 1.1a.

2- A spiral column is usually of square or circular shape, in which the longitudinal reinforcement is an arrangement in circular shape and twisted by a continuous closely spaced spiral, Fig. 1.1b.

3- The composite column is column in which a structural steel shape, pipe or tubing is used beside concrete, with or without longitudinal bars, Fig. 1.1c.

The ratio of longitudinal steel area (A_{st}) to gross concrete cross section (A_g) is in the extent from 1% to 8%, according to (ACI 318-19, 2014).

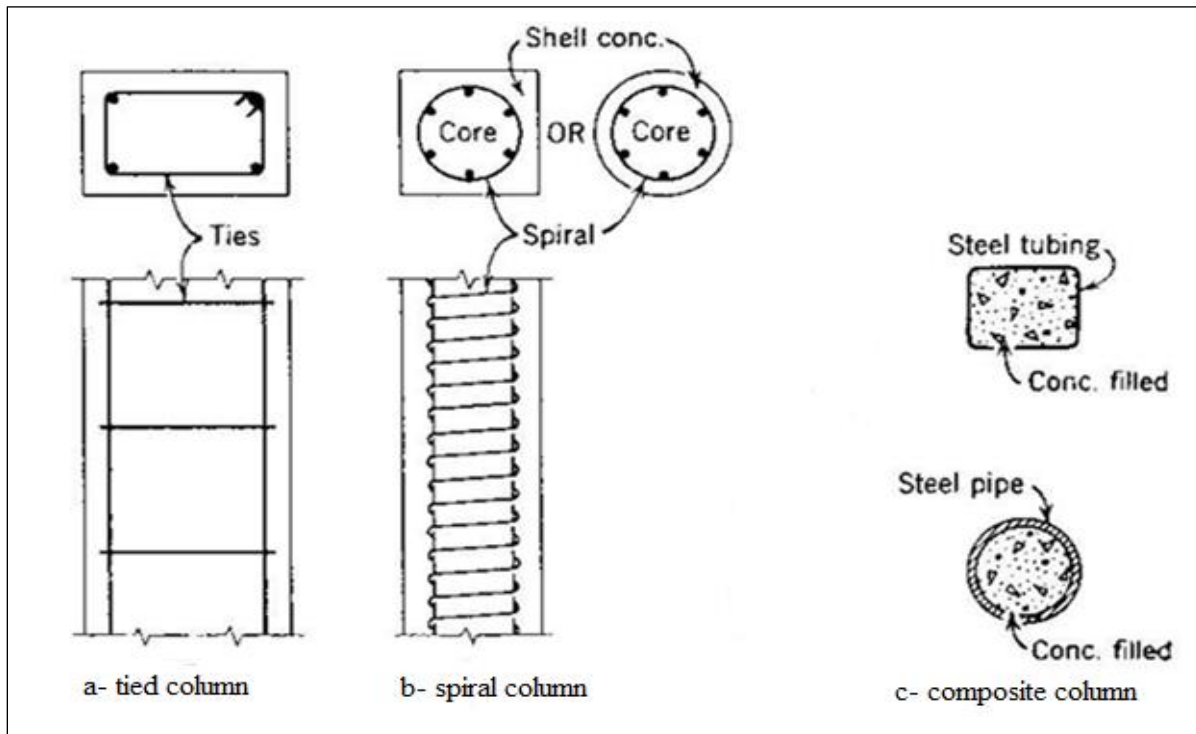


Fig. 1.1 Types of reinforced concrete columns (Ferguson et al, 1981).

While, the classification of columns according to type of loading includes (Park and Paulay, 1975).

1- Axially loaded column, Fig. 1.2a.

2- A column with uniaxial eccentric loading, Fig. 1.2b.

3- A column with biaxial eccentric loading, Fig. 1.2c.

Columns subjected to pure axial load rarely exist. All columns under some moment, which may be due to end restraint arising from the monolithic placement of floor beams and columns or due to accidental eccentricity resulted from imperfect alignment and variable materials (Wang et al., 2007).

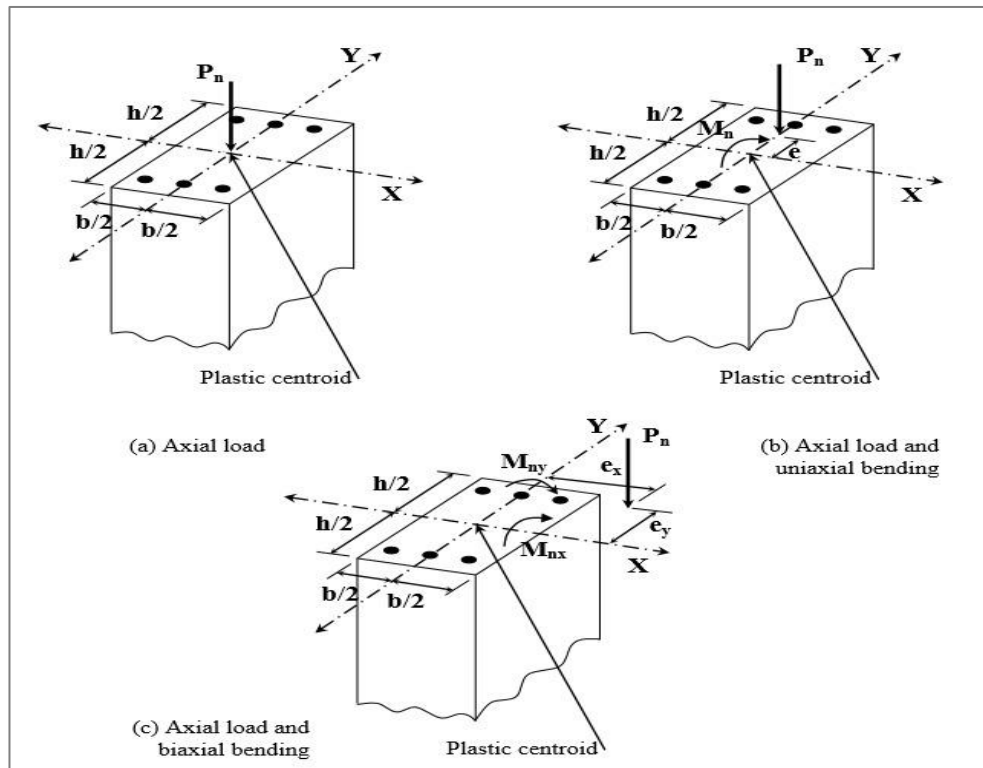


Fig. 1.2 Columns subjected to different types of loading (Park and Paulay, 1975).

Columns may be classified according to height:

- 1- Short columns: where the columns failure is due to the crushing of concrete and the yielding of the steel bars under the full load capacity of the column, as shown in Fig. 1.3.
- 2- Long columns or slender column: where buckling effect and slenderness ratio must be taken into consideration in the design, thus reducing the load capacity of the column relative to that of a short column, as shown in Fig. 1.4 .



Fig. 1.3 Short columns failed (Games and Musa, 2016).



Fig. 1.4 Buckling failure (Module, 2017).

1.3 Slender column

The ratio of the length of a column to the least radius of gyration of its cross section can be defined as slenderness ratio. It is used extensively for finding out the design load as well as in classifying various columns in short or long. The degree of slenderness is generally expressed in terms of the slenderness ratio as presented in Eq. 1.1 (ACI 318-19, 2014: Nadim and Akthem, 1976: Mrema et al, 2011: Chanakya, 2009: Fiona, 2004).

$$\lambda = kl/r$$

1.1

Where:

λ = Slenderness ratio

l = the unsupported length of the member.

r = the radius of gyration of its cross section, equal $\sqrt{I/A}$ for square or circular members, the value of (r) is the same about either axis; for other shapes, r is smallest about the minor principal axis, and it is generally this value that must be used in determining the slenderness ratio of a freestanding column.

k = effective length factor is the shortest distance between the top and bottom most points of the column at the point of bending is termed as length which effectively resists against the buckling. Columns having various types of supports as shown in Fig. 1.5.

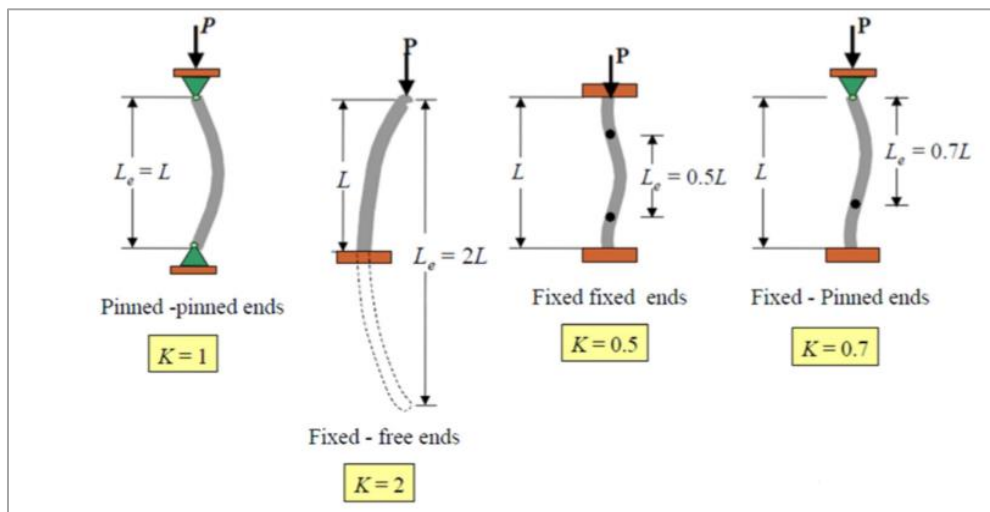


Fig. 1.5 Effective length of factor (Bijan et al. 2018).

Some codes specified the limitation of the slenderness ratio, that can be summarized in Table 1.1 according to the British standard (BS-8110, 1985), Euro code (EC2) (Bill et al., 2007) and American code (ACI 318-19, 2014)., as follows in Table 1.1.

Table 1.1 Summary of code procedures to determine slenderness ratio and column classification (Webber et al., 2015).

Parameters		BS 811	EC 2	ACI 318
Slenderness ratio		$\frac{l_{ex}}{h}$ or $\frac{l_{ey}}{b}$ Where: l_{ex}, l_{ey} = effective lengths h = depth of the column. b = width of the column.	$\lambda = l_0 / i$ Where: l_0 = effective height i = Radius of gyration $= \sqrt{I/A}$	$\frac{kl_u}{r}$ Where: k = effect length factor l_u = unsupported length r = Radius of gyration $= \sqrt{I/A}$
Column Classification	For Braced /Non-sway Frame	Short if both $\frac{l_{ex}}{h}$ and $\frac{l_{ey}}{b} < 15$ Slender if both $\frac{l_{ex}}{h}$ and $\frac{l_{ey}}{b} > 15$	Short if $\lambda \leq \lambda_{lim}$ Slender if $\lambda > \lambda_{lim}$ Where $\lambda_{lim} = \frac{20ABC}{\sqrt{n}}$ (Refer code for A,B,C)	Short if $\frac{kl_u}{r} \leq 34 + 12 \left(\frac{M_1}{M_2} \right)$ and $\frac{kl_u}{r} \leq 40$ Slender if $\frac{kl_u}{r} > 34 + 12 \left(\frac{M_1}{M_2} \right)$ and $\frac{kl_u}{r} > 40$ M_1/M_2 is (+ve) for single curvature (-ve) for double curvature bending
	For Unbraced /sway Frame	Short if both $\frac{l_{ex}}{h}$ and $\frac{l_{ey}}{b} < 10$ Slender if both $\frac{l_{ex}}{h}$ and $\frac{l_{ey}}{b} > 10$	Short if $\lambda \leq \lambda_{lim}$ Slender if $\lambda > \lambda_{lim}$ Where $\lambda_{lim} = \frac{20ABC}{\sqrt{n}}$	Short if $\frac{kl_u}{r} \leq 22$ Slender if $\frac{kl_u}{r} > 22$

1.4 Eccentricity

Eccentrically loaded reinforced concrete columns are commonly exist in practice due to the existence of some bending moments. The eccentricity of the supported beams as well as the unavoidable imperfections of construction are the main sources of the developed bending moments in the columns under gravity loads. In addition, lateral loads due to wind or earthquake loading are another source of the developed bending moments on the columns. Therefore, the strength of the columns is controlled by the compressive strength of concrete, the tensile strength of the longitudinal reinforcements and the geometry of the column cross-section (Park and Paulay, 1975). If columns have axial loads and bending moment about either the x or y axes only, they are classified as uni-axially eccentrically loaded columns. The peripheral columns located on the sides of a building are of this category. On the other hand, the corner columns of a building are loaded vertically and in addition they have moments about the x and y axes. These columns are known as bi-axially eccentrically loaded columns. Due to initial crookedness, non-uniformity of concrete and possible eccentricity in loading, all columns may be conceived to be bi-axially eccentrically loaded (Richart,1948).

All columns shall be taken the bending moment if have minimum eccentricity equal to :

According to (ACI 318-19, 2014)

$$e_{\min} = 0.6 + 0.03 h \quad 1.2$$

h= minimum lateral dimension in column.

1.5 Hollow reinforced concrete columns

Most tropical countries have heavy rains throughout the year. This requires an efficient and appropriate drainage system for any building. Hiding PVC

(Polyvinyl Chloride) pipes inside reinforced concrete columns and walls in buildings is a common practice. This requirement was imposed by architects who claimed that dropping pipes outside the columns would affect the appearance of the building (Mohammed, 2020). Also in some industrial buildings, these tubes may carry gases or liquids that are very harmful to the safety of the buildings in the event of a fire.

Providing such openings in reinforced concrete columns may result in a loss of strength and stiffness, and consequently, significant structural damage may occur, if the availability of the openings is not carefully checked during the design or construction stages (Mousavian, 2010). The benefit of using hollow concrete columns may be summarized by several points:

- 1- Transverse openings and longitudinal holes are often provided in reinforced concrete columns to allow arrival for services such as pipes for plumbing and electric wiring (Mousavian, 2010).
- 2- In location, where the cost of concrete is comparatively high, or in cases where the weight of concrete members is to be kept to a minimum, it may be economical to use hollow reinforced concrete columns (Zahn et al., 1990).
- 3- To reduce contribution of the column to seismic response and high carrying demand on foundation, it is desirable to use hollow cross section for columns (Lignola et al., 2007).

1.6 Fiber reinforced polymer (FRP)

Fiber reinforced polymer (FRP) materials have been attractive new materials for structural engineers in the concrete construction field. It has been used to retrofit concrete members such as columns, slabs, beams and girders in structures such as bridges, parking, decks, and buildings. FRP is a composite material composing of high strength fibers and polymer matrix. The FRPs mostly used for

civil engineering applications are carbon fiber reinforced polymer (CFRP), glass fiber reinforced polymer (GFRP), and aramid fiber reinforced polymer (AFRP) (Mohammed, 2007). During the last decades, the use of FRP has gained increasing popularity due to several properties such as: high strength to weight ratio; corrosion resistance; ease and speed of application; minimal change of cross-sections; possibility of installation without interruption of structure functions. For these reasons, FRP has been widely used in the retrofitting and strengthening of reinforced concrete structures, especially in regions under high seismic risk (Lignola, 2006). Fiber materials commonly used are carbon, glass or aramid. The different FRP materials and systems have varying properties and behavior. Table 1.2 presents typical properties of FRP composites. It should be noted that the ranges given in this table are indicative, and a particular product may have properties outside the ranges given in the Table, particularly when the fiber content is different from the ranges considered in the Table (1.2). It should further be noted that, in discussing the elastic modulus and tensile strength for a FRP composite formed in a wet lay-up process, the thickness of the FRP composite is generally difficult to control or define precisely. This has led to the use of the fiber sheet thickness or a nominal thickness as recommended by the manufacturer (Yousif, 2012).

Table 1.2 Typical mechanical properties of FRP composites (Yousif, 2012).

Unidirectional advanced composite materials	Tensile strength (MPa)	Longitudinal tensile modulus (GPa) of fiber	Density (kg/m ³)	Fiber content (by weight%)
Glass fiber/polyester GFRP laminates	400-1800	20-55	1600-2000	50-80
Carbon/epoxy CFRP laminate	1200-2250	120-250	1600-1900	65-75
Aramid/epoxy AFRP laminate	1000-1800	40-125	1050-1250	60-70

Carbon fiber reinforced polymers (CFRP) are the choicer suited to the post strengthening of structure. They are much stronger and stiffer than most other fibers, and are more corrosion resistant and more widely available as a raw material. CFRP do not absorb water and are resistant to many chemical solutions (Mohammed, 2007).

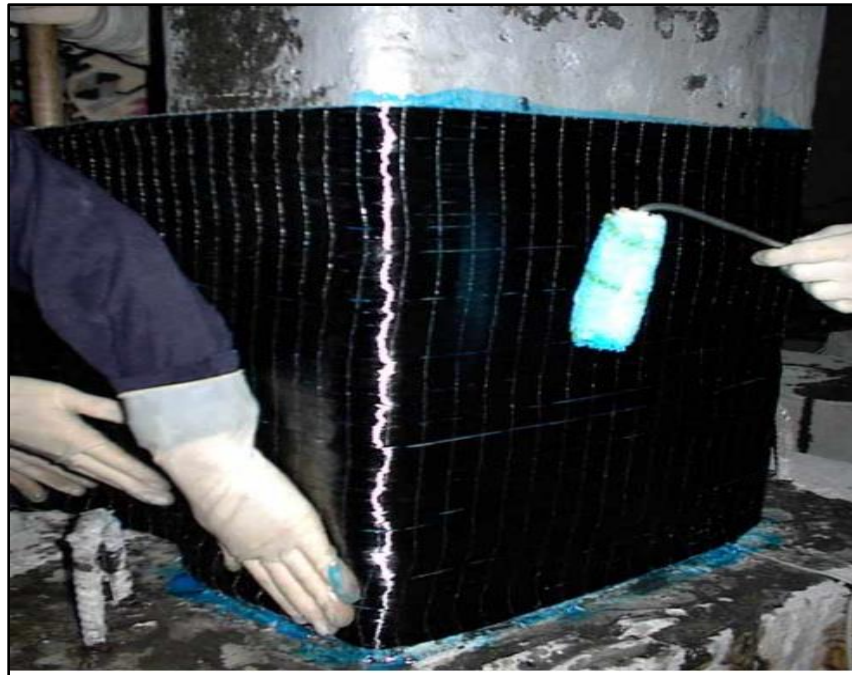


Fig. 1.6 Strengthening of reinforced concrete columns by CFRP (Cem and Osman, 2004).

1.7 Objectives of research

The principal objective of this research are summarized as follows:

- 1- Investigating experimentally the behavior of reinforced concrete slender columns with longitudinal holes. These holes are either rectangular or circular in shape. Columns are to be subjected to axial compression load and uniaxial bending up to failure.
- 2- Studying the effect of tie lateral reinforcement on the behavior of the hollow slender columns.

- 3- Studying the effect of strengthening by CFRP on the behavior of the hollow slender columns. The study also includes finding the ultimate load, maximum lateral displacement at any height, ultimate moment, ductility, energy absorption and failure mode of the column specimens.
- 4- Clarify the behavior of the column when exposed to an eccentricity load, and the effect of the value of the eccentricity displacement on the buckling of the hollow slender column studied.
- 5- Demonstrating the effect of the hole shape on the behavior of the slender column.

1.8 Thesis layouts

The study includes five chapters, as follows:

- 1- Chapter One: presents the general introduction to the columns and their strengthening.
- 2- Chapter Two: briefly reviews the previous researches, it is divided into two sections, the first part is the experimental work on slender reinforced concrete columns. The second part is related to the experimental work on hollow reinforced concrete columns.
- 3- Chapter Three: deals with the experimental program and test setup. Material properties, concrete mix design, details of hollow concrete slender columns, method of strengthening by CFRP and test program are described also.
- 4- Chapter Four: discusses and analyses the results of experimental.
- 5- Chapter Five: the conclusions obtained from the current research and provide many suggestions and recommendations for future studies to avoid the negatives that have been recorded and to develop these new types of hollow slender concrete columns on a larger scale.

CHAPTER TWO

LITERATURE REVIEW

2.1 General

Due to the lack of studies related to hollow slender concrete columns, two categories of researches were covered in this chapter. The first part was through which the previous researches were studied for the experimental works on slender reinforced concrete columns. While, the second part was studied for experimental works on short or slender hollow reinforced concrete columns.

The purpose of previewed these previous studies is to obtain sufficient information on the factors affecting on the behavior of hollow slender reinforced concrete columns that have not been previously studied.

2.2 Experimental work on slender reinforced concrete columns

(Elimihilmy, 2003) studied behavior of square slender reinforced concrete columns. Seventeen slender reinforced concrete columns with different slenderness ratios were tested under axial and flexure load. The main purpose of the test was to examine the behavior of slender columns subjected to pure axial loads or to axial loads with small eccentricity. The research program studied slenderness ratio, lateral and vertical steel reinforcement ratios, tie and spacing eccentricity of the axial load. The results are summarized that columns with closely spaced transverse reinforcement showed more ductile behavior at higher ultimate loads. The test results indicated that tie arrangement effects on both peak loads and ductility. The vertical reinforcement ratio altered both the ultimate loads and lateral deflections. It was noticed that the recorded lateral deflection increased by the amount of the initially applied eccentricity.

(Sumajouw et al., 2006) carried out a test program on slender reinforced geopolymer concrete columns. Twelve square slender column tests under axial load and uniaxial bending. The column cross-section was 175 mm square. The height of the columns was 1500 mm. The variables of the test program were longitudinal reinforcement ratio 1.47% and 2.95% respectively, compressive strength (40 and 60 Mpa) and load eccentricity ($e= 15, 35$ and 50 mm). The results presented in this work were the column load capacity increased as the load eccentricity decreased about 39.47% and 68.36% respectively. The column capacity also increased with an increase in the longitudinal reinforcement ratio about 31.59% and an increase in the concrete compressive strength about 52.82%.

(Gajdosova and Bilcik, 2013) investigated the effect of carbon fiber reinforced polymer (CFRP) on slender rectangular reinforced concrete columns in two manners. The first approach is a well-known form of CFRP sheet jacketing, and a second is a relatively new retrofit method of near surface mounted (NSM) CFRP strips. Eight columns with cross section (150×210) mm and length 4100 mm ($\lambda= 65$) in four series are tested. The first series consisted of non-strengthened columns; the second series was composed of concrete columns strengthened with CFRP laminate strips in the grooves; the third was composed of columns confined with a CFRP sheet; and the last series was composed of columns strengthened with a combination of these methods. All the columns loaded in the same way. The results of this study show the increase in resistance to strengthening can be expressed as an enhancement of maximum actualized compression force beside the non-strengthened reinforced concrete column, 12.9% for columns strengthened by longitudinal (NSM) CFRP strips, 2.4% for columns strengthened by confining with one layer of transverse CFRP sheet, and 15.4% for columns strengthened by a combination of CFRP strips and CFRP sheet. Also, the results showed a significant

difference in slender and short column strengthening in accordance with the predominant stress manner. It was confirmed that the effect of CFRP wraps on the increase in column strength is proportionally greater for short RC columns subjected to general compression.

(Youcef et al., 2013) investigated the effectiveness of strengthening by CFRP on behavior of four slender reinforced concrete columns, subjected to monotonic eccentrically axial load. Four columns with cross section (55×55) mm and length 1600 mm ($\lambda= 100$) were tested. The strengthening configuration were, one control column, and three columns, differently strengthened with a composite of CFRP. The control column without strengthening, the second strengthening with composed of 2-layers CFRP. The third column strengthening consists of a layer of CFRP which the fibers are disposed longitudinally to the column axis and the fourth column strengthening consists of two layers, one the same as that of the third column, on this is added another CFRP layer, such as the fibers are arranged perpendicularly to the column axis. The results of this study showed the three types of strengthening used in this research had relatively increased resistance significantly. An increase in the load bearing capacity of 76% was observed in the case of strengthening with an envelope of the CFRP which the fibers disposed longitudinally to the column. By adding a layer of the same CFRP with fibers arranged transversely, the increase reached 103%. The particular arrangement of two CFRP layers resulted in a 52% increase.

(Nadeem et al., 2014) carried out a test program on slender circular RC columns strengthened with FRP composites. A total of 12 small-scale circular RC columns of (150) mm diameter were cast in three groups, each group containing four columns of the same height. The first group of columns belonged to short columns of 600 mm height, whereas the height of the second and third groups (900

and 1200) mm heights respectively represented slender columns. The strengthened columns were prepared using three different strengthening schemes. The first strengthening scheme, included wrapped columns using a single layer of hoop CFRP sheet, whereas other strengthening schemes employed two and four longitudinal CFRP sheets in addition to one layer of hoop CFRP wrap. The column strengthened with single layer of hoop FRP not only increases the load carrying capacity but also the ductility substantially. CFRP-strengthening improves the strength and ductility of slender RC columns substantially. The results of this study showed the percent increase in load carrying capacity due to FRP strengthening. The increase in load carrying capacity for strengthening scheme varies from 34% to 73% which is mainly due to the increase in the confining strength of concrete. The effect of hoop wraps on the strength of columns is more significant for short columns (73%) than slender columns (61% for 900 mm and 34% for 1200 mm columns).

(Hamdy and El-Tony, 2016) presented a detailed experimental analysis on the overall structural behavior of fifteen columns with a cross section (150×100) mm and length 1200 mm were divided into four groups as well as a control axially loaded column. The first two groups represented columns bent in single curvature modes, while the other two groups represented columns bent in double curvature modes. Three end eccentricities ratios were studied, namely, 0.1b, 0.3b and 0.5b, where b is the column width. The results of this study show providing end eccentricities resulted in a decrease in the axial capacity proportionally with respect to the value of the end eccentricity. For equal end eccentricities ratio 0.5b, the column had lost about 75% of its axial capacity. In addition, columns bent in double curvature modes can sustain a higher load than those bent in single

curvature modes having the same end eccentricities combinations. Fig. 2.1 shown the mode failure of this group.



Fig. 2.1 Final failure modes for all columns a- group No. (1)

b- group No. (2). c- group No. (3) and d- group No. (4) (Hamdy and El-Tony, 2016).

(Mohammed and Ali, 2019) investigated the strengthened column by steel-fibre-reinforced (SFR) and carbon fiber-reinforced polymer (CFRP) on a part or a whole of the length of the column under axial force. And to obtain the effective length, which is responsible for the increasing of the ability of the column to resist buckling. Seven samples with cross section (120×60) mm and length 2000 mm was designed as slender reinforced columns. The results showed that the strengthening of the middle half of the column length by SFR gave an ultimate load similar to the strengthening of the whole column with same material. Also, it was found that the column strengthened by SFR increased its ultimate load by 42.6%, 42.1% and 33.3% for strengthened lengths of dimensions L, L/2 and L/3, respectively, compared to the non-strengthened column. The increase in ultimate load that could be borne by the column strengthened by CFRP were 53.0% and 33.8% for strengthened lengths of L and L/2, respectively.

2.3 Experimental work on hollow reinforced concrete columns

(Bakhteri and Iskandar, 2005) investigated the effect of concealing rain water pipes inside reinforced concrete columns in multi-storey buildings. Fourteen columns with length 1500 mm and different cross section in seven sets, with a PVC drain pipe positioned at the center of cross section of each one of them have been tested. The load subjected axially to the columns and when the columns reach the failure of the collapse load (ultimate) and maximum axial strain for each column has been recorded. Based on the ultimate strength/failure load of the specimens, the safety factor for each specimen can calculate by dividing the collapse load (experimental) by the design strength of the specimen. The study indicates that the factors of safety of the models obtained from the experimental investigation, vary from 1.20 to 1.79 using the BS 8110 code. Based on ACI code evaluation, the corresponding factors vary from 1.12 to 1.59. In both cases, the

obtained values are less than the nominal value of 2 as recommended by the codes. Research also revealed that the positioning of a drain pipe (PVC) inside the column significantly reduces the load carrying capacity and the effective cross-sectional area of the specimens.

(Lignola et al., 2007) carried out experimental tests on seven square hollow reinforced concrete short columns confined with CFRP. The cross section of the tested columns was (360×360) mm with a wall thickness of 60 mm. The longitudinal reinforcement was 16 \varnothing 10 mm longitudinal bars with 25 mm concrete covers and \varnothing 4 mm stirrups at 80 mm spacing as shown in Fig. 2.2. The hollow portion of the column had a height of 1300mm and was made of foam-polystyrene.

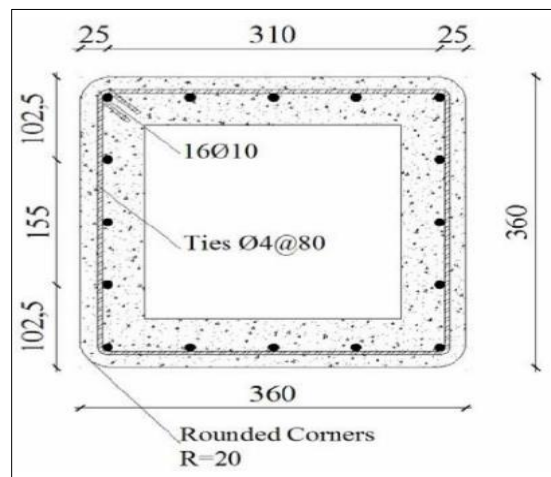


Fig. 2.2 Detailing of hollow columns (Lignola et al., 2007).

The heads had solid sections to distribute the load and to avoid local failures. Three eccentricities of 50, 200, and 300 mm have been selected to study the behavior of the hollow members. The results are summarized that the strength improvement was more relevant in the case of specimens loaded with smaller eccentricity, while the ductility improvement was more relevant in the case of higher eccentricity. In un-strengthened columns the curvature ductility ranged between 1 and 1.54, while

for strengthened columns the curvature ductility was significantly increased, attaining values ranging between 3.02 and 8.27. Since the failure of un-strengthened members is strongly affected by the occurrence of premature mechanisms (compressed bars buckling and concrete cover spalling), the CFRP confinement allows delaying these mechanisms, thus resulting in both strength and ductility increases of members, even under large eccentricities.

(Yazici and Hadi, 2009) investigated effects of CFRP wrapping on hollow core circular reinforced concrete columns. Eight circular short columns were studied in this experiment and divided into two groups. Four columns defined as (C) for externally unconfined and four columns (L) for externally confined in the hoop direction by wrapping with three layers of lateral FRP sheets were cast and tested. The hollow core reinforced concrete columns of 205 mm diameter, 56 mm hollow core diameter, and 925 mm height were tested under concentric axial loads and also under eccentric loads. A PVC pipe having an inner diameter of 205 mm was used as the outer mold, and a 56 mm outer diameter PVC pipe was used to form the hollow part. Two eccentricities have been taken into this study 25 and 50 mm. They summarize that CFRP wrapping proved to increase both the strength and the ductility by increasing axial and lateral deformation capacities is more effective on the axial load carrying capacity. When the loading is concentric, there was 50.91% increase in the axial load carrying capacity of the FRP wrapped specimen and 178.67% increase in the axial deflection corresponding to the maximum load (Δ) when compared to the unwrapped specimen.

(Yuliarti and Hadi, 2010) studied the behavior of hollow columns confined with FRP composites. A total of twelve short RC columns made of high strength concrete (HSC) having a height of 925 mm were cast and tested. Deformed steel bars (12 and 16 mm diameter) which had a nominal tensile strength of 500 MPa,

were used as longitudinal reinforcement in the columns. While, for the ties and spirals (transversal reinforcement), a plain steel bar (8 mm diameter) having a nominal tensile strength of 250 MPa with a pitch of 50 mm were used. Six columns had a circular cross section (two solid columns, two hollow columns each having a circular hole, and two hollow columns each having a square hole) and the remainder columns had a square cross section (two solid columns, two hollow columns each having a circular hole, and two hollow columns each having a square hole). The test result showed that solid circular column confined with (CFRP) has a higher ultimate load (3783kN) compared to solid circular column without (CFRP) confinement that has an ultimate load of 2507 kN. Also, circular column with a square hole confined with (CFRP) has a higher ultimate load (2666 kN) compared to circular column with a square hole without (CFRP) confinement that carries an ultimate load of (1789 KN) and circular column with a circular hole, confined with (CFRP) carries a higher ultimate load (2668 kN) compared to circular column with a circular hole without (CFRP) confinement that has an ultimate load of (1991 kN). So, It was found that FRP confinement increased hollow RC columns axial load and ductility capacities; and hollow columns having circular holes had better performance compared to hollow columns having square holes.

(Jabor, 2013) studied behavior of reinforced concrete hollow circular columns with steel fiber. This research included test twelve hollow circular columns with 1200 mm long and outer diameter of 210 mm and inner diameter of 80 mm, resulting in a wall thickness of 65 mm used in this investigation where reinforced with $\varnothing 10$ mm deformed bars as longitudinal reinforcement of $f_y = 420$ MPa and $\varnothing 6$ mm plain bars as lateral hoops of $f_y = 350$ MPa and fiber inclusion. The test results showed a direct relationship between absorbed energy and the spacing of lateral reinforcement. The addition of steel fibers with $V_f = 1\%$ (for the

fiber type used) to a hollow circular RC columns enhances the ductility with an increment of (40 to 60)%, allowing these columns to absorb an energy of about (40-50)% greater than that needed to deform a similar columns made of ordinary reinforced concrete to the same load level .

(Ihsan et al., 2018) studied the behavior of reinforced concrete slender columns with longitudinal hole under axial compression load and uniaxial bending. This research included testing of ten slender columns with dimensions (150×150×1300) mm with the details shown in Fig. 2.3. The investigation deals with the effect of using different diameters of column hole on the values of the load carrying capacity and cracking loads, mid-height lateral deflection and longitudinal shortening of the columns. The research program studied the hole size (hollowing ratios of 2.3%, 5.1%, 9% and 20.3%), the load eccentricity, (eccentricity column depth ratio of 0.33 and 1), tie spacing, height of columns, locations of the vertical holes (central hole, hole at compression side of the cross-section and hole at tension side of cross-section). All samples had four different diameter holes (0, 25.4, 38.1, 50.8, 76.2 mm). Test results have shown that when the holes were located at the center of the column cross-section and the column was loaded with high load eccentricity, the effect of hollowing ratio on load capacity is insignificant. For hollowing ratios used in this study the ultimate load is decreased by 0%, 0.28%, 1.03%, 3.28% and 6.48% respectively. The effect of hollowing ratio on columns loaded with small eccentricity of 50 mm ($e/h=0.33$) is greater than the effect of the hollow ratio of columns with 150 mm eccentricity ($e/h=1.0$) which reduces the load capacity for the columns by 0.00%, 0.66%, 2.65%, 4.97% and 11.26% for hollowing ratios the hollowing ratios used respectively.

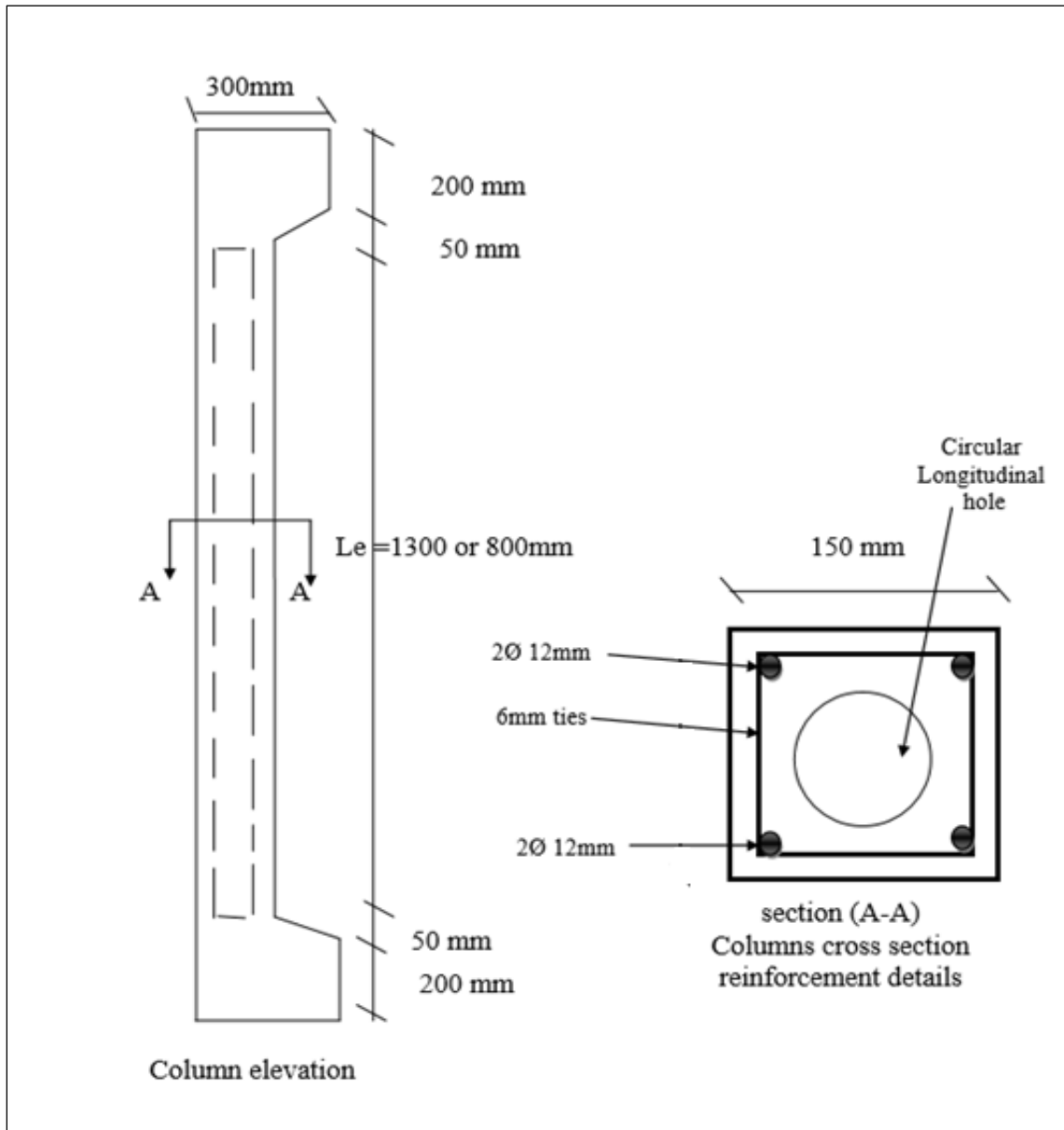


Fig. 2.3 Column elevation and cross section (Ihsan et al., 2018).

(Hadi et al, 2018) studied the behavior of hollow core Reactive Powder Concrete (HCRPC) columns confined with a circular Carbon-Fibre-Reinforced polymer (CFRP) tube. Sixteen circular hollow core specimens (206 mm in diameter, 800 mm in height and a 90 mm circular hole) were made with Reactive Powder Concrete (RPC) of 105 MPa compressive strength. These specimens were

divided into four groups. The first group was the control group that consisted of four unconfined HCRPC specimens reinforced with conventional longitudinal steel bars and steel helices. The specimens of the second group had the same configuration as the first group except that these specimens were externally confined with CFRP tube. The specimens of the third group were externally confined with a CFRP tube and internally confined with a Polyvinyl chloride (PVC) tube. Finally, the specimens of the fourth group had no steel reinforcement and were only made with an external CFRP tube and an internal steel tube. These specimens were subjected to different loading conditions: concentric, eccentric (25 mm and 50 mm) and four-point bending. It was found that the CFRP tube confinement slightly increased the strength of the HCRPC columns, whereas the ductility was significantly enhanced.

2.4 Summary

From the previous researches, it was found that many researches had been carried out on the behavior of solid slender columns or hollow short columns. However, it can be conclude that until now a little experimental work has been done on the presence of longitudinal openings in columns. One reference (Al-Zaidy et al., 2018) only studied the experimental behavior of hollow slender reinforced concrete column with many variable. The columns are square with dimensions of (150×150×1300) mm. Therefore, the present work was devoted to studying experimentally the hollow slender reinforced concrete columns under axial loading and uniaxial eccentric loading. Also, the effect of CFRP and lateral reinforcement (ties) on the strengthening of the hollow slender concrete column had been studied.

CHAPTER THREE

EXPERIMENTAL WORK

3.1 General

In this chapter, the details of the experimental program were presented. It showed of the details of the materials used (cement, sand, coarse aggregate and CFRP sheet), preparation, mixing, casting procedures, curing, and testing program of column specimens. Experimental tests were carried out in the laboratory of the Technical Institute of Amara.

3.2 Material properties

3.2.1 Cement

Ordinary Portland cement used in this study. It was placed in a dry place to keep the properties of cement from the impact of moisture. The results of the physical and chemical properties of the cement are shown in Tables 3.1 and 3.2, respectively. The tests are done in the laboratory of the Technical Institute of Amara according to the (Iraqi Specification No.5/1984).

Table 3.1 Physical properties of the cement.

Physical Properties	Test result	Limit of IOS 5:1984
Fineness using Blaine air permeability apparatus (m^2/kg)	312	≥ 230
Setting time using Vicat's instruments Initial (hrs: min.) Final (hrs: min)	130 min 4:00 hrs	≥ 45 min ≤ 10 hrs
Compressive strength 3 days (MPa) 7 days (MPa)	20.5 28.8	≥ 15 ≥ 23

Table 3.2 Chemical composition of the cement.

Compound composition	Chemical composition	Percentage by weight	Limits of IOS 5:1984
Lime	CaO	62.00	–
Silica	SiO ₂	21.00	–
Alumina	Al ₂ O ₃	5.26	–
Iron Oxide	Fe ₂ O ₃	3.00	–
Magnesia	MgO	2.70	≤5
Sulfate	SO ₃	2.10	≤2.8
Loss on Ignition	L.O.I	3.2	≤4
Insoluble residue	I.R	0.8	≤1.5
Lime saturation factor	L.S.F	0.92	0.66-1.02
Main Compounds (Bogue's equation) percentage by weight of cement			
Tri calcium silicate (C ₃ S)		48.10	
Di calcium Silicate (C ₂ S)		20.82	
Tri calcium Aluminate (C ₃ A)		8.16	
Tetra calcium Alumino ferrite (C ₄ AF)		9.18	

3.2.2 Fine Aggregate

The sand that has been used in all concrete mixtures is a natural sand. Table 3.3 shows the grading of fine aggregate and the limits of the (Iraqi Specification No.45/1984). Table 3.4 shows the physical properties of the used fine aggregate. The fineness modulus was 2.6.

Table 3.3 Grading of the fine aggregate.

No.	Sieve size (mm)	Passing by weight %	
		Fine aggregate	Limits of IOS No. 45/1984
1	10	100	100
2	4.75	98	90-100
3	2.36	92	75-100
4	1.18	76	55-90
5	0.60	54	35-59
6	0.30	18	8-30
7	0.15	2	0-10

Table 3.4 Physical properties of the fine aggregate.

Physical properties	Test results	Limits of IOS No.45/1984
Specific gravity	2.74	-
Sulfate content(SO ₃ %)	0.41%	≤ 0.5 %
Absorption %	1.6	-
Chloride content (Cl)	0.072%	≤ 0.1 %

3.2.3 Coarse Aggregate

Coarse aggregate is natural gravel obtained from Ali algarby. A maximum size aggregate of 10 mm was used. The results indicate that the coarse aggregate grading is within the requirements of (Iraqi specification No. 45/1984). The coarse aggregate was washed to remove the dust, then exposed to air to dry the surface, and then used in a saturated-surface dry state before use. Grading and properties of the aggregate are presented in Tables 3.5 and 3.6.

Table 3.5 Grading of coarse aggregate.

Sieve size mm	Passing by weight (%)	
	Coarse aggregate	Limits of IOS No.45/1984
14	100	100
10	84	85-100
5	7	0-25
2.36	0	0-5

Table 3.6 Properties of coarse aggregate.

Physical properties	Test results	Limits of IOS No.45/1984
Specific gravity	2.65	-
Sulfate content(SO ₃)	0.07 %	≤ 0.1 %
Absorption	0.59 %	-

3.2.4 Mixing water

The reverse osmosis (R.O) water was used for casting and curing all the specimens.

3.2.5 Carbon fiber reinforced polymer (CFRP)

SikaWrap®-300 C/60 carbon fiber was used to externally strengthen the reinforced concrete columns, as shown in Fig. 3.1. CFRP when loaded in tension, does not exhibit any plastic behavior before rupture. The tensile behavior of CFRP is characterized as a linearly elastic stress-strain relationship up to failure, which is sudden and can be disastrous (Falah, 2015; Mustafa, 2018). The properties of CFRP sheet are showed in Table 3.7 according to manufacturing specifications.



Fig. 3.1 CFRP sheet.

Table 3.7 Technical properties of CFRP sheet.

Property	CFRP
Areal weight	$300 \text{ g/m}^2 \pm 15 \text{ g/m}^2$
Fabric design thickness	0.166 mm (based on fiber content).
Fiber density	1.79 g/cm^3
Mechanical/ Physical properties	Tensile strength: $3,900 \text{ N/mm}^2$ (nominal) Tensile E-modulus: $230,000 \text{ N/mm}^2$ Elongation at break: 1.5% (nominal)

3.2.6 Adhesive materials

Sikadur-330 was used in this work as shown in Fig. 3.2 for bonding the carbon fiber reinforced polymers to the surface of reinforced concrete column specimens. The mixing ratio of the epoxy was four parts resin of component A (white paste) to one part hardener of component B (grey paste) by volume.



Fig. 3.2 Adhesive (Sikadur-330).

3.2.7 Steel reinforcement

Deformed steel bars with diameter of 6 mm were used for both lateral and longitudinal reinforcement in all columns. And deformed steel bars used with nominal diameters of 8 mm and 12 mm for corbel reinforcement in columns. 500 mm long specimens were tested to determine the yield stress (f_y) and the ultimate strength (f_u) as shown in Fig. 3.3. The test was conducted according to (Iraqi limits 2091/1999). The properties of the tested bars are presented in Table 3.8.



Fig. 3.3 Stress-Strain relationship for steel.

Table 3.8 Properties of reinforcing bars.

Bar diameter (mm)	Actual diameter (mm)	Area (mm ²)	Yield stress (f_y) (N/mm ²)	Tensile Strength (f_u) (N/mm ²)	Elongation %
6	5.9	27.3	424.5	533.7	12
8	7.82	48.03	480.3	553.7	13.6
12	12	113	570.8	670.4	15

3.3 Models description

The aim of the experimental work was to study the behavior of hollow reinforced concrete columns under concentric and eccentric loads. It was based on the study of fifteen concrete columns that were casted and tested in two stages. The first stage included seven specimens tested under axial loads. And the second stage included eight specimens that were designed with a corbel at the ends of the column for testing under eccentric load. Corbels have been added to the columns that are applied on it eccentricity loads for two main reasons. The first reason was to prevent a failure near the ends of the columns due to the occurrence of shear stress in the area opposite to the direction of the eccentric distance because of its small area. The second reason was that the load can be applied with an eccentric distance outside the column, so the presence of the corbel is to provide support for the purpose of applying the load according to the required distance. The details of

columns without corbels and with corbels are shown in Fig. 3.4 and Fig. 3.5, respectively. All columns are symmetrical in this study, with a cross section of (140×80) mm and 2000 mm in length. Each column was reinforced by 6Ø6 mm for longitudinal reinforcement and Ø6 mm bars were used for transverse reinforcement (ties). Four experimental factors were studied for the columns specimens. The factors were lateral reinforcement (ties), strengthening by carbon fiber polymer (CFRP) sheet, opening shape and eccentric load. The details of columns shown in in the Tables 3.9 and 3.10. The fifteen columns were dived into nine groups according to the effect of experimental factors.

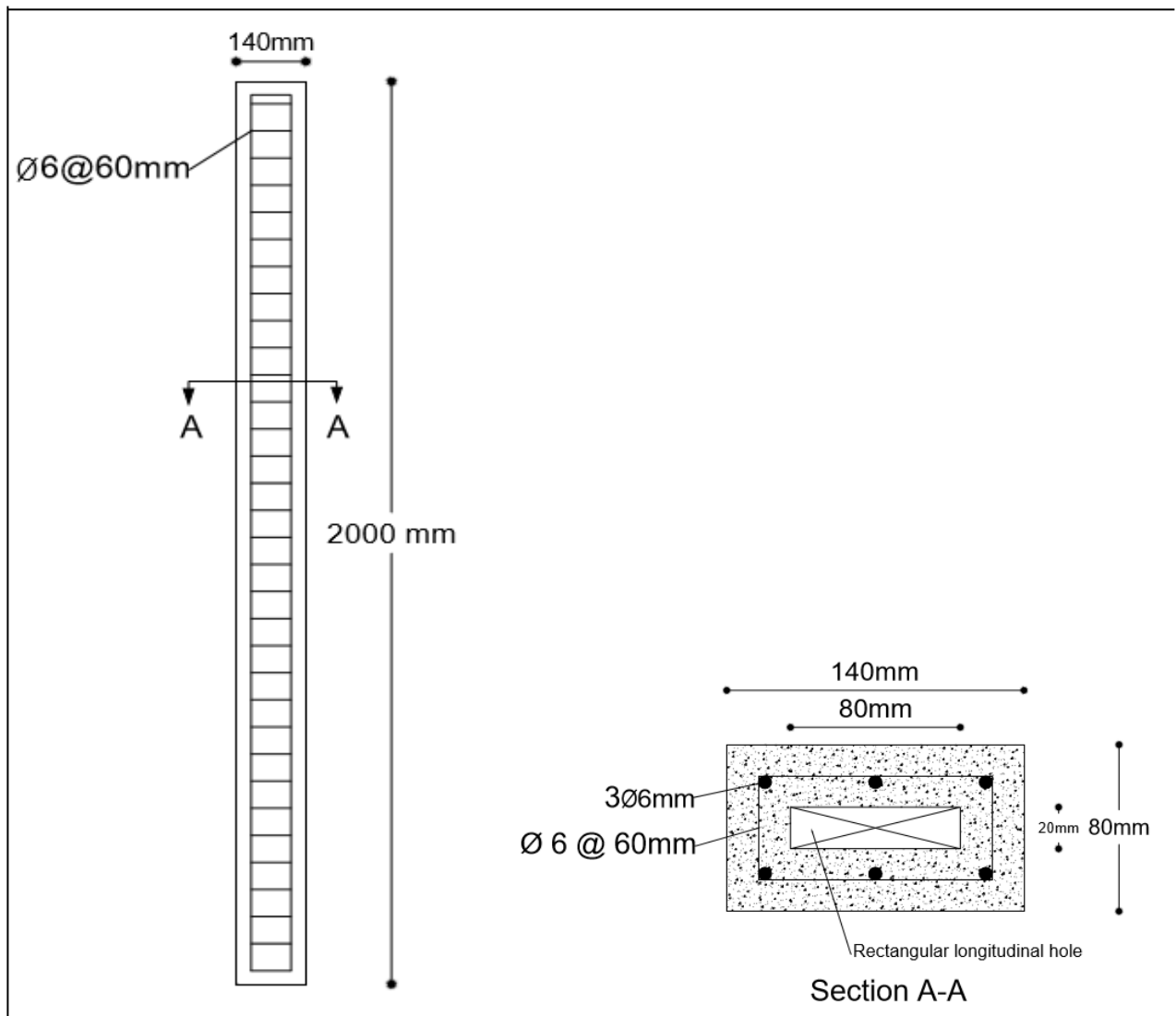


Fig. 3.4 column details without corbel.

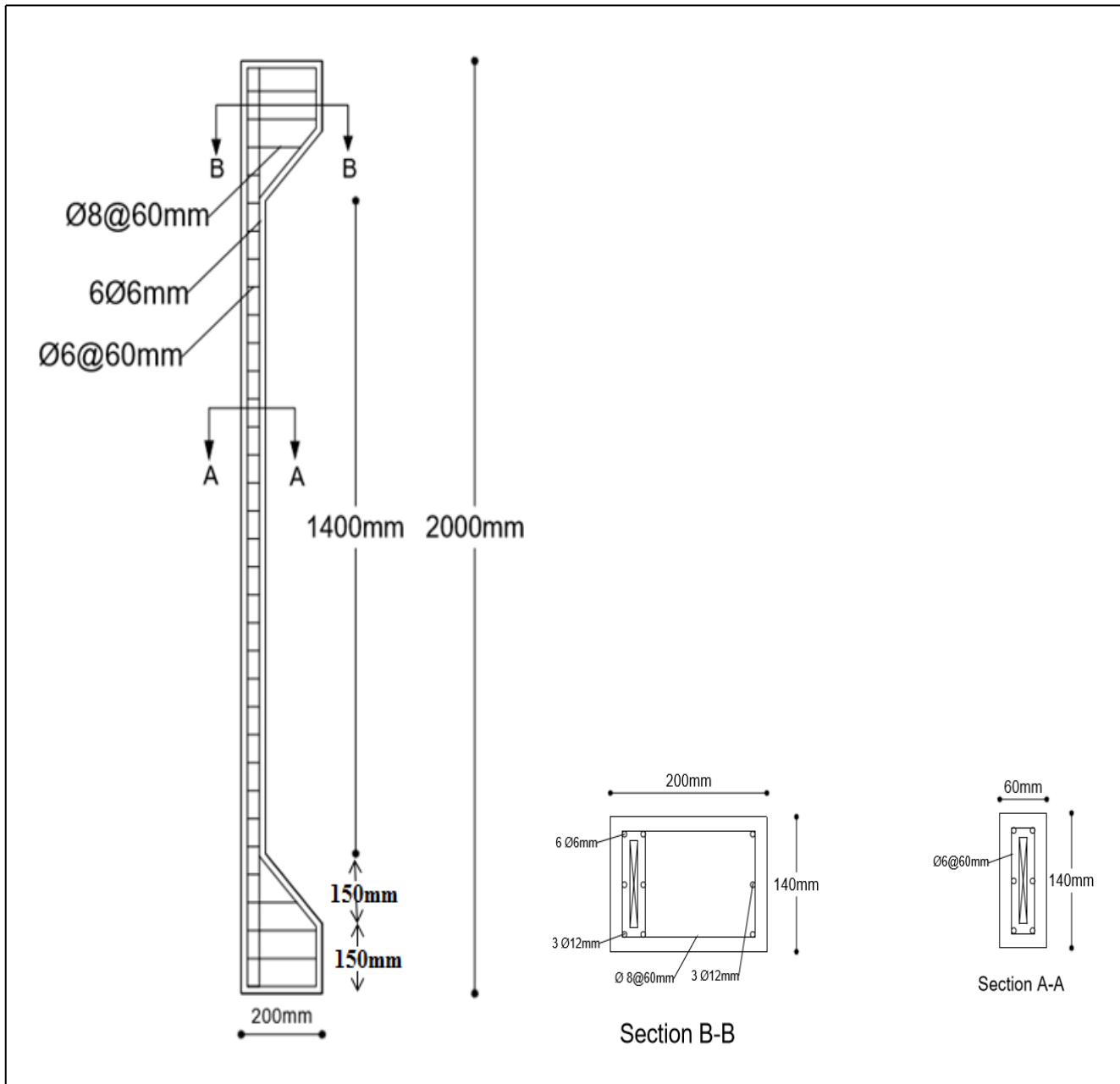


Fig. 3.5 Details of column with corbel.

* All columns are symmetrical in this study, so half of the column length (1000mm) was depended in Tables 3.9 and 3.10.

Table 3.9 Details of columns subjected to axial load.

Column ID	Distance of strengthening by adding addition lateral reinforcement (ties) at the ends of columns $\emptyset 6@60$ mm (mm)	Distance of strengthening by (CFRP) from the end of ties	Distance of Strengthening by lateral reinforcement + (CFRP) (mm)	Shape of Opening
C1	-	-	-	Rectangular
C2	140	-	140	Rectangular
C3	333	-	333	Rectangular
C4	500	-	500	Rectangular
C5	140	360	500	Rectangular
C6	333	167	500	Rectangular
C7	-	500	500	Rectangular

Table 3.10 Details of columns subjected to eccentric load.

Column ID	Distance of Strengthening by (CFRP) from the inner end of corbels (mm)	Shape of Opening	Eccentricity (mm)
C8	-	Rectangular	20
C9	-	Rectangular	40
C10	-	Circular	20
C11	-	Circular	40
C12	200	Rectangular	40
C13	200	Circular	40
C14	1400	Rectangular	120
C15	1400	Circular	40

3.3.1 Effect of lateral reinforcement

This group included four columns, C1, C2, C3, and C4, with variables included strengthening by additional lateral reinforcement (ties) at both ends of column and opening shape (rectangular opening shape). The first concrete column specimen C1 was kept without strengthening as a reference. The specimen C2 was reinforced by ties $\text{Ø}6@30$ mm for 140 mm distance of column ends. The reinforced distance is equal to the least column size (140) mm the specimens C3 and C4 were also reinforced by $\text{Ø}6@30$ mm as in specimens C2 but the reinforcement distance extended to 333 mm and 500 mm, respectively. Columns were strengthened by lateral reinforcement for specified distances from the ends to locate the column failure. This distance of strengthening was increased from 140 mm to 500 mm (quarter of the length of column) from each end to reach the maximum column capacity, which is obtained by buckling in the middle of the column. Details of the group are shown in Fig. 3.6.

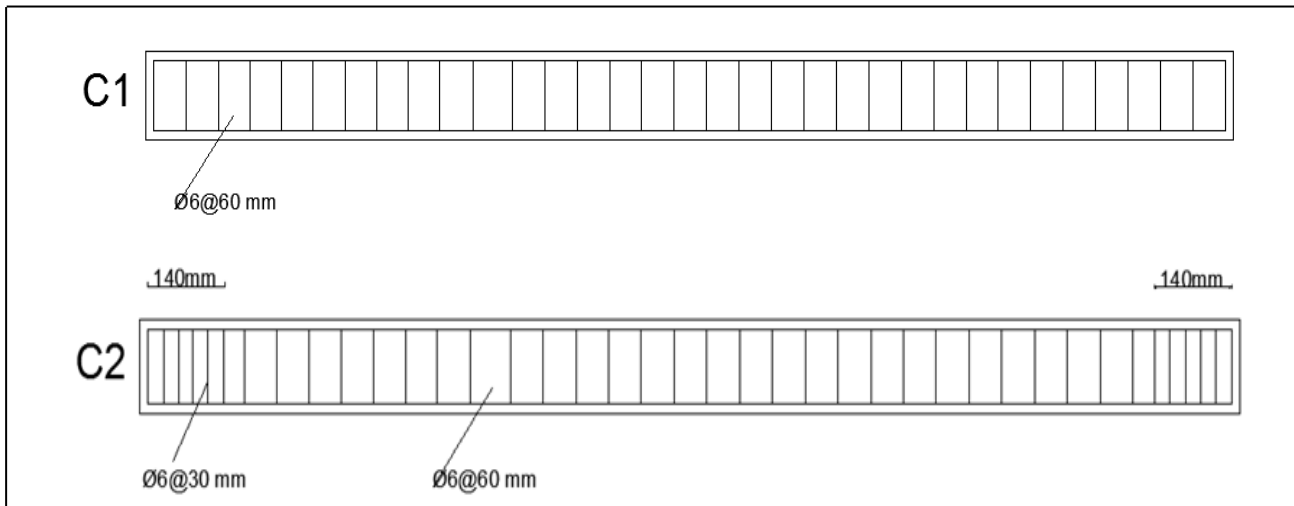
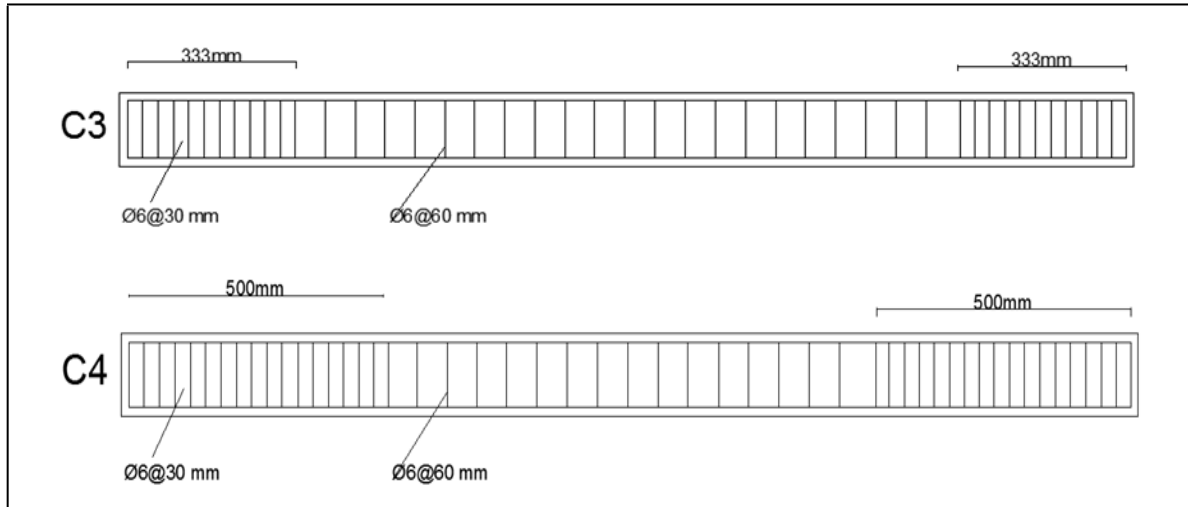


Fig. 3.6 First group details.



Continue.

3.2.2 Effect of lateral reinforcement and CFRP sheet

This group was included four columns, C4, C5, C6, and C7. The variables included were strengthening by lateral reinforcement (ties) at both ends of column and strengthening by CFRP at opposite sides of the width of column. C5 column was strengthened with lateral reinforcement (ties) at a distance of 140 mm and strengthened by CFRP sheet at distance of 360 mm. C6 column was strengthened also with lateral reinforcement and a CFRP at a distance of 333 mm and 167 mm respectively. The last column C7 strengthened only with CFRP at a distance of 500 mm. This group was done to find out the effect of the strengthening of the quarter of the column from each side by using CFRP and ties together in different proportions to know their effect on the behavior of the column. Also to find out the optimum ratio at the strengthening by CFRP which gives the best capacity of column with the least cost because CFRP is more expensive compared to ties. A quarter of the column had been strengthened on each side to make the column behaves at full capacity and the buckling occurs within the middle third of the column. Details of the group are shown in Fig. 3.7.

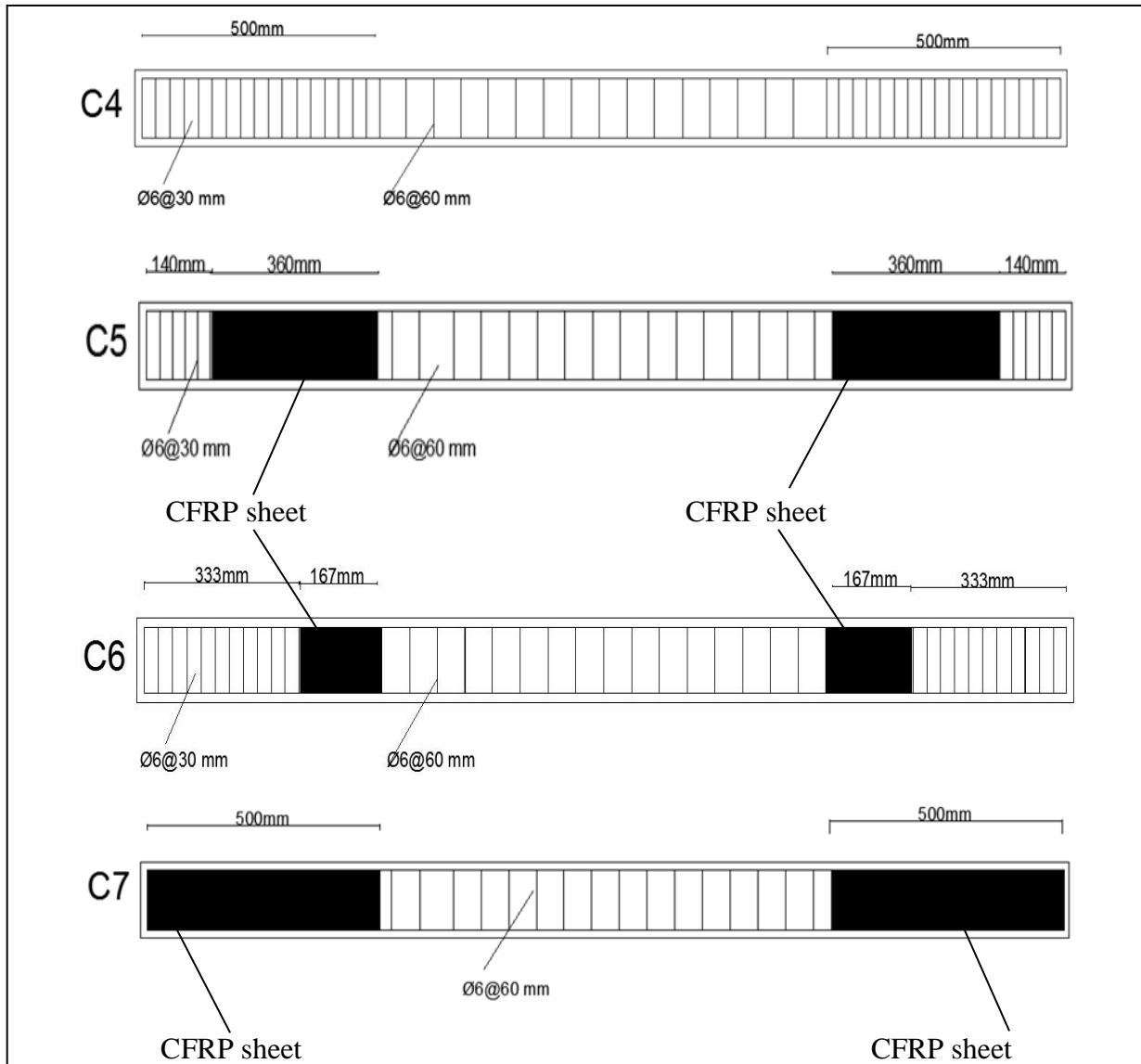


Fig. 3.7 Second group details.

3.3.3 Effect of eccentricity ($e= 20, 40$) mm

Through this group the effect of the eccentricity on slender columns was studied. C3 was chosen to be similar to the behavior of column C8 and column C9. Since column C3 is strengthened with an additional lateral reinforcement with a distance of 333 from each end, and this strengthening is approximately equivalent to the additional concrete in the corbel of columns C8 and C9, especially since the strengthening distance and the depth of the corbel are approximately equal. Where,

column C8 was tested by subjecting it on the load with an eccentric distance perpendicular to the width of the column, equivalent to one fourth of the column thickness, which was 20 mm. Also, C9 column was tested with an eccentric distance equal to half of the column thickness, which was 40 mm. Both columns were compared with the reference column C3, which was tested under axial load. The opening in all the columns in this group was rectangular. The details of columns (C3, C8 and C9) are shown in Fig. 3.8.

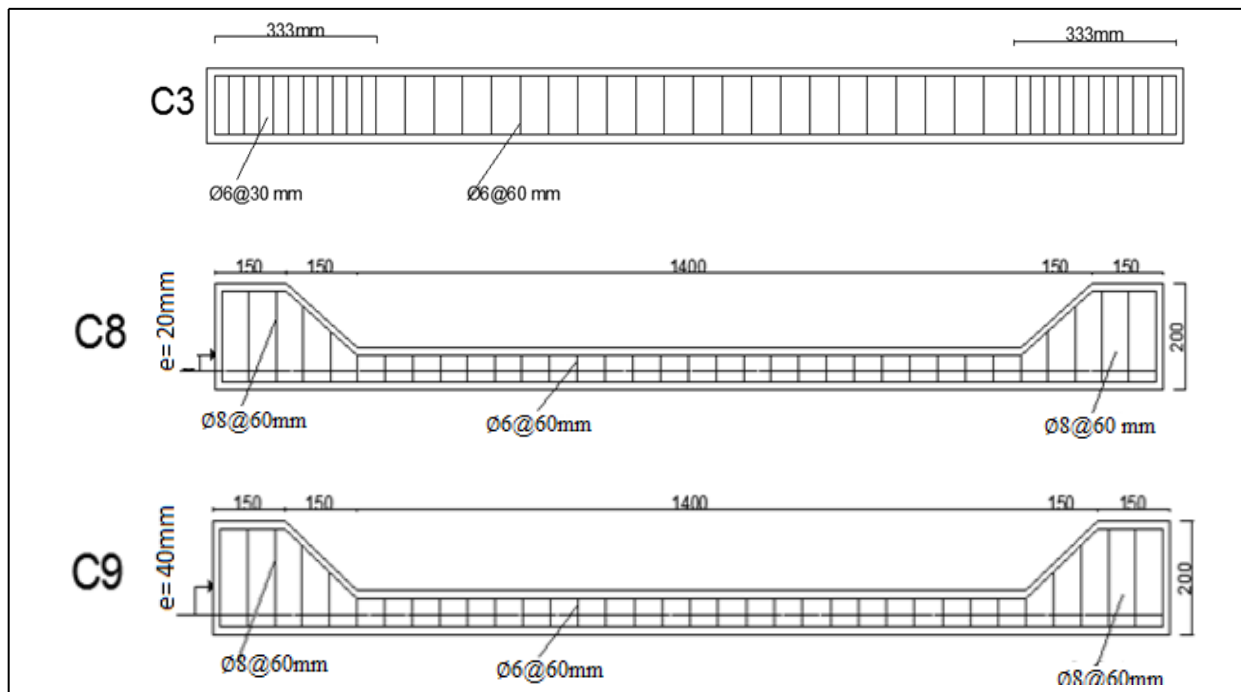


Fig. 3.8 Third group details.

3.3.4 Effect of opening shape with eccentricity ($e=20$ mm)

Two columns, C8 and C10, were included in this group. The columns have a 20 mm eccentricity and a different of opening shapes. The purpose of the group was to understand the effect of the eccentricity on the hollow slender columns with various shaped openings (circular and rectangular with approximately equal areas). Fig. 3.9 shows the specifics of the columns (C8 and C10).

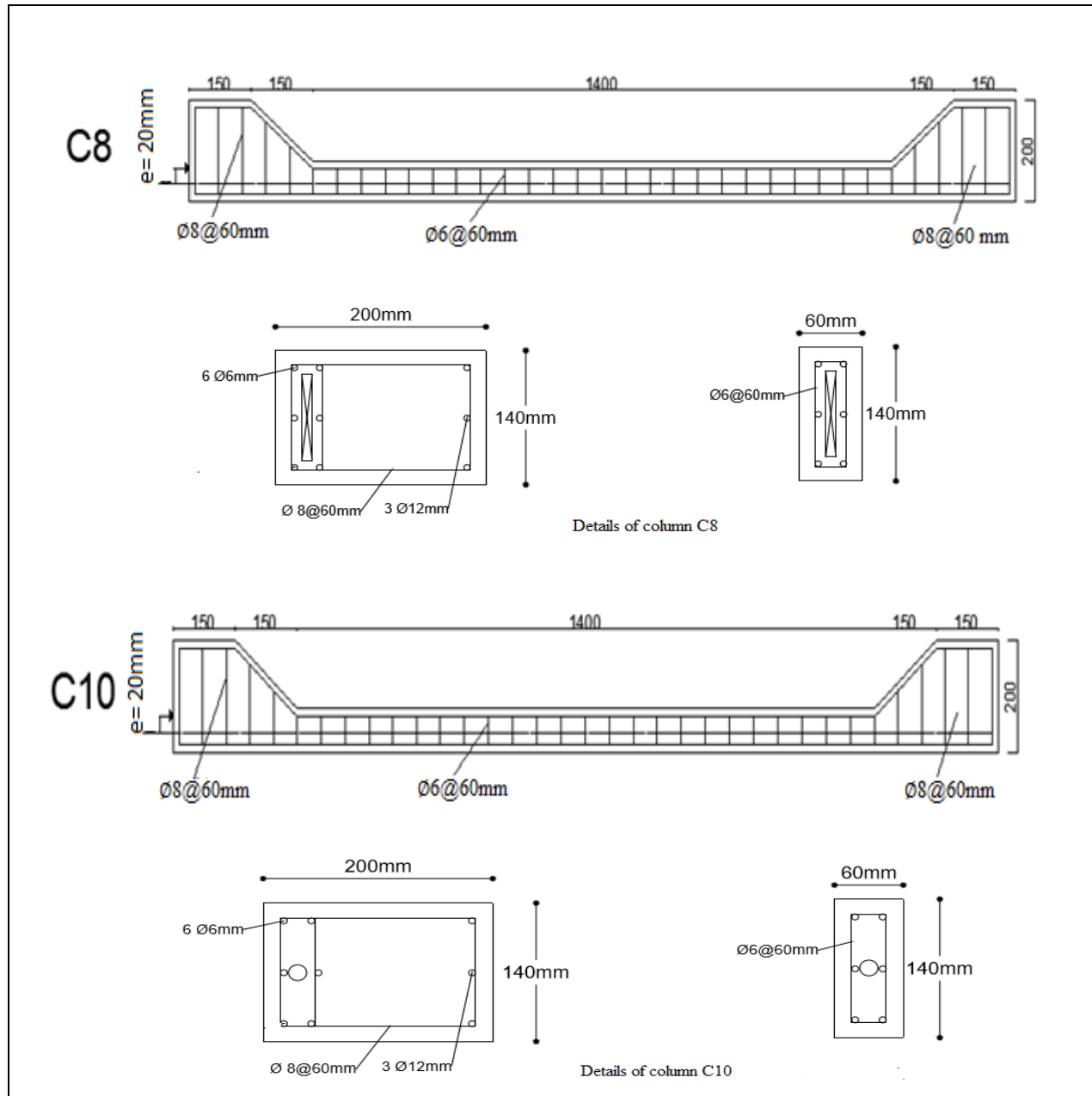


Fig. 3.9 Fourth group details.

3.3.5 Effect of opening shape with eccentricity ($e=40 \text{ mm}$)

Two columns C9 and C11 were included in this group. The columns C9 and C11 have eccentricity equal to 40 mm with opening of different shapes. The objective of the study was to understand the effect of the eccentricity on the hollow

slender columns with openings of different shapes (circular and rectangular with approximately equal areas). The columns were not strengthened by CFRP sheets. All details shown in Fig. 3.10.

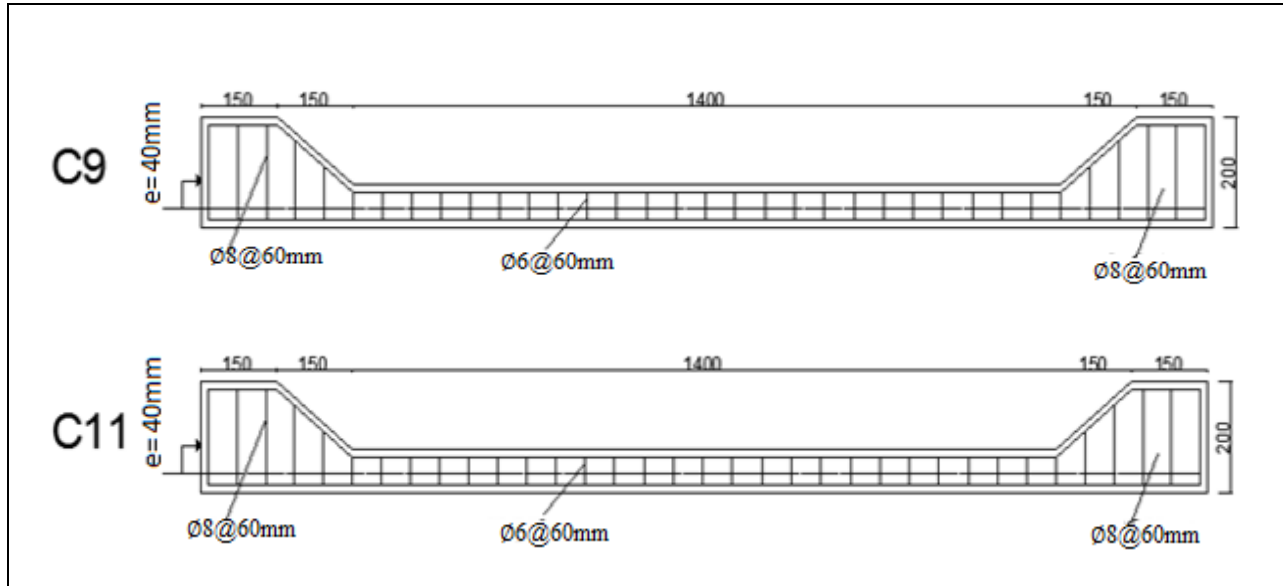


Fig. 3.10 Fifth group details.

3.3.6 Effect of eccentricity with CFRP sheet

In this group, the effect of eccentricity on strengthened columns with CFRP was studied. Where, C7 column was tested by subjecting an axial load and strengthened with CFRP at distance of 500 mm. While, C12 was tested with an eccentric distance equal to half of the column thickness, which was 40 mm and strengthened with CFRP at distance of 200 mm from both internal corbels. Actually, the above strengthening distance was chosen not at arbitrary, but rather to strengthen the column for a distance equal to a quarter of the length of the column from each end. But the presence of the corbels at a distance of 300 mm from each end denied the need to strengthen this area with CFRP and remaining distance of 200 mm was strengthened. The details are shown in Fig. 3.11, noting that the shape of the opening is a rectangular of all the columns.

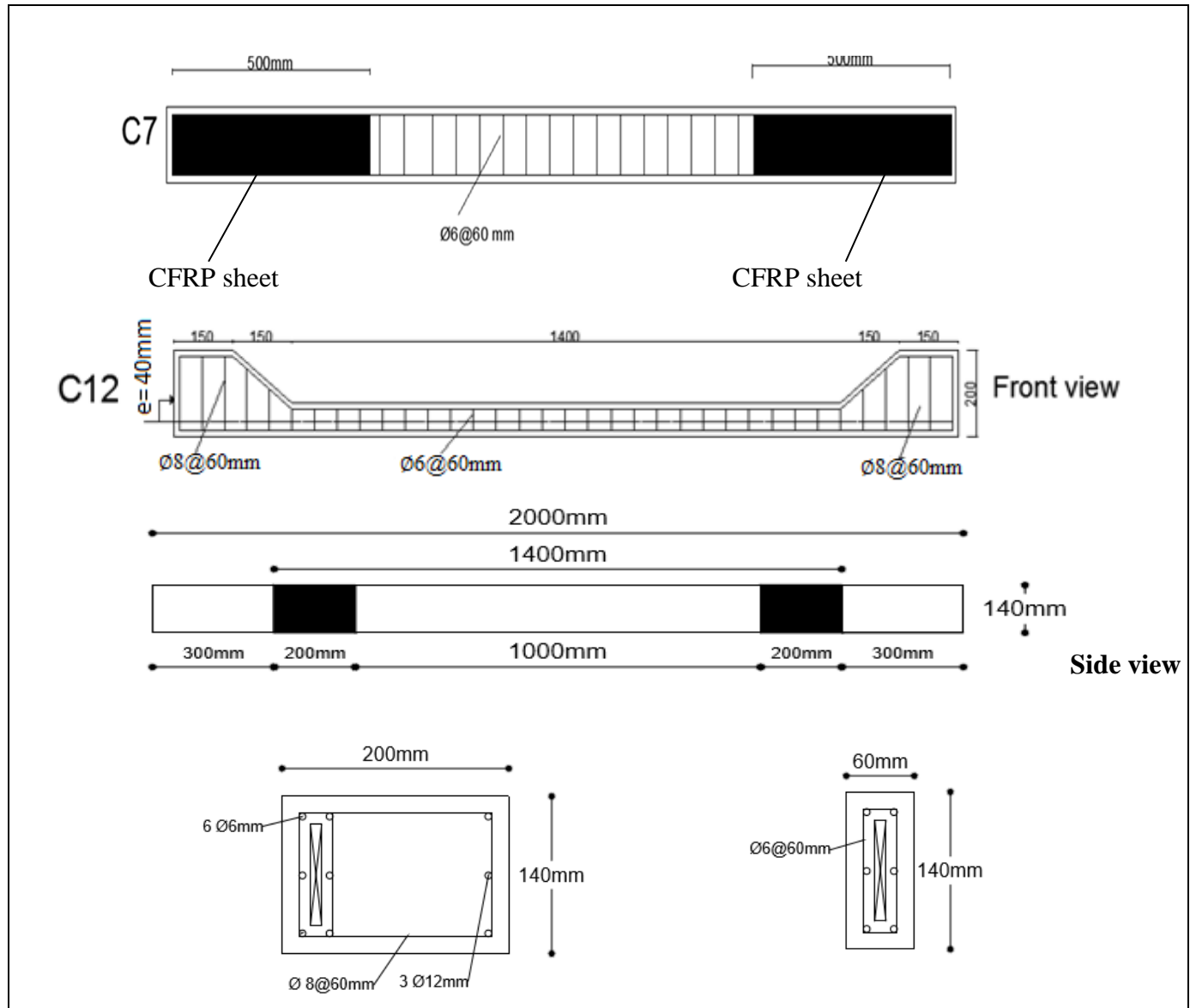


Fig. 3.11 Sixth group details.

3.3.7 Effect of opening with CFRP sheet

This group there were two columns C12 and C13 studied. The columns having the same eccentricity and strengthened with opening of different shapes. The purpose of this group was to study the effect of eccentricity with different hollow and strengthened by CFRP sheet with the same length. Details of this group shown in Fig. 3.12.

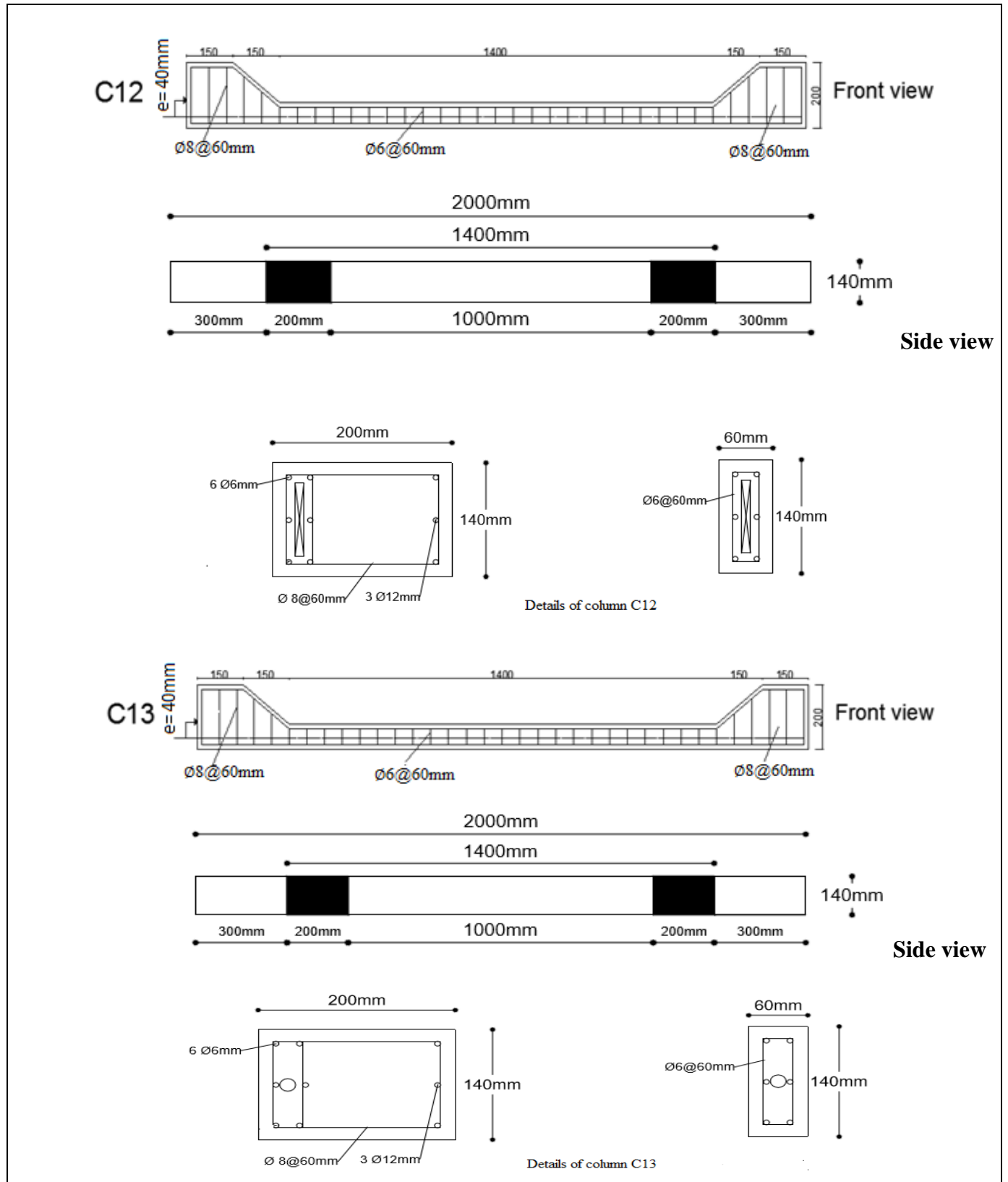


Fig. 3.12 Seventh group details.

3.3.8 Effect of high eccentricity

C14 column was strengthened at a distance of 1400 mm between both internal ends of the corbels. Thus, the whole column was strengthened with CFRP except for the corbels area, which did not need to strengthen. This column was selected for the purpose of applying an eccentric load at a distance of one and half times of the thickness of column and was 120 mm. The purpose of choosing this distance is to test a column that the load is applied on it at a distance outside the bounded of the column dimensions to know how this column behaves. It is expected that there will be a high moment due to the large eccentric distance, so a fully strengthened column was chosen. No previous studies have studied the existence of eccentricity outside the bounded of the dimensions of the column, so this specimen was studied in a group alone. The details of C14 are shown in Fig. 3.13.

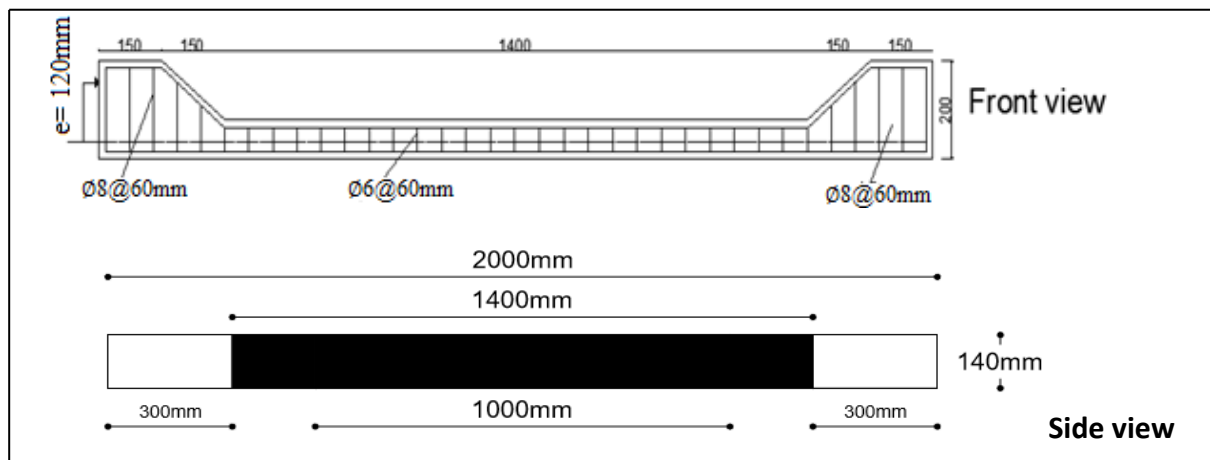


Fig. 3.13 Eighth group detail.

3.3.9 Effect of CFRP sheet with same eccentricity

In this group there were three columns C11, C13, and C15, with variable strengthened by CFRP in different lengths. The values of all other parameters were remain constants ($e=40 \text{ mm}$ and the same hollow (circular)). Each column has the same properties of the geometric aspects. The C11 was kept without strengthened.

While C13 and C15 were strengthened using CFRP sheet in 200 mm and 1400 mm respectively at opposite sides of the width of the column. The objective of this group to study the effect of eccentricity on the column having a circular hollow and strengthened by CFRP sheet in different lengths. Details are shown in Fig. 3.14.

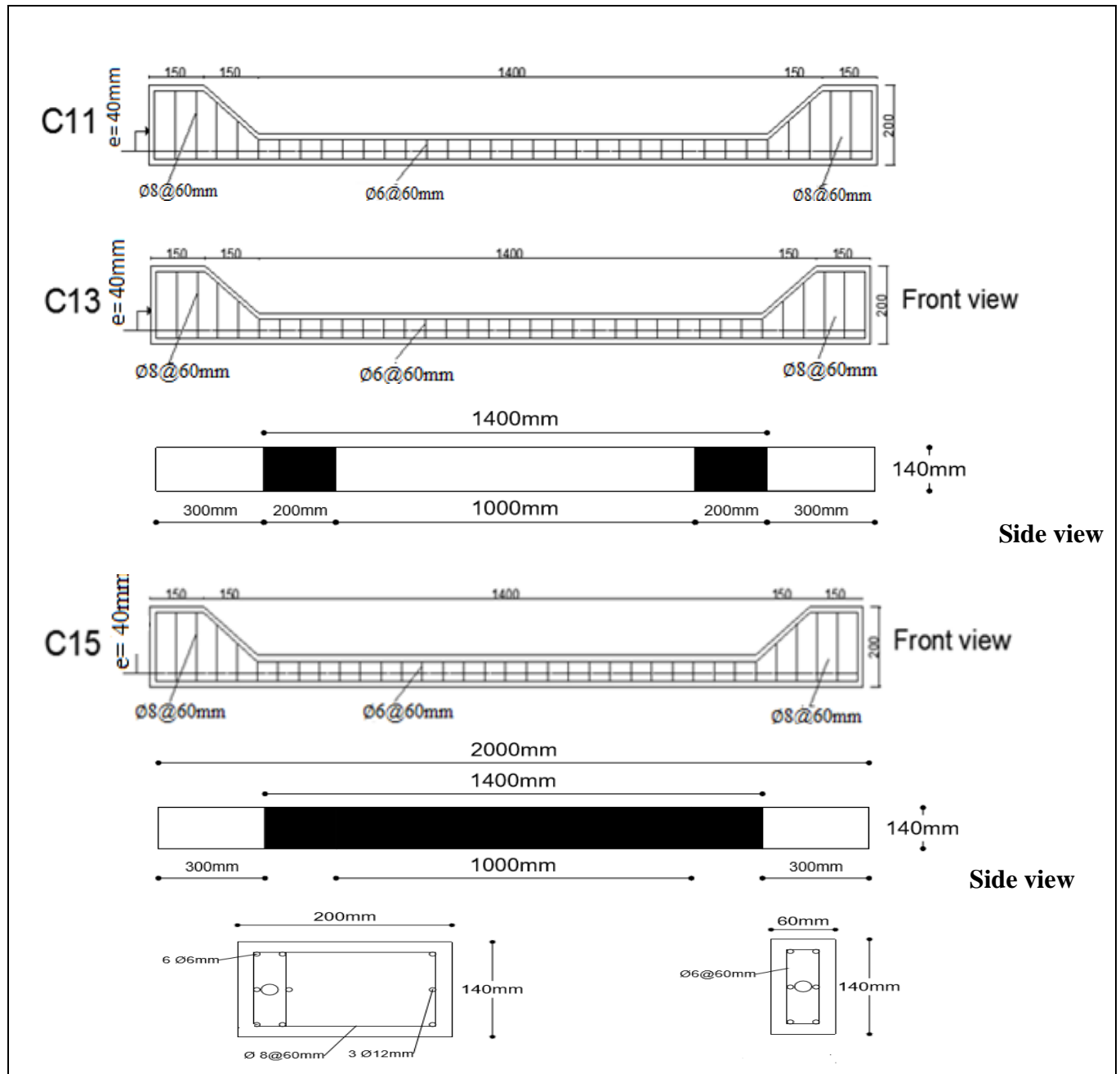


Fig. 3.14 Ninth group details .

3.4 Formwork and reinforcement cages

Longitudinal reinforcement and ties are shown in Fig. 3.15 a and b which represents steel reinforcement. All the column specimens used in this work were cast in iron molds to obtain a column specimen having cross-section (140×80) mm in the middle and total length 2000 mm as shown in Fig. 3.16. However, some of the column molds had top and bottom corbels with a cross-section (200×300) mm to facilitate eccentric loading during the test as shown in Fig. 3.17. The corbels were designed to have strengths well by using deformed steel bars $\varnothing 8$ and $\varnothing 12$ to prevent premature failure at this portion of the specimens during the tests and to concentrate the failure in the middle portion as shown in Fig. 3.18. The iron molds consist of a base and four iron sides, two of which are attached to the base and two of them are movable to facilitate the mold opening process. A thin wood mold used to form a rectangular hole inside the column with dimensions of (20×80) mm as shown in Fig. 3.19a. While a thin plastic tube (PVC pipe) was used to form a circular hole inside the column with a diameter of 45 mm with an area roughly equivalent to the area of the rectangular hole, as shown in Fig. 3.19b.



Fig. 3.15a Cage of steel reinforcement for columns (C1-C7).



Fig. 3.15b Cage of steel reinforcement with corbels for columns (C8-C15).



Fig. 3.16 Steel Reinforcement cage and molds without corbel.



Fig. 3.17 Steel Reinforcement cage and mold with corbel.



Fig. 3.17 Continue.



Fig. 3.18 The reinforcement of corbels.



Fig. 3.19a Rectangular hole.



Fig. 3.19b Circular hole.

3.5 Mix proportion

In this study, the mix proportion (1:1.23:1.67) as a concrete mixes by weight was designed according to American method of mix proportions selection (ACI 211.1-91). The weights of cement, sand and gravel for each cubic meter in this mixture were (531.7, 655.32, 890), respectively. The water cement ratio was 0.41.

3.6 Mixing procedure

The laboratory mixing procedure used in this study as stated in the following steps:

- 1- All ingredients for each mixture are weighed and placed in a clean area.
- 2- Coarse aggregate was washed with clean water and left to dry before mixing.
- 3- Prepare and clean the mixer and ensure continuous mixing during the mixing period.
- 4- After homogenization of the mixture, water was added to mix with admixture gradually, with continuous mixing.
- 5- The concrete was then discharged and tested for fresh properties and finally cast inside the molds.

3.7 Casting and curing procedure

The procedures were included lubricating the internal sides of the molds and fixing the reinforcing cages inside them. The concrete was mixed by using a rotary mixer available at the structural laboratory of the Technical Institute of Amara. Fig. 3.20 represents a concrete mixer used in this work. Then casting the concrete into the molds and using the vibrator, taking into consideration the leveling of the upper outer surface of each mold as shown in Fig. 3.21. While, Fig. 3.22

represented to finish of casting of column specimens. After 24 hours, the samples were removed from the molds and treated in a water for (27) days with approximately constant laboratory temperature and covered with a cotton cloth and treated with water. After 27 days, the covers was removed from the columns and tested according to the standard specifications. Fig. 3.23 represents the treatment of column samples, and Fig. 3.24 shows samples before testing.



Fig. 3.20 Concrete mixer used in the present work.



Fig. 3.21 using the vibrator during casting of column specimens.



Fig. 3.22 Finishing casting of column specimens.



Fig. 3.23 Curing of column specimens.



Fig. 3.24 Painting of the column specimens by white emulsion.



Fig. 3.24 Continue.

3.8 Tests of Hardened Concrete

The columns were cast in two categories, the first category represented the columns to which the axial load applied and the second category represented the columns to which the eccentric load was applied. For each category were cast, six cubes, three cylinders and three prism were casted to measure the compressive, tensile and flexural strengths respectively as follow:

3.8.1 Cube compressive strength (f_{cu})

The test of compressive strength of concrete was done by using cubical specimens with dimension (150×150×150) mm according to the British standard (BS 1881: part 116-1983, 1983). This test was taken at the using a compression machine (2000 kN) in the of laboratory of the Technical Institute of Amara as shown in Fig. 3.25. The result shown in Table 3.11.



Fig. 3.25 Concrete compressive strength test.

3.8.2 Splitting tensile strength (f_{ct})

The splitting test was conducted in compliance with (ASTM-C496, 2004). A total of three cylinders (150×300) mm were tested. Two bearing strips of 3 mm thick plywood and 300 mm long were placed upper and lower the specimen to provide the concentrated stress and the applied uniform load on the test surface of cylinder as shown in Fig 3.26. The test result shown in Table 3.11 and the result calculated using the following formula:

$$f_{ct} = \frac{2P}{\pi DL} \quad 3.1$$

Where:

f_{ct} : splitting tensile strength (N/mm^2).

P: Maximum applied load (N).

D: diameter of specimen (mm).

L: Length of the specimen (mm).



Fig. 3.26 Splitting tensile strength test.

3.8.3 Flexural strength test (f_r)

The modulus of rupture is calculated in accordance with (ASTM-C78, 1992). Three prisms of dimensions (150×150×500) mm were cast for each category at the same time as the columns were cast. This test was conducted at the laboratory of the Technical Institute of Amara. The modulus of rupture was obtained using a 100-ton machine as shown in Fig. 3.27. The expression given

below is used to calculate the modulus of rupture and the result shown in Table 3.11.

$$f_r = \frac{3PL}{2bd^2} \quad 3.2$$

where:

f_r : modulus of rupture (MPa).

P: maximum applied load (N).

L: span length (mm).

b: average width of specimen (mm).

d : average depth of specimen (mm).



Fig. 3.27 Flexural strength test.

Table 3.11 Results of mechanical properties of concrete.

column		f_{cu} (MPa)	f_r (MPa)	f_{ct} (MPa)
Category one at 28 days	Sample 1	43.92	3.67	2.89
	Sample 2	43.10	3.64	2.91
	Sample 3	44.43	3.68	2.92
	Average	43.81	3.66	2.91
Category two at 28 days	Sample 1	43.22	3.80	2.88
	Sample 2	44.31	3.68	2.92
	Sample 3	44.00	3.80	2.94
	Average	43.84	3.76	2.92

3.9 Important factors before starting works

3.9.1 End Column Cap

According to previous research carried out by several researchers, it was found that the ends of the tested slender column had failure first at the beginning of the loading, which gave inaccurate results about the actual behavior of the column. Therefore, most research restored to strengthen these ends. In this study before starting to test the main columns, an experimental columns were used. The ends were strengthened by capping them with a confining iron jacket. But, during loading a slippage occurred between the end of the column and the jacket, which resulted in the pressure of jacket on the column and caused its failure, as shown in Fig. 3.28. So it's replaced by two pieces of steel plate and their dimensions were (200×200×10) mm to prevent crushing the head of the column and to avoid stress concentration on the head of the columns during loading, then to prevent crushing failure at the end. The plate has screws to prevent the plate cover from slipping or being disassembled during the loading as shown in Figs. 3.29. Also, a steel plate cap with dimension (200×50×8) mm is provided at both ends to facilitate the application of eccentric loading. A 20 mm rod was used in the plate and device to

restrict the horizontal and vertical movements of the specimens, as shown in Fig. 3.30.



Fig. 3.28 Plate cap jacket.



Fig. 3.29a column cap (side view).



Fig. 3.29b end column cap (top view).



Fig. 3.30 Plate cap of eccentric load.

3.9.2 Number of specimens

To determine the number of specimens for each cases, another experimental column shown in Fig. 3.31 similar to column C1 was tested with the same details. It was found during the test that it gave completely similar results to the result of column C1. So only one model was relied on for each column to represent a specific case.



Fig. 3.31 The failure of experimental work of an experimental column.

3.10 Application of CFRP sheet

Before adhering CFRP to the surface of concrete for strengthening purposes, preparation of the surface should be done as a preliminary stage to ensure a high quality bond. These included preparation the substrate of concrete, ensuring the flatness of the concrete surface for adhering to the strengthening system and setting out the strengthening material in an exact location. The surface of concrete to which the strengthening material is bonded should be sufficiently to avoiding developing any out of plane stresses. The bonding of strengthening CFRP on to the surface of concrete include the following steps:

- 1- It should be removed a layer of concrete surface of 0.5 – 1.0 mm. Coarse aggregate using grinding tool as shown in Fig. 3.32. Further, any materials and dust should be removed using water and a brush.
- 2- First of all, the CFRP was cut into the required lengths.
- 3- Two parts of epoxy (A and B) adhesive (Sikadur-330) was mixed together in proportion (4:1) respectively until the color became uniform light gray. The adhesive was also applied, then the sheet was placed on concrete.
- 4- After that, putting CFRP sheet on the column surface on the coated region by epoxy and pressure applying by a rubber roller to seat the sheet by that cause epoxy forced out from both sides of the sheet. And excess epoxy removed from the sides of CFRP.
- 5- Finally the columns be ready to test after curing for 7 days. Fig. 3.33 showed some of these steps.



Fig. 3.32 Surface grinding.



Fig. 3.33 Steps of installation CFRP sheet

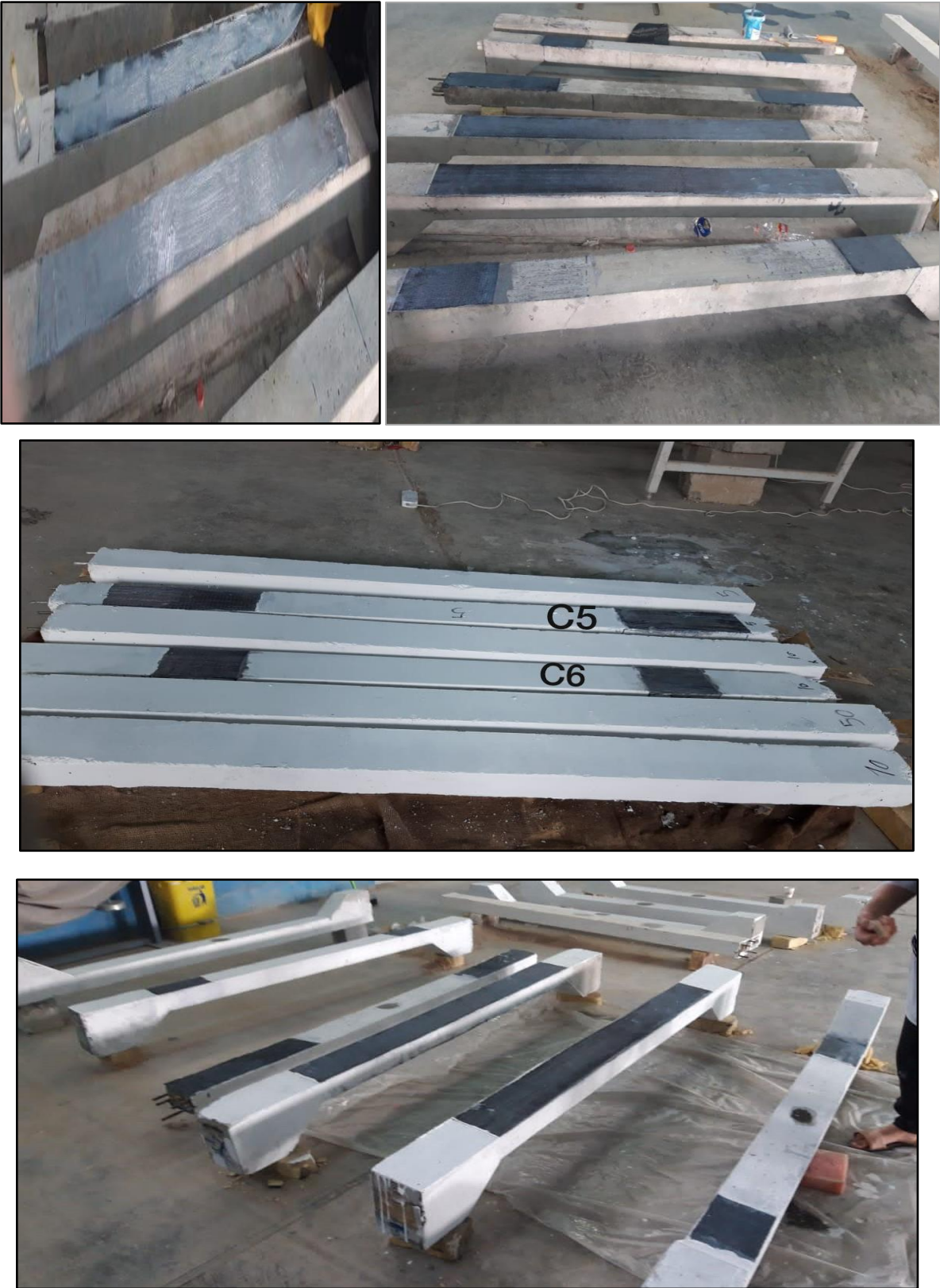


Fig. 3.33 Continue.

3.11 Measurement of lateral deflection

Two dial gauges were fixed to measure the lateral deflection for each column specimen at each loading stage. The dial gauges had an accuracy of 0.01 mm. The dial gauges were placed on the surface of the column at the positions shown in Fig. 3.34. The mid-height lateral displacement of columns were recorded immediately after the application of the load by using Camera.



Fig. 3.34 Dial gauges used in the test.

3.12 Testing machine

Steel rig had been fabricated and assembled at the Reinforced Concrete Laboratory of the Technical Institute of Amara, Iraq, in order to facilitate the execution of the experimental work program as shown in Fig. 3.35. Steel caps were provided at both ends of the column in order to distribute the column compression load at both ends as well as to facilitate the application of eccentric loading. Concerning the test procedure, after 28 days the specimens was carried out after strengthening casting. All specimens were cleaned, strengthened by (CFRP) and painted with white paint before testing. While the column was loaded using compression test machine of 600 kN capacity. Column specimens were tested

vertically, the load was applied on the top end of the column. The columns are placed under the test frame socket and adjusted so that the midline. Before the test, to adjust the supports and loading system a small load was applied, and then the initial readings were taken. At each stage of the download, order scale readings were taken. This behavior took some time until the failure occurred. After this stage, the column sample was removed from the testing machine.



Fig. 3.35 Test arrangement.

CHAPTER FOUR

RESULTS AND DISCUSSION

4.1 General

The main aim of this study is to investigate experimentally the behavior of hollow slender reinforced concrete columns. This chapter includes the main parts, (strengthening by lateral reinforcement (ties), strengthening by carbon fiber polymer (CFRP) sheet, opening shape and eccentric load) which were the results of testing of fifteen concrete column specimens. In addition the ultimate load, maximum lateral displacement at any height, ultimate moment, ductility, energy absorption and failure mode of the column specimens are presented.

4.2 The concluded factors from the results

4.2.1 Ductility of column specimens

Ductility is the ability of members to undergo considerable deformations prior to failure. Ductility plays an important factor in reinforced concrete members, especially that designed for seismic zones (Yuliartri and Hadi, 2010). The ductility of the test columns are computed using two methods. The first method was proposed by (Pessiki and Pieroni, 1997) which called "displacement ductility" at which the ratio of the axial displacement of the column at an axial load corresponding to 85% of the maximum axial load on the descending branch of the axial load-displacement curve (Δ_{85}), to the displacement at the limit of elastic behavior (Δ_y) as shown in Fig 4.1 a. This mean the ductility is calculated using Eq. 4.1.

$$\text{The displacement ductility index } (\mu_{85}) = \Delta_{85} / \Delta_y \quad 4.1$$

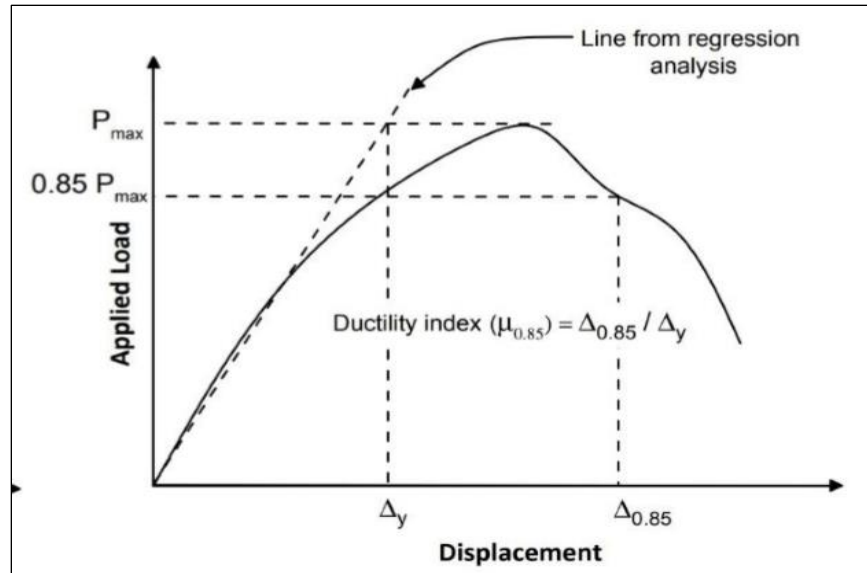


Fig. 4.1 a Determination of the displacement ductility (Azizinamini et al., 1999).

While, the second method proposed by (Lian and Thomas, 1995) defined the displacement ductility as the ratio between the maximum deflection (Δu) on the yield deflection (Δy) as presented in Eq. 4.2.

$$\text{The ductility index } (\mu) = \Delta u / \Delta y \quad 4.2$$

Where

μ = ductility index, unit less.

Δu = Maximum deflection corresponding to maximum strength, mm.

Δy = Deflection corresponding to yield behavior limit, mm.

The load-displacement curves proposed by (Thomas and Cooper, 1995) were used in this study, as shown in Fig. 4.1 b. The results of the ductility index of hollow slender columns were tabulated in Table 4.1.

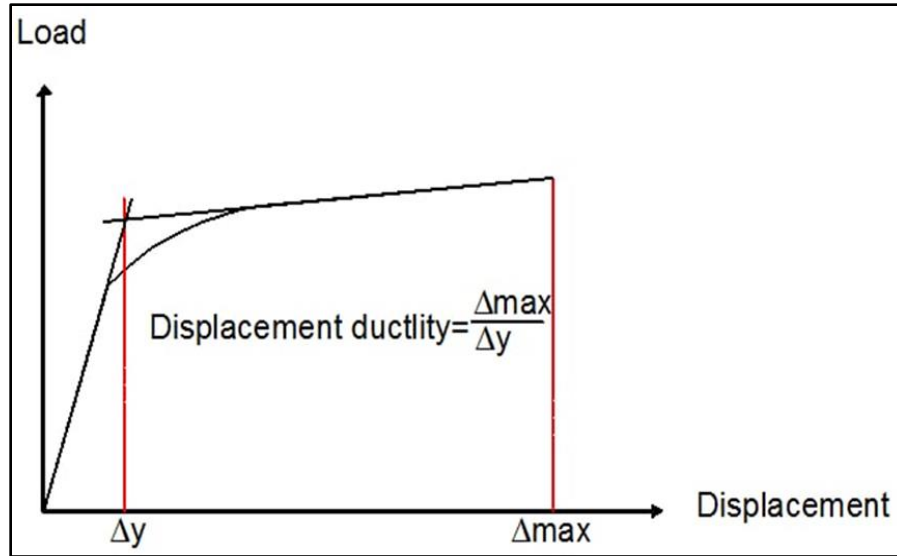


Fig. 4.1 b Determination of the displacement ductility (Lian and Thomas, 1995).

4.2.2 Energy absorption

Energy absorption values equals the area under the curve of load deflection response of tested specimens. Energy absorption is the ability of a material to absorb energy and plastically deform without fracturing. The results of energy absorption of hollow slender column was tabulated in Table 4.1.

4.2.3 First and second order moment

To calculate the moment, the method of Vianello's (Aleksandar, 1997) was proposed for axially loaded columns with an initial eccentricity as shown in Fig. 4.2. In this case, an initial eccentricity, Δ , which follows the buckled shape of the column, assumed. The initial eccentricity can be resultant of many factors, such as imposed lateral deformations, or imperfections during construction. As axial load P is applied, a moment equal to $P \Delta$ is generated. This moment is referred to as a first-order moment as presented in Eq. 4.3. The first order moment generated causes the column to undergo further lateral deformations, until a total maximum deformation equal to $e_{tot, max}$ is achieved. e_{tot} is equal to the sum of the first-order deformation Δ and the second-order deformation e . The magnitude of e along

the length of the column is affected by both material and geometric nonlinearities. The moment resulting from the applied axial load P and the second-order deformation e is known as a second-order moment. Total moment M is the sum of the first-order moment and second-order moment and presented in Eq. 4.4.

$$M = P \times \Delta \quad 4.3$$

$$M = P (\Delta + e) \quad 4.4$$

The term $P \Delta$ is referred to as the first order moment M by (Salonga, 1998) since it corresponds to what is known as first-order analysis. First-order analysis is based on a determined state of equilibrium based on the structure's initial geometry. The term $P(\Delta + e)$ is representative of additional second-order moments M caused by member deformation and change in flexural stiffness EI .

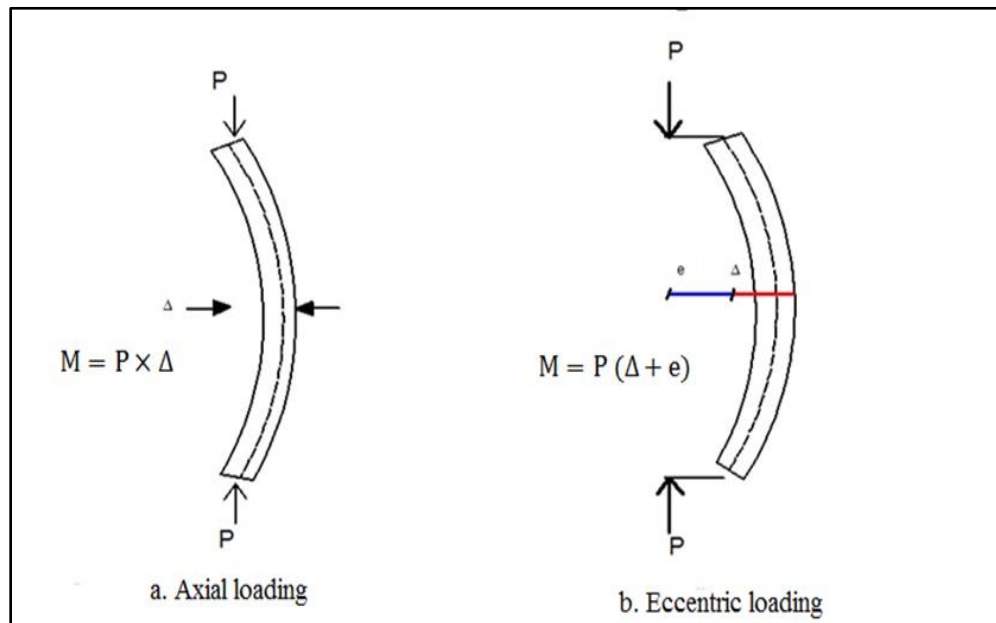


Fig. 4.2. Axial and eccentric loading in the column.

4.3 Test Results of columns specimens

The details of tests result of hollow slender column that include the ultimate load of columns and maximum lateral displacements of the specimen are given in Table 4.1.

Table 4.1 Experimental test results of column specimens.

Column ID	Ultimate load (kN)	Maximum lateral displacement (mm)	Location of failure from the top of the column (mm)	Ductility Index	Energy absorption (kN.mm)	Moment (kN.m)
C1	180	1.82	-	2.02	209.18	0.3276
C2	185	2.20	-	3.13	302.18	0.41
C3	195	3.70	340	4.11	612.63	0.72
C4	290	20.00	590	8.00	2165.12	5.80
C5	337	14.00	890	9.00	4000.50	4.73
C6	310	12.00	630	8.80	3077.50	3.72
C7	400	17.81	900	10.00	6298.80	7.12
C8	175	4.32	500	3.11	584.57	4.24
C9	160	3.00	345	2.50	320.79	6.88
C10	200	6.50	840	4.33	1074.47	5.30
C11	190	5.75	800	4.10	870.95	8.69
C12	210	6.80	820	4.22	1121.82	9.82
C13	240	7.50	1450	4.40	1431.21	11.40
C14	100	2.50	300	4.11	195.85	12.25
C15	335	11.00	1550	6.11	2948.08	17.10

4.3.1 Result of effect lateral reinforcement

The first group involved testing of four columns (C1,C2,C3 and C4) with different lateral reinforcement (ties) from the ends the column comparison with the reference column, these columns tested to the failure under axial loads.

4.3.1.1 Ultimate load and maximum lateral displacement

The outcomes exhibited that the obtained increase in lateral reinforcement caused an increase in ultimate load by 2.7%, 8.33% and 61.11%, for C2, C3 and C4 respectively compared to the un-strengthened column C1 as shown in Table 4.1. The variance in the ultimate load was due to the change in the lateral reinforcement up to 50% of the length of column. It can be observed that the increase in the lateral reinforcement caused a decrease in the lateral displacement at the same load level as shown in Fig. 4.3. Increasing the lateral reinforcement at the ends of columns caused also increase the max. lateral displacement by (20.8, 103.3 and 998)% for columns C2, C3 and C4 respectively compared to the column C1. Lateral reinforcement is effective at increasing of the ultimate strength and maximum lateral displacement of reinforced concrete columns because it confines the concrete and longitudinal reinforcement in the additional closer spacing of lateral reinforcement is known to increase the uniformity of lateral pressure.

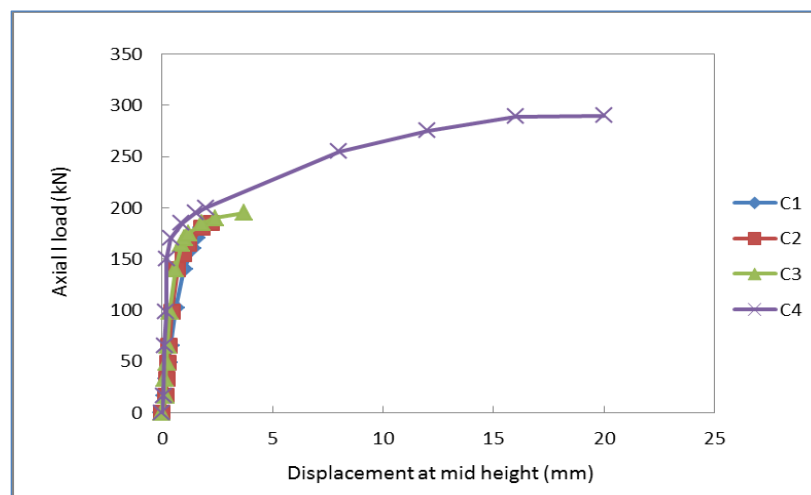


Fig. 4.3 Load-displacement curves.

4.3.1.2 Ultimate moment

The strengthening of columns by lateral reinforcement (ties) from ends of columns at different proportion from the length of column, caused an increase in the ultimate first moment by 24.2%, 120.2% and 1670.4% for columns C2, C3 and C4 respectively compared with the column C1. This occurred as a result of the increase in the applied load. The result shown in Table 4.1.

4.3.1.3 Ductility index

The use of the lateral reinforcement at different distances from the ends of the column has been shown to have significant effects on ductility. The ductility of confined concrete increase with an increase in ties reinforcement by 54.9%, 103.5% and 296% for columns C2, C3 and C4 respectively compared to the reference column C1 as shown in Table 4.1. The lateral reinforcement (ties) produced higher results in terms of ultimate load and maximum displacement than unstrengthened specimens. Therefore, the effect of ties confinement on the bearing capacities increased with an increase the amount of ties. Fig. 4.4 showed the effect of lateral reinforcement on ductility index.

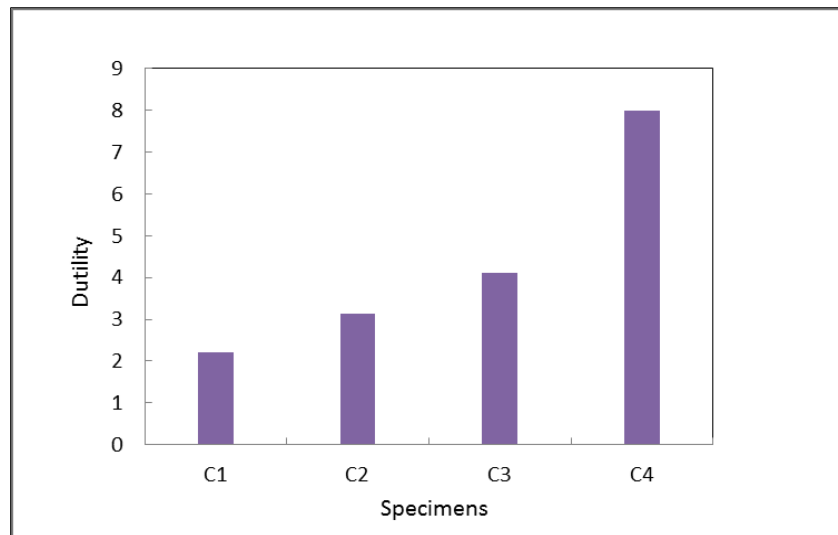


Fig. 4.4 Effect of lateral reinforcement on ductility index.

4.3.1.4 Energy absorption

The energy calculated from the area under the load-displacement curve. Fig. 4.5 shows the effect of ties on energy absorption. The energy in the first group caused an increase in the displacement by 44.5%, 192.9% and 935% for columns C2, C3 and C4 respectively compared to the column C1 as shown in Table 4.1. The results showed that the energy absorption capacities of RC columns with a high amount of ties were improved compared with this of an RC column with low amount of ties.

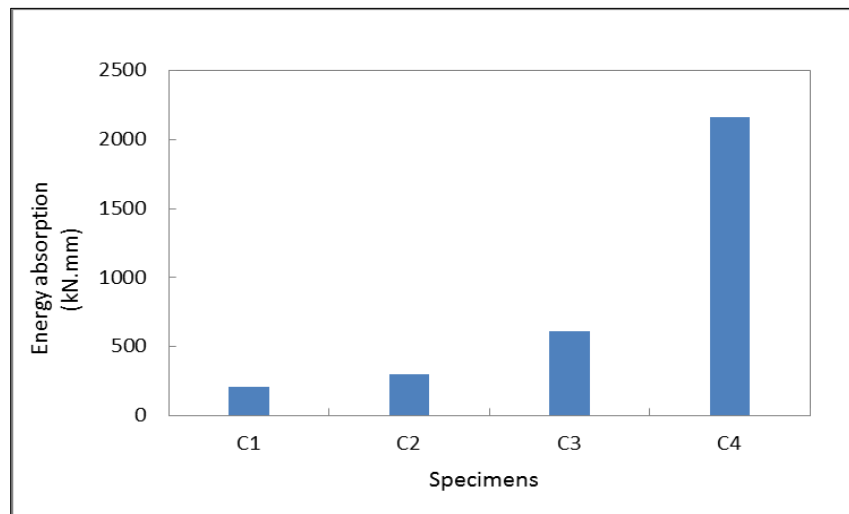


Fig. 4.5 Effect of lateral reinforcement on energy absorption.

4.3.1.5 Mode of failure

Fig. 4.6 and Table 4.1 display the failure modes and location of the maximum lateral displacement of the first group columns specimens. In general, two failure modes are observed for columns strengthened by lateral reinforcement in different distances from the length of column; crushed failure and local buckling. The columns C1 and C2 suddenly failed due to the concrete crushed (brittle failure) at the ends. The failure mode of columns C3 and C4 were local buckling but the failure happened at a different distances which were (340 mm and 590 mm) respectively from the top end of the column. So, the increase in the ratio

of lateral reinforcement caused an increase in the stiffness of the column, and it could longer resist the applied axial load



Fig. 4.6 Mode failure of first group.

4.3.2 Results of the effect of lateral reinforcement and CFRP sheet

This group deals with the effect of strengthening by lateral reinforcement (ties) at both ends of the column and strengthening by (CFRP) at opposite sides of the width of column together in different proportions to know their effect on the behavior of the column. These columns tested to the failure under axial loads.

4.3.2.1 Ultimate load and maximum displacement

The externally strengthened reinforced concrete columns with bonded CFRP sheets in second group generally showed a significant increase in ultimate loads.

The ultimate load for columns C5, C6 and C7 increased by 16.4%, 6.9% and 37.9% respectively compared with the column C4. Also, CFRP sheet and ties reduced the lateral displacement at the same load by (5, 15 and 35)%, respectively compared with the column C4 as shown in Table 4.1. Fig. 4.7 represented to the effect of strengthened by lateral reinforcement and CFRP sheet on lateral deflection at mid height of columns.

The variance in the ultimate load was happened due to the using of CFRP in different lengths to complement the existing strengthening by lateral reinforcement, in order to reach the total strengthening distance, which is equivalent to half the column length. When used CFRP sheet in column C5 at a distance of 360 mm from the end of ties gave a better result than column C6 when strengthened by CFRP at distance of 167 mm. When compared the column C7 (strengthened by CFRP at distance of 500 mm) with the column C4 (strengthened by ties at distance 500 mm), it is observed column C7 gave a good result than column C4 because, CFRP has excellent material characteristics like high strength to weight ratio.

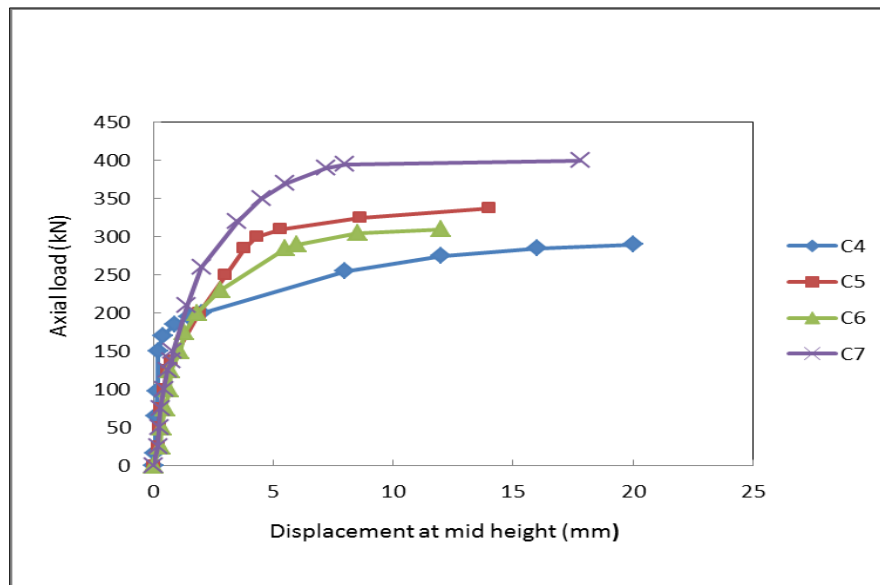


Fig. 4.7 Load-displacement curves for second group.

4.3.2.2 Ultimate moment

The strengthening columns by CFRP from the end of ties at different distances from the length of column, and which were 360 mm and 167 mm caused an decrease in the ultimate first moment in the columns C5 and C6 by 18.5% and 35.8% respectively due to reduction in maximum displacement from 20 mm to 14 mm and 12 mm in these columns compared with the column C4. While, the ultimate moment increased for the column C7 by 22.8% compared with the column C4 when the column strengthened only with CFRP at distance 500 mm from the ends of column. The results shows in Table 4.1.

4.4.2.3 Ductility

Table 4.1 shows the values of ductility index of column specimens of second group. The results calculate from Eq. 4.1. The effect of CFRP is shown in Fig. 4.8. It is observed that specimens strengthened by CFRP with distance 360 mm, 167 mm and 500 mm showed an increase in ductility index more than reference column C4 about (12.5, 10 and 25)% respectively.

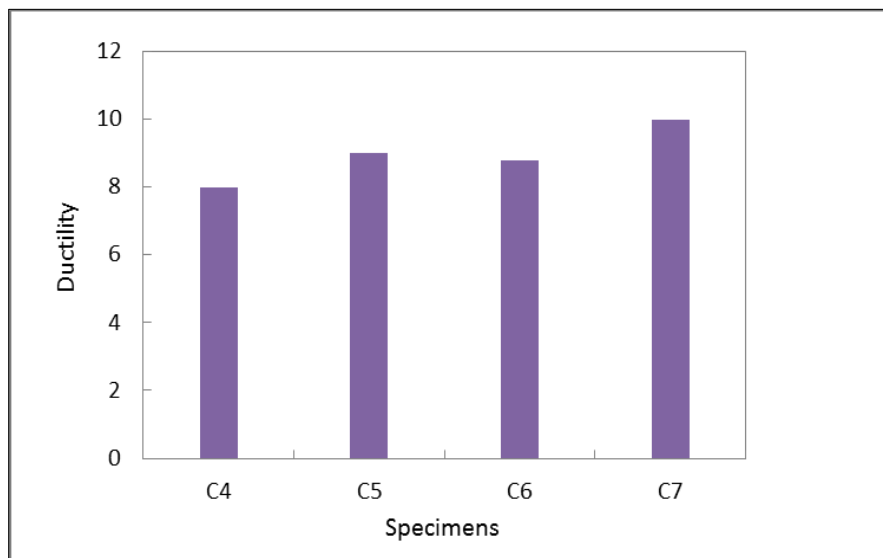


Fig. 4.8 Effect of strengthening on ductility index.

4.3.2.4 Energy absorption

In the specimens of group two improved the energy absorption by a range of (42.1 to 190.9)% with respect to the column C4. The enhanced in energy in the columns C5 and C6 due to using strengthened by CFRP sheet and ties reinforcement at a different distances. Fig. 4.9 showed the effect of using lateral reinforcement and CFRP sheet on energy absorption. The values of energy absorption are recorded in Table 4.1.

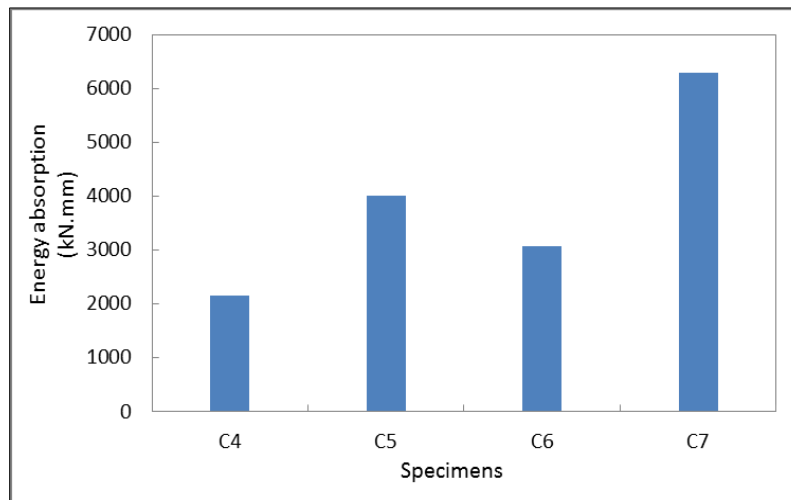


Fig. 4.9 Effect of strengthening on energy absorption.

4.4.2.5 Mode of failure

Fig. 4.10 shows columns before testing and Fig. 4.11 shows the representative failure modes in each column in group two observed from the tests. When the columns are exposed to loads, they start to buckle without obvious cracks in the areas of tension and compression of the column and then the column suddenly fails in the form of an explosion. The failure mode of column C4 is local buckling but the failure happened at 590 mm from the top end of the column. Using a CFPP sheet with a length of 360 mm from the end of ties change the mode failure from local buckling to buckling at mid-height (maximum point deflection) in column C5. The addition of CFRP increased the stiffness of the column, and it could longer resist the applied axial load. But, in column C6 the mode failure is

local buckling and occurring at a distance of 630 mm from the end of the CFRP sheet. And with the continuous increase in the applied load on the column C7 (strengthening with CFRP sheet up to 50%), the stresses transferred from the stronger region (CFRP) to the weaker region (at the ends of the CFRP material itself). This led to the increase in the curvature of the column in mid-point, and this was ultimately the reason for its failure.



Fig. 4.10 Columns before testing (second group).



Fig. 4.11 Failure mode of second group (after testing).



Fig. 4.11 Continuous.

4.3.3 Results of the effect of eccentricity ($e= 20, 40$) mm

This case included three specimens (C3, C8 and C9). This section deals with the effect of eccentricity of columns on the values of the ultimate load, maximum displacement, ultimate moment, ductility and energy absorption under two variable eccentricities 0, 20 mm (which equivalent $e/h= 25\%$), and 40 mm (which equivalent $e/h= 50\%$). The values of all other parameters were kept constants.

4.3.3.1 Ultimate load and maximum displacement

Eccentricity of load was one of the important factors on load carrying capacity of columns especially slender columns. The behavior affected by the eccentricity. It can be observed that increasing the eccentricity of the applied load caused an increasing in the lateral displacement at the same load level. Increasing of the eccentricity from 0 to 20 and to 40 mm caused an increasing in the lateral displacement by 110.5% and 215.8% respectively at a level of load equal to 160 kN (the minimum ultimate load in this group) as shown in Fig. 4.12. Two eccentricity values (20 mm and 40 mm) caused decreasing in the load carrying capacity of columns by (10.26 and 17.95)% for columns C8 and C9 respectively compared with the column C3 as shown in Table 4.1.

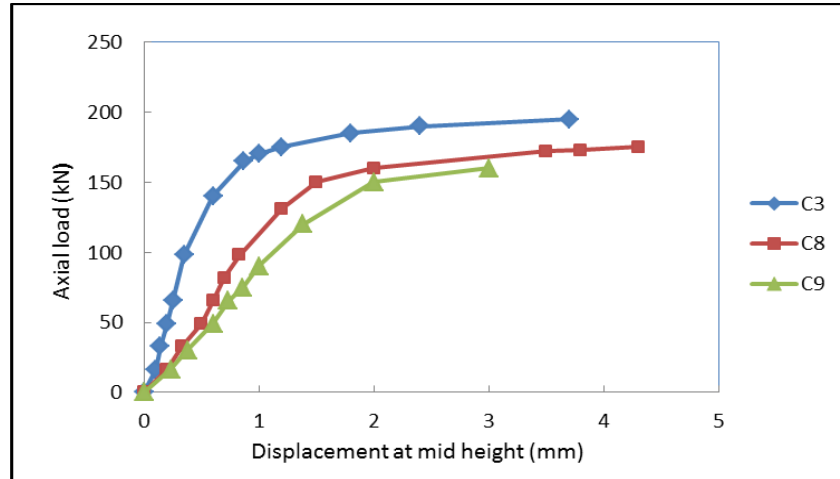


Fig. 4.12 Load-displacement curves for third group.

4.3.3.2 Ultimate moment

When the eccentric load on the column is further increased, it will tend to increase the applied moment. The moment increased by 487.66% and 853.56% in column C8 and C9 respectively compared with the column C3 as shown in Table 4.1 .

4.3.3.3 Ductility index

It can be noted from the results of this group increasing the eccentricity led to decrease in the ductility index by (24.33 and 39.17)% for columns C8 and C9 respectively compared with the column C3. Fig. 4.13 showed the effect of eccentricity on ductility. The result shows in Table 4.1.

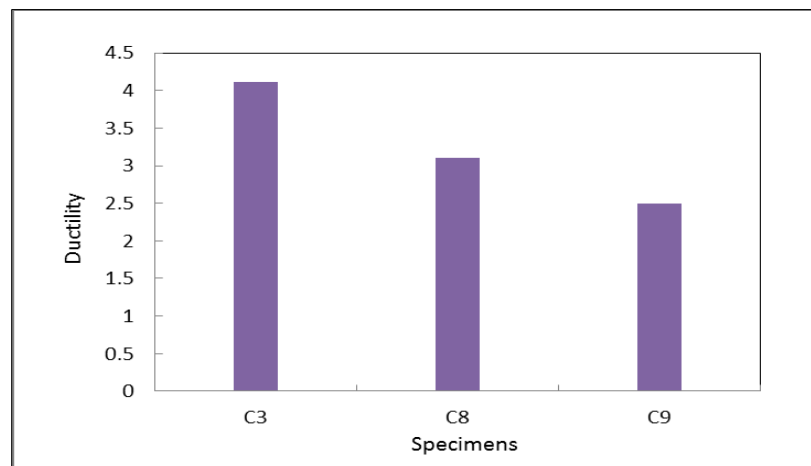


Fig. 4.13 Effect of eccentricity on ductility index.

4.3.3.4 Energy absorption

It can be concluded from Table 4.1 that the increase in eccentricity of applied load in columns C3, C8 and C9 resulted in a decrease in the energy absorption, increasing of the eccentricity from zero to 20 and 40 mm caused a decrease in energy by (4.58 and 47.63)% respectively as shown Fig, 4.14.

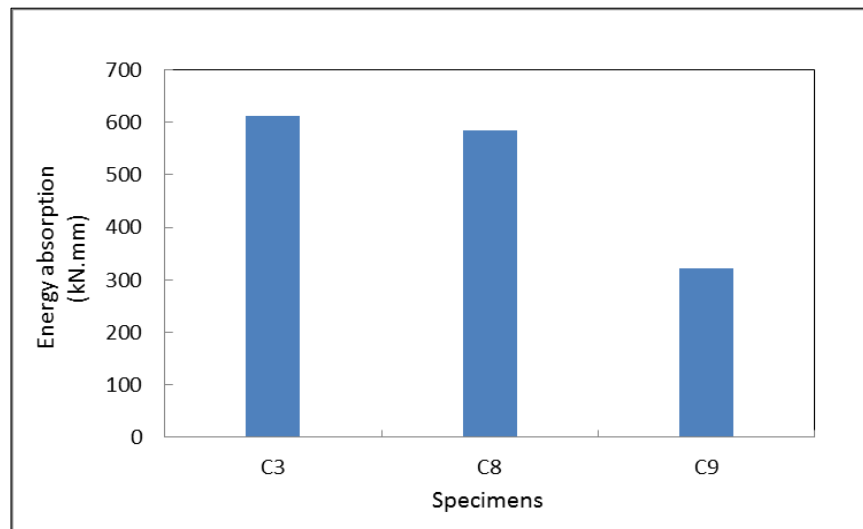


Fig. 4.14 Effect of eccentricity on energy absorption.

4.3.3.5 Mode of failure

Regarding to the failure mode of group three, Figs. 4.15 and 4.16 shows the representative failure mode of these columns during and after the testing. The failure types shed light on the different types of possible failures for these columns. when the load on the column is further increased it will tend to increase the moment capacity of the columns and they start to buckle slightly and then the column suddenly fails without warning. C8 failed due to local buckling at a distance of 500 mm from the top end of column, this failure occurred under lower eccentricity ratio (25%) and showed evidence of bar buckling without obvious cracks. In column C9, the mode failure was local buckling but at a distance of 340 mm under higher eccentricity ratio (50%).



Fig. 4.15 Mode failure of columns during the test for third group.



Fig. 4.16 Mode failure of columns after the test for third group.

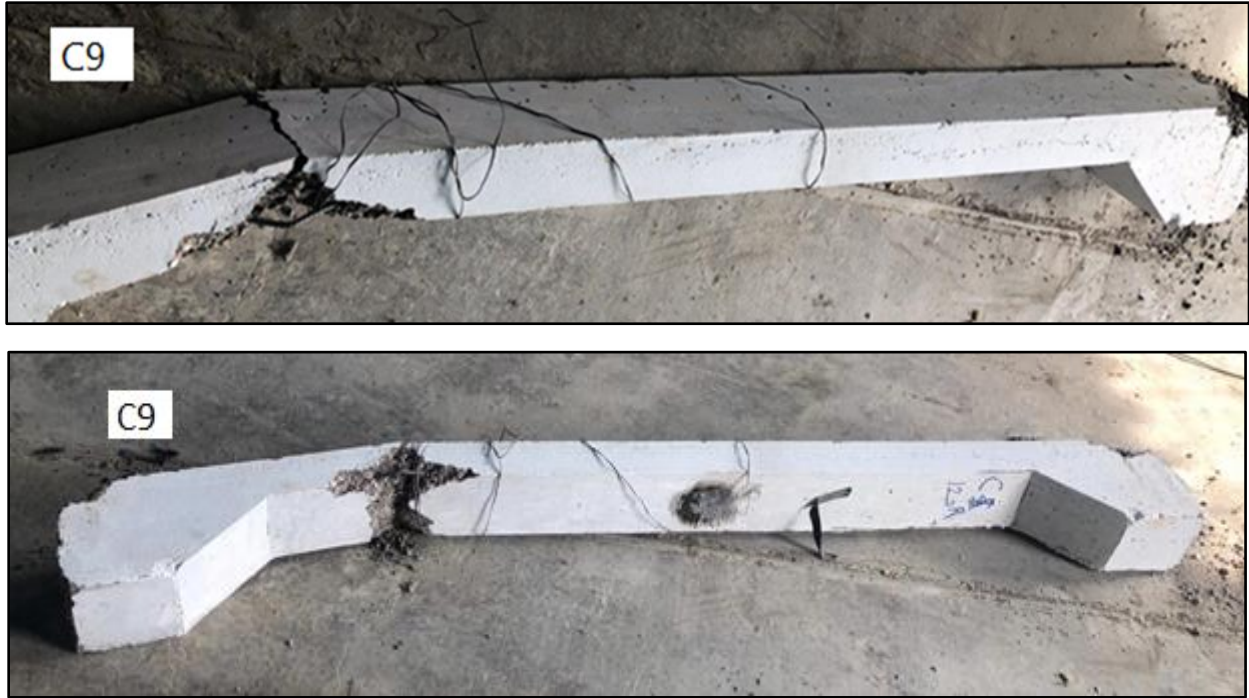


Fig. 4.16 Continue.

4.3.4 Result of effect of opening shape with eccentricity ($e= 20$ mm)

This group consists of two column specimens (C8 and C10) with the same eccentricity ($e= 20$ mm) and different opening shapes. The tested was carried out up to failure under eccentric loads.

4.3.4.1 Ultimate load and maximum displacement

The results proved that the columns with circular hole have a good performance compared to the columns have rectangular hole in terms of ultimate load. The increased in ultimate load and deflection were (14.29 and 51.16)% respectively in column (C10) compared with the column (C8). Fig. 4.17 represented the effect of opening shape under the same eccentricity ($e=20$ mm) on load-displacement curve. From the result above the increase in maximum lateral displacement and ultimate load in column C10 due to the use of a circular hole instead of a rectangular hole in column C8. This is due to the fact that the

distribution of the load was more uniform in the circular opening shape because there is no weak point at the corners as in the rectangular section.

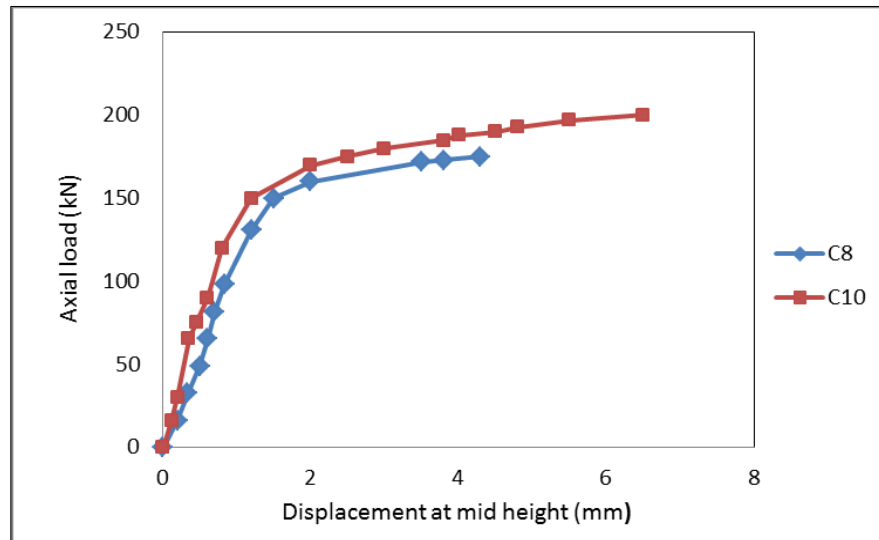


Fig. 4.17 Load-displacement curve for fourth group.

4.3.4.2 Ultimate moment

The moment also increased by 25% in column C10 compared with the column C8. The increase in ultimate load due to the fact that the distribution of the load was more uniform in the circular opening shape because there is no weak point at the corners as in the rectangular section.

4.3.4.3 Ductility index

Ductility index of column specimens C8 and C10 are shown in Table 4.1. Changing the opening shape of columns from rectangular to circular enhanced the performance of the column in terms of ductility as illustrated in Fig. 4.18. It is obvious from the results that the columns have the equivalent area, column with circular hollow C10 have ductility higher than column with rectangular opening by 39.23%.

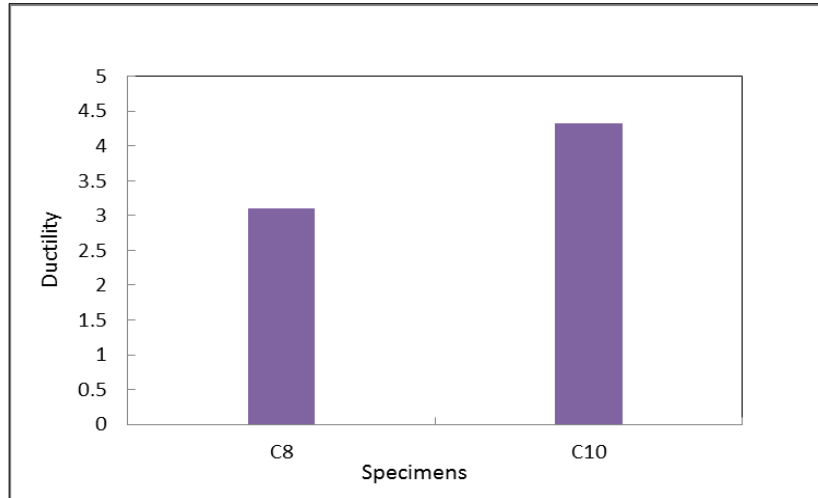


Fig. 4.18 Effect of shape opening on ductility index.

4.3.4.4 Energy absorption

Result of energy absorption of fourth group shown in Table 4.1. As shown in Fig.4.19 the column C10 with circular openings has energy absorption greater than C8 by 83.8%. From the result the increase in the index of ductility and energy absorption in column C10 due to the use of a circular hole instead of a rectangular hole in the column C8.

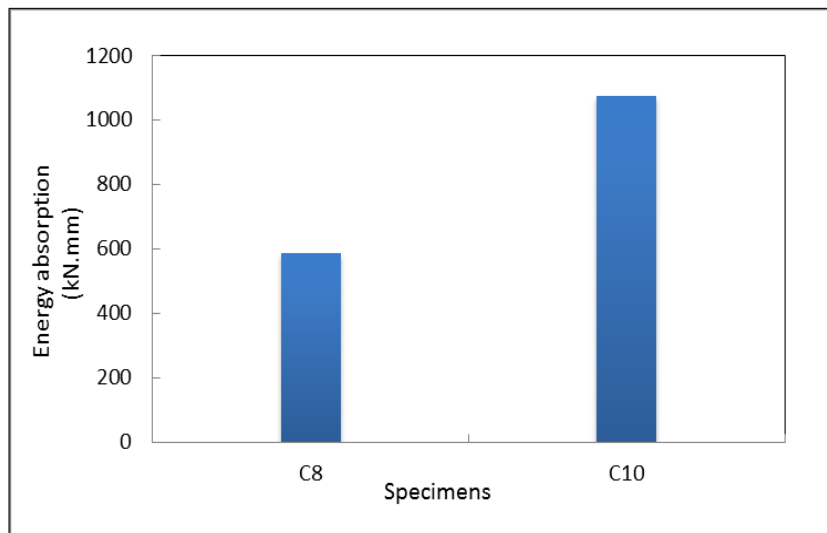


Fig. 4.19 Effect of shape opening on energy absorption.

4.3.4.5 Mode of failure

Regarding the failure mode of the fourth group, Fig. 4.20 show the representative failure mode of these columns. In general, when the columns are exposed to loads, they start to buckle slightly and then the column suddenly fails without warning. Column C8 failed due to local buckling at a distance of 500 mm from the top end of column this failure occurred under eccentric load ($e= 20$ mm) with rectangular opening shape without obvious cracks. When changing the opening type to circular opening and under eccentricity 20 mm, the column C10 failed due to buckling at distance 840 mm.



Fig. 4.20 Mode failure of fourth group.

4.3.5 Result of the effect of opening shape with eccentricity ($e= 40$ mm)

This group consists of two column specimens (C9 and C11) with the same eccentricity and different opening shapes. The tested was carried out up to failure under eccentric loads ($e= 40$ mm).

4.3.5.1 Ultimate load and maximum displacement

The shape opening under eccentric load ($e= 40$ mm) played a remarkable role in the ultimate load and maximum displacement. The ultimate load and max. displacement of column C11 increased by an average of 18.75% and 91.7% respectively compared with the column C9. It is clear that increase the ultimate load and maximum displacement of the hollow circular column exceeds that of hollow rectangular column for the same cross sectional area, possibly due to the distribution of the load being more regular in the columns having circular holes due to the absence of corners. The effect of eccentricity on displacement at mid height of columns shown in Fig. 4.21.

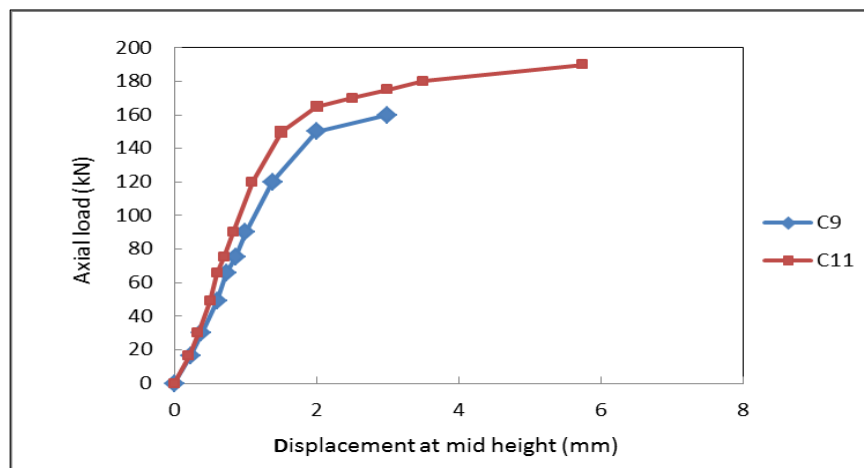


Fig. 4.21 Load-displacement curve for fifth group.

4.3.5.2 Ultimate moment

When the value of displacement increased from 3 to 5.75 mm under the same eccentricity and as result of the increase in the applied load in fifth group the

moment increased by 26.3% in column C11 compared with the column C9. The increase in ultimate load due to the fact that the distribution of the load was more uniform in the circular opening shape because there is no weak point at the corners as in the rectangular section.

4.3.5.3 Ductility index

The ductility index of column specimens (C9 and C11) is shown in Table 4.2. It is observed from Fig. 4.22 that C11 has ductility greater than C9 by 64% with circular openings.

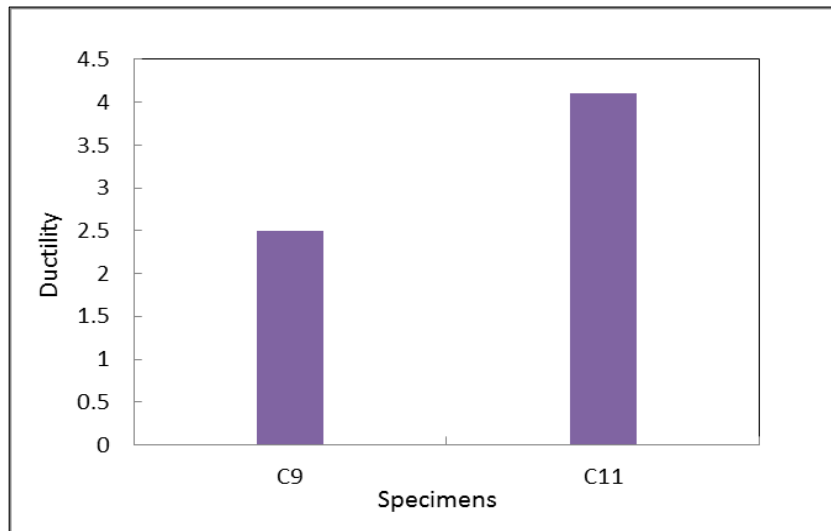


Fig. 4.22: Effect of shape opening on ductility index.

4.3.5.4 Energy absorption

Energy absorption is shown in Table 4.2. The column C11 with circular openings have an energy absorption of 171.5% greater than C9, as shown in Fig. 4.23. It is clear that the hollow circular column's increase in ductility and energy absorption exceeds that of the hollow rectangular column for the same cross-sectional area, possibly due to the more regular load distribution in the columns having a circular hole due to the absence of corner.

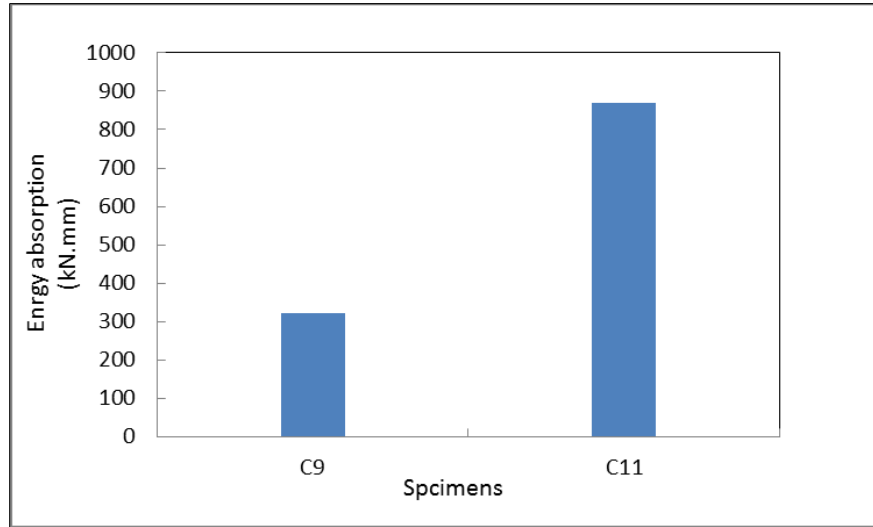


Fig. 4.23 Effect of shape opening on energy absorption.

4.3.5.5 Mode of failure

The failure modes and location of the maximum lateral displacement of the fifth column group specimens are shown in Table 4.1 and Fig. 4.24. The tested columns exhibited two different failure types: local buckling and buckling in mid-height. When the columns are exposed to loads, they start to buckle slightly and then the column suddenly fails without warning. The mode failure in column C9 was local buckling but at a distance of 340 mm with eccentricity equal to 40 mm and this failure was accompanied by buckling of longitudinal reinforcement. But, the mode failure in C11 was buckling at a distance of 800 mm with circular opening and under eccentricity 40 mm. In some cases it results from sudden fails and reinforcement yielding of the columns. All concrete removed from the failed columns was loose and able to be removed easily by hand.



Fig. 4.24 Mode failure for fifth group .



Fig. 4.24 Mode failure for fifth (after testing).

4.3.6 Result of the effect of eccentricity with CFRP sheet

This section considers to study the effect of eccentricity of columns strengthened columns (C7 and C12) with CFRP on ultimate load, ultimate moment, maximum lateral displacement, ductility and energy absorption.

4.3.6.1 Ultimate load and maximum displacement

The test results for two columns strengthened by CFRP at the same distance from the length of column under different eccentric load showed that the ultimate load and maximum lateral displacement decreased by (47.5 and 61.8)% respectively when the eccentricity increased from 0 to 40 mm in column C12 compared with the column C7 as shown in Fig. 4.25.

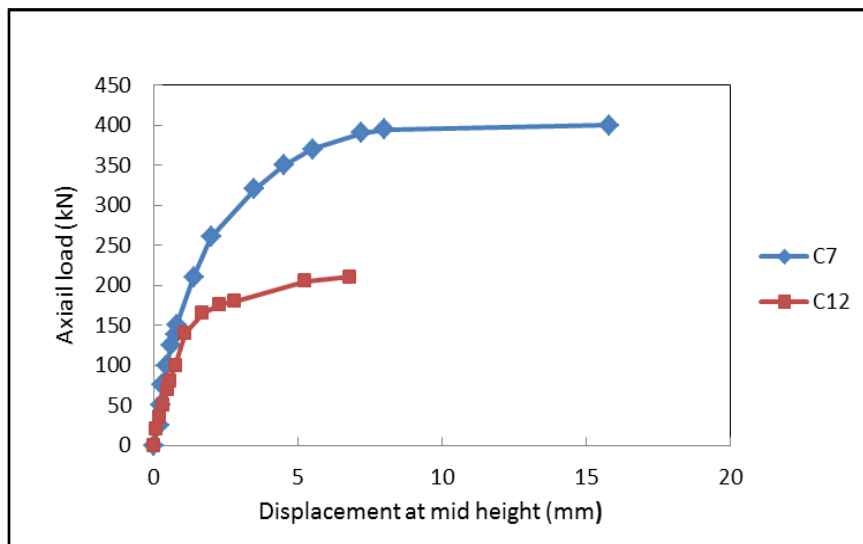


Fig. 4.25 Load-displacement curve for sixth group.

4.3.6.2 Ultimate moment

Increasing eccentric load from zero to 40 mm with strengthening by CFRP in the column C12 means that the moment is greater than in column C7 by 37.90% as shown in Table 4.1221`. The presence of eccentricity caused an increase in ultimate moment on the columns, causing buckling and early failure.

4.3.6.3 Ductility index

It can be noted from the results of Table 4.1 that the increase in eccentricity of the load resulted in a revised effect on the ductility. Increasing the eccentricity from 0 to 40 mm led to a reduction in the displacement ductility index, accompanied with a reduction in the load carrying capacity. The ductility in the column C12 decreasing by 57.8% compared with column C7. Fig. 4.26 shows the effect of using CFRP under eccentric loading on ductility.

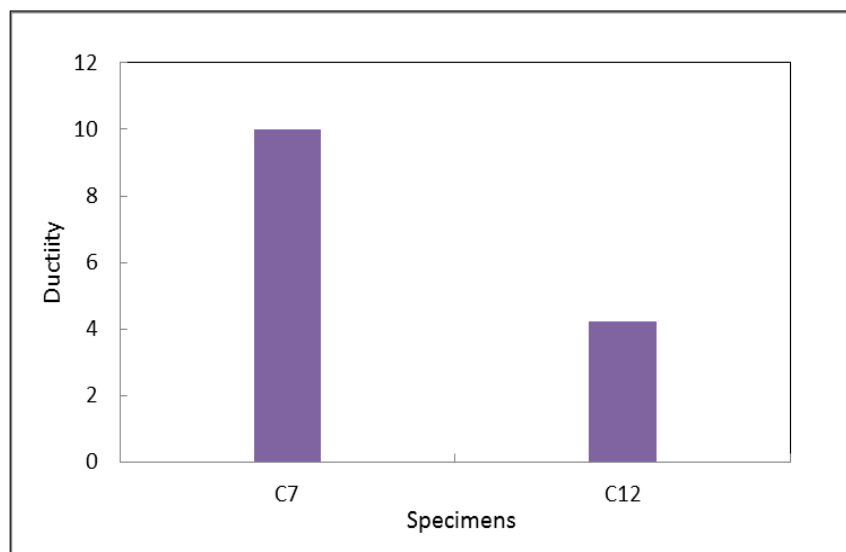


Fig. 4.26 Ductility index for sixth group.

4.3.6.4 Energy absorption

It can be concluded from Table 4.1 that the increase in eccentricity of the applied load resulted in decreased the energy absorption. Increasing the eccentricity from zero to 40 mm caused a reduction in energy by 82.2% in column C12 compared with the column C7. Fig. 4.27 show the effect of using CFRP under eccentric loading on energy absorption.

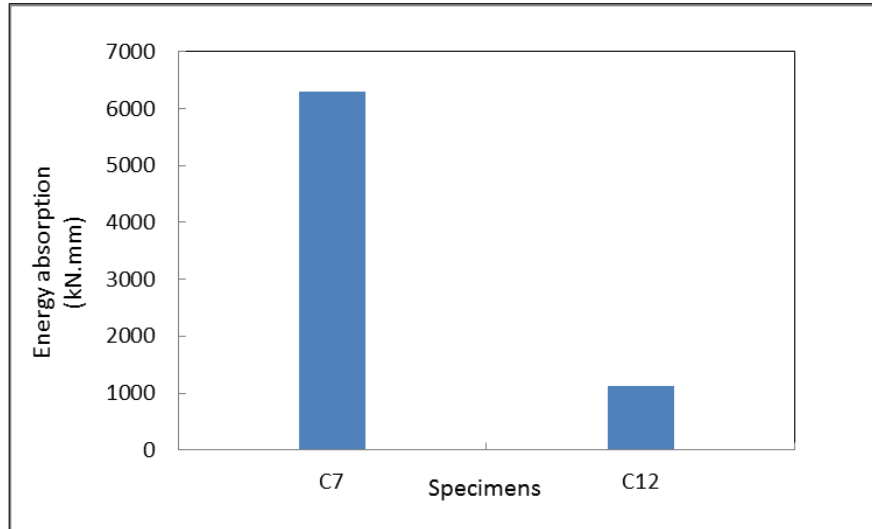


Fig. 4.27 Energy absorption for sixth group.

4.3.6.5 Mode of failure

Regarding the failure mode of sixth group, Figs.4.28 and 4.29 show the representative failure mode of columns (C7 and C12) during and after the test. In general, two failure modes are observed for columns strengthened by CFRP at the same length under different eccentricity; buckling at mid-height and bar buckling. The failure in column C7 was buckling at mid-height because used CFRP sheet at a distance of 500 mm from both ends of column under concentric load, The pressures have therefore been transferred from the stronger region (CFRP) to the weaker region (at the ends of the CFRP material itself). The mode failure in C12 (strengthening with CFRP at a distance of 200 mm) was buckling at the mid-height of the column under eccentric load ($e=40$ mm). This failure accompanied with buckling in longitudinal reinforcement. Strengthening of the half of the column length by CFRP caused an increase in resistance to buckling. In this group was no sign of rupture of the CFRP and in some cases it results from a sudden explosion fails and reinforcement yielding of the columns. All concrete removed from the failed columns was loose and able to be removed easily by hand.



Fig. 4.28 Mode failure of sixth group (during the test).

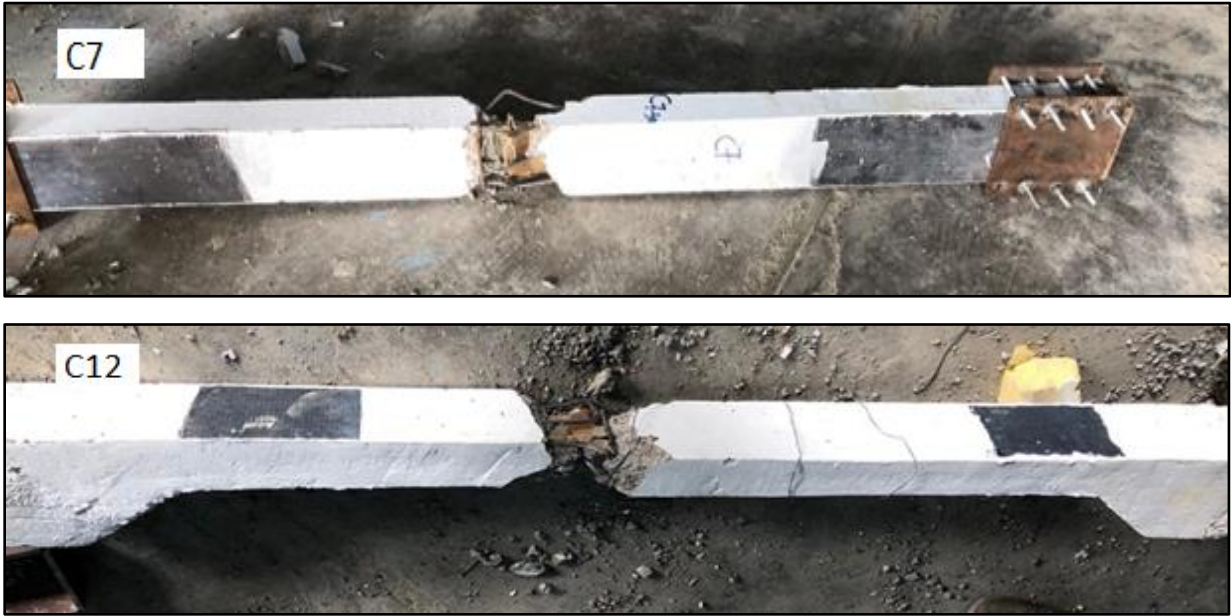


Fig. 4.29 Mode failure of sixth group (after the test).

4.3.7 Result of the effect of opening shape with CFRP sheet

This section considers to study the effect of external strengthening by CFRP with the same length 200 mm (from the end of corbel) under the same eccentricity ($e=40$ mm) and with different opening shape in columns (C12 and C13) on ultimate load, ultimate moment, maximum lateral displacement, ductility and energy absorption.

4.3.7.1 Ultimate load and maximum displacement

The hollow reinforced concrete column had circular hole C13 carry higher ultimate load and displacement, compared with column had rectangular hole C12. The increased in ultimate load and maximum displacement by (14.3 and 10.3)% respectively as shown in in Table 4.1. Load-displacement curve for seventh group shown in Fig. 4.30. The gain in strength and displacement for RC columns increases with the change the type of opening shape from rectangular hole to circular hole and the use of carbon fiber led to increased confinement in the columns and thus increased the strength in columns.

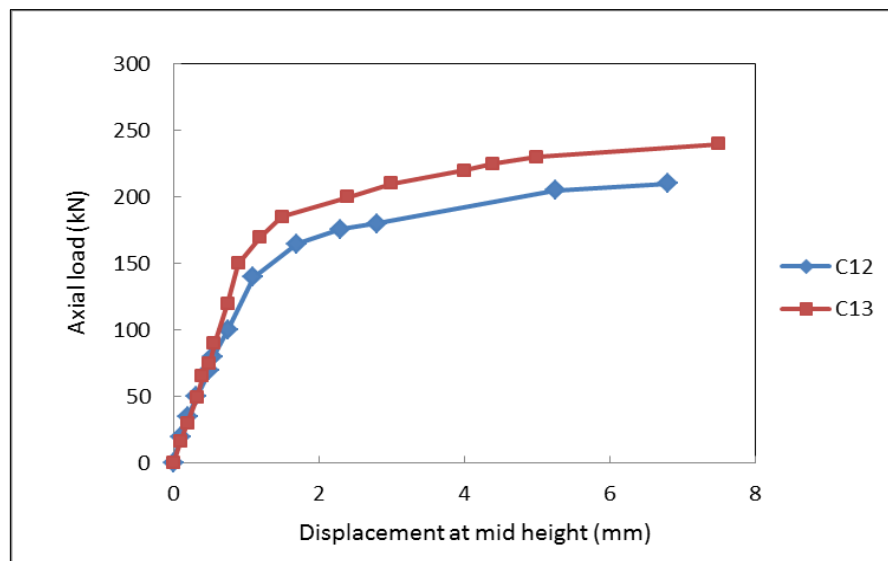


Fig. 4.30 Load-displacement curve for seventh group.

4.3.7.2 Ultimate moment

It can be concluded from Table 4.1 that strengthening the columns using CFRP at the same length with circular hole led to a higher ultimate moment than rectangular hole. It was found that the increasing in moment was 16.1% in column C13 compared with the column C12. From these results the increased in values of the column C13 due to the fact that the load distribution was more uniform in circular holes because they do not have any points of weakness and the strengthening by CFRP mainly improved the performance of the specimens under eccentric loading.

4.3.7.3 Ductility index

Changing the hollow of columns from rectangular to circular enhanced the performance of the column in terms of ductility as illustrated in Fig. 4.31. It is obvious from the test results that the column with circular hole have ductility higher then rectangular column by 4.27%. The result shows in Table 4.1.

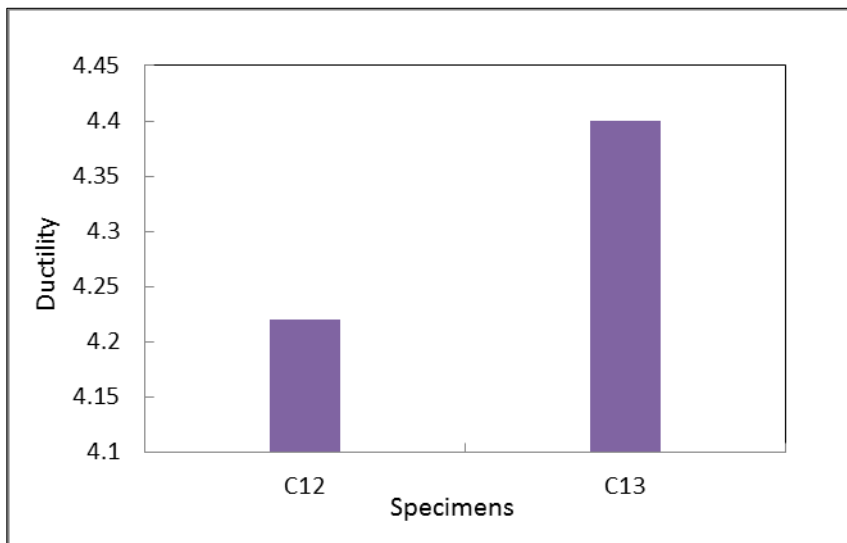


Fig. 4.31 Effect of CFRP with different opening on ductility.

4.3.7.4 Energy absorption

The energy absorption for columns C12 and C13 shows in Table 4.1. When changing the hole of specimens from rectangular C12 to circular C13 hole CFRP was more effective in enhancing the energy absorption. The increased in energy absorption in the column C13 was 27.5% compared with the column C12 as illustrated in Fig. 4.32.

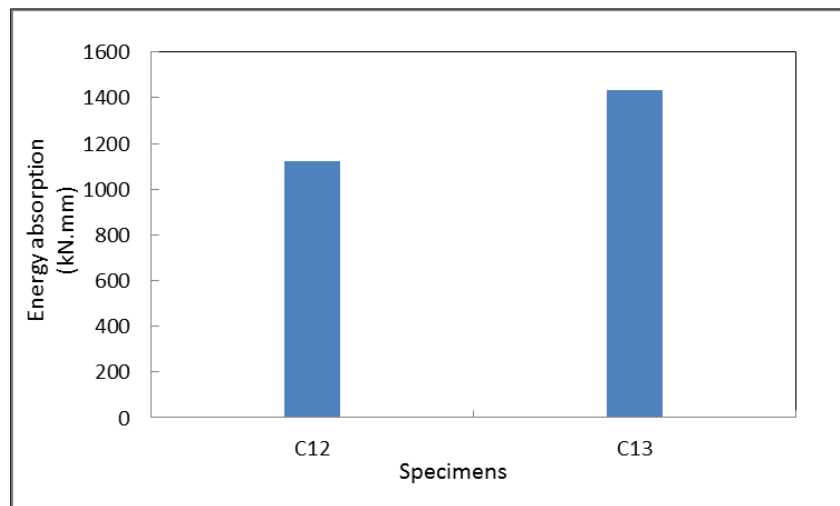


Fig. 4.32 Effect of CFRP with different opening on energy absorption.

4.3.7.5 Mode of failure

Regarding the failure mode of seventh group, Fig. 4.33 shows the representative failure mode of columns (C12 and C13). The mode failure in C12 (strengthening with CFRP at a distance of 200 mm) was buckling in the mid-height of the column and this failure accompanied with buckling in longitudinal reinforcement, meanwhile, C13 also strengthening in the same way as C12 with different opening shape (circular opening), the failure occurred suddenly in the last third of the length column at end of CFRP sheet and this failure did not accompanied with buckling in longitudinal reinforcement. Strengthening of the half

of the column length by CFRP (from internal corbel) caused an increase in resistance to buckling. In this group was no sign of rupture of the CFRP.



Fig. 4.33 Mode failure of sixth group.

4.3.8 Result of the effect of high eccentricity

As previously described in Chapter 3, this column was studied in a group alone. C14 column was strengthened at a distance of 1400 mm between both internal ends of the corbels. The ultimate load and max. lateral displacement record 100 kN and 2.5 mm, respectively. It was also noted that these values are few compared to the others column due to the presence of high eccentricity. The ultimate moment equal to 12.25 kN.m. The ductility and energy absorption were 4.1 and 195.85 respectively. Fig. 4.34 showed mensuration of load-displacement

relation result for C14 tested under high eccentricity ($e= 120$ mm). C14 column failed early and the failure occurred from the top at the end distance of the corbel because the stresses were concentrated in the upper third of the column under the corbel area due to the high eccentricity as shown in Fig. 4.35.

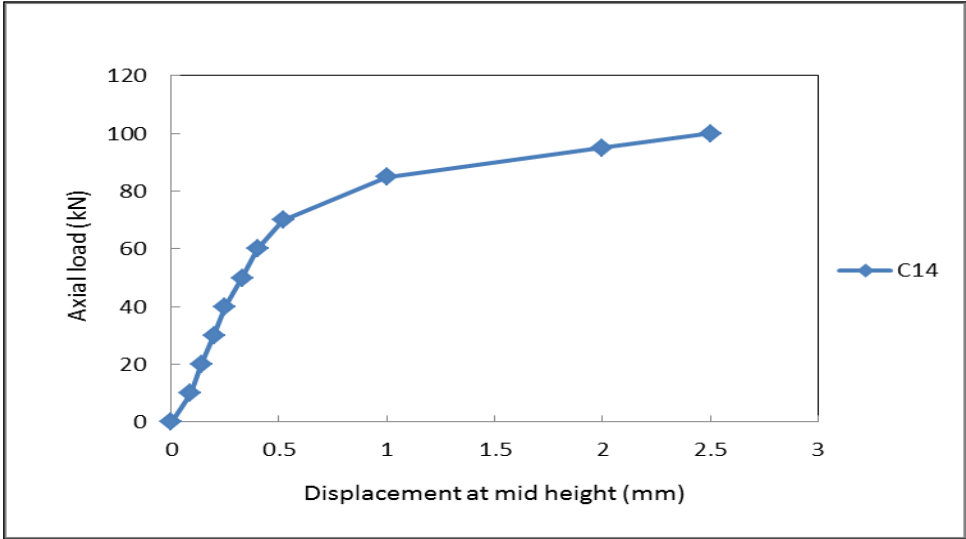


Fig. 4.34 Load-displacement curve for C14.



Fig. 4.35 Mode failure of column C14.

4.3.9 Result of the effect of CFRP sheet with same eccentricity

This case included three specimens (C11,C13 and C15) tested under the same eccentricity 40 mm and circular hollow with different CFRP sheet lengths.

4.3.9.1 Ultimate load and maximum displacement

The Fig. 4.36 and Table 4.1 presented result of load-displacement relation for ninth group tested hollow columns. The max. lateral displacement increased in C13 and C15 by (26.1 and 91.3)% respectively compared with column C11. When the CFRP sheet is fixed along the width of column, the ultimate load in the column C15 was increased by 76.3 %. Also column C13 gave a good result when fixed CFRP sheet on the quarter of length. Where the increase in C13 was 26.3% when compared to the non-strengthened column C11. The increase in ultimate load due to used CFRP in different lengths because the use of CFRP has properties such as: high strength to weight ratio; corrosion resistance; ease and speed of application; minimal change of cross-sections; possibility of installation without interruption of structure functions. For these reasons, CFRP has been widely used in the retrofitting and strengthening of reinforced concrete structures, especially in regions under high seismic risk (Lignola, 2006).

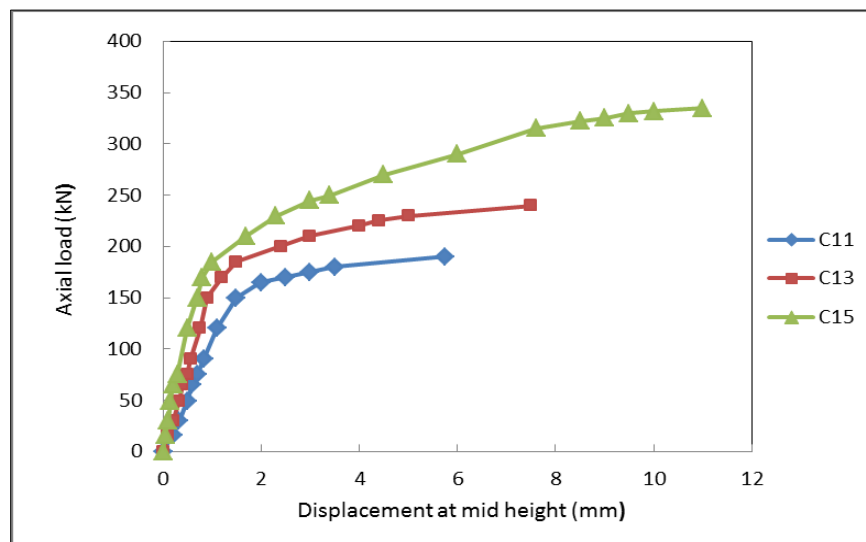


Fig. 4.36 Load-displacement curve for ninth group.

4.3.9.2 Ultimate moment

The moment increased by 31.2% and 96.8% for C13 and C15 respectively compared with the column C11 as shown in Table 4.1.

4.3.9.3 Ductility index

It can be noted from the results of this group the increasing in the length of CFRP from 200 mm (quarter of length) to 1400 mm (along the width of column) led to an increase in the ductility index by (7.32 and 49.02)% for columns C13 and C15 respectively compared with the column C11. Fig. 4.37 and Table 4.1 showed the effect of CFRP with circular hole on ductility.

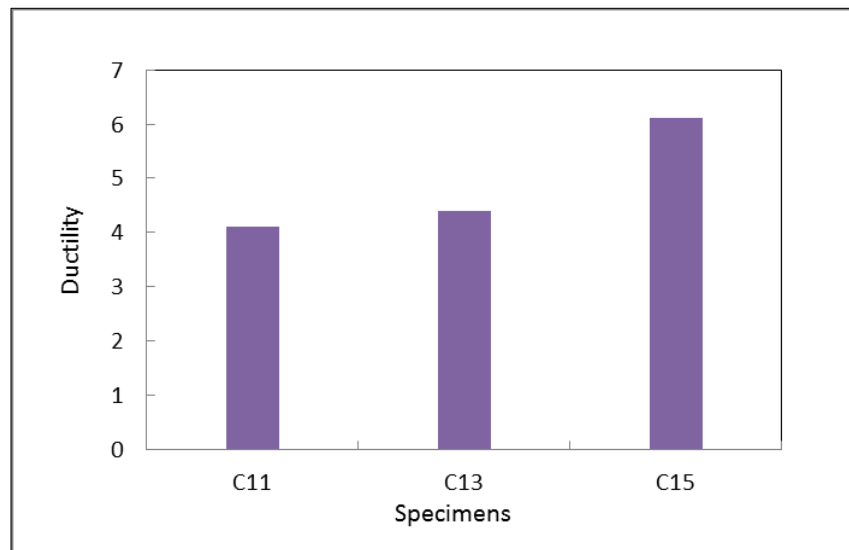


Fig. 4.37 Effect of CFRP with circular hole on ductility.

4.3.9.4 Energy absorption

In ninth group strengthening the columns by CFRP improved the performance of the column in terms of energy absorption as illustrated in Fig. 4.38. It is obvious from the results in Table 4.1 when the CFRP sheet is fixed along the width of column, the energy absorption in the column C15 was increased by 238.5% compared with un-strengthened column C11, and the column C13 gave a

good result when fixed CFRP sheet on the quarter of length. Where the increase in C13 was 64.3% when compared to the un-strengthened column C11.

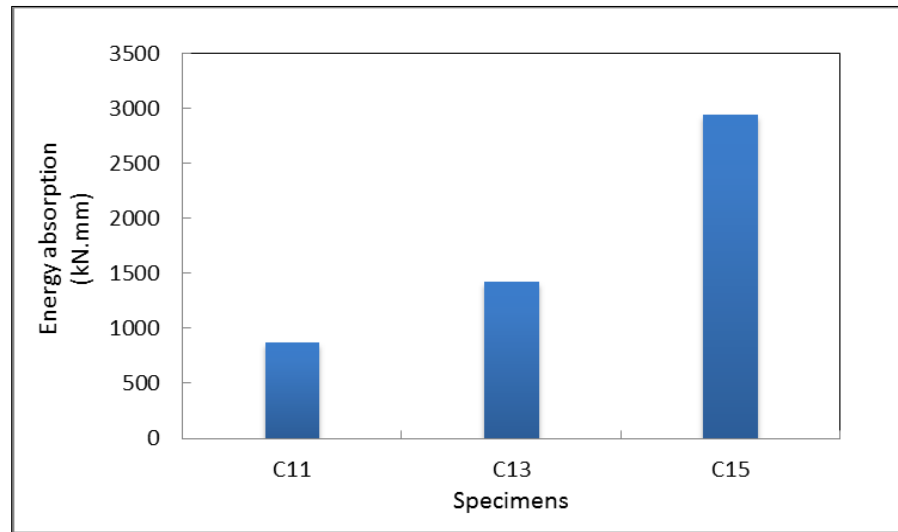


Fig. 4.38 Effect of CFRP with circular hole on energy absorption.

4.3.9.5 Mode of failure

Regarding the failure mode of ninth group, Fig. 4.39 shows the representative failure mode of columns C11, C13 and C15. The tested was carried out up to failure under eccentric loads ($e=40$ mm). The failure mode in column C11 was buckling at a distance of 800 mm with circular opening. meanwhile, the failure occurred suddenly in the last third of the length column, at a distance of 1450 mm from the top of the column without any rupture in CFRP sheet in the column C13. In column C15, the failure occurred in the last third of the length column, at a distance of 1550 mm from the top of the column accompanied by a rupture in CFRP sheet, a ripple in CFRP, buckling in longitudinal reinforcement and rupture in CFRP. Fig. 4.40 represented the failure mode of slender columns of column C15. The modes failure of columns are listed in Table 4.2.



Fig. 4.39 Mode failure of ninth group.

Table 4.2 Mode failure of columns.

Column ID	Failure mode
C1	crushed (brittle failure) at the ends
C2	crushed (brittle failure) at the ends
C3	Local buckling
C4	Local buckling
C5	Buckling
C6	Local buckling
C7	Buckling
C8	Local buckling
C9	Local buckling
C10	Buckling
C11	Buckling
C12	Buckling
C13	Failure at the last third of column
C14	Failure at the first third of column (at the end of corbel)
C15	Failure at the last third of column+ rupture in CFRP+ corrugating in CFRP.

CHAPTER FIVE

CONCLUSIONS AND RECOMMENDATIONS

5.1 Conclusion

Based on the investigated variables in this research, different conclusion points concerning the structure behavior of hollow concrete column specimens under axial loading and eccentric loading are drawn:

5.1.1 Behavior of columns under axial loading

1. For columns strengthened by ties $\emptyset 6@30$ mm for different distances at each ends of columns in addition to the original lateral reinforcement $\emptyset 6@30$ mm, and which were 140 mm, 333 mm and 500 mm, caused an increase in the ultimate load, ultimate moment, ductility and absorption energy. The percentage of the obtained ultimate load, ultimate moment, ductility and absorption energy results ranged between (2.7-61.11)%, (24.2-1670.4)%, (54.9-296)% and (44.5-935)% respectively compared to un-strengthened column.
2. For columns strengthened by lateral reinforcement (ties) and CFRP from the ends of ties at opposite sides of the width of column for lengths 360 mm, 167 mm and 500 mm caused an increase in the ultimate load, ductility and energy absorption by ranges of (16.4, 6.9 and 37.9)%, (12.5, 10 and 25)% and (42.7, 42.1 and 192.1)%, respectively compared with un-strengthened column.
3. The reinforced concrete columns strengthened with lateral reinforcement and CFRP sheet showed a lower deflection at corresponding loads from those of un-strengthened column.
4. The buckling occurred within the middle third of the column at maximum lateral displacement, when increased the lateral reinforcement (ties) in columns at both ends from 140 mm to 500 mm.

5. Strengthening of the half length of the column length by CFRP caused an increase in resistance to buckling.

5.2.2 Behavior of columns with eccentric loading

1. Effect of increasing the eccentricity values of reinforced concrete slender columns led to reduce ultimate load capacity by (10.26 and 17.95)% for ($e=20$ mm and $e=40$ mm) respectively. The ductility index decreased by (24.33 and 39.17)% when the value of (e) is increased from (0) to (20 mm and 40 mm) respectively. Also when the values of (e) increased from (0) to (20 mm and 40 mm), the energy absorption decreased by (4.58 and 47.63)% respectively.
2. For 20 mm load eccentricity, it was found that the column having circular opening shape caused an increase in the load capacity, ultimate moment, ductility and energy absorption than column having rectangular by (14.29, 24.7, 39.23 and 83.8)% respectively.
3. For (40 mm) eccentricity, it was found that the column having circular opening shape gave an increase in the load capacity, ultimate moment, ductility and energy absorption than column having rectangular by (18.75, 26.3, 64 and 171.5)% respectively.
6. For column strengthened by CFRP at distance of 200 mm from both internal corbels and having a rectangular opening shape under eccentricity of 40 mm led to decrease in the ultimate load, ductility and energy absorption by (47.5, 52.5 and 82.2)% respectively. But, the ultimate moment increased by 37.9%.
7. In columns strengthened by CFRP at distance of 200 mm from both internal corbels with different opening shape under eccentricity (40 mm), the result presented an increase in the ultimate load, ultimate moment, ductility and energy absorption in the column having circular opening by (14.3, 16.1, 4.27

and 27.5)% respectively compared to the column having rectangular opening and strengthened by CFRP in the same way.

8. For column with eccentricity 120 mm and whole column was strengthened by CFRP, the ultimate load, ductility and energy absorption were 100 kN, 4.1, and 195.85 kN.mm respectively. And ultimate moment was 12.25 KN.m. It was noted that these values are few compared to the others columns with eccentricities (20 mm and 40 mm), therefore, it can be advise don't take a high eccentricity, and take a value of eccentricity with a distance equal to quarter or half of the column thickness, which were (20 mm and 40 mm) to avoid early failure.
9. For columns tested under the same eccentricity of 40 mm and circular hollow with different CFRP sheet lengths, it was found the column strengthened by CFRP sheet along the width of column from both internal corbels. The ultimate load, ultimate moment, ductility and energy absorption increased in this column (76.3, 96.8, 49.02 and 238.5)% respectively compared with un-strengthened column. Also when fixed CFRP sheet on the quarter of length from both internal corbels column gave a better performance in terms of ultimate load, ultimate moment, maximum lateral displacement, ductility and energy absorption compared with un-strengthened column.

5.2 Recommendation for future works

1. Experimental and analysis investigations are required to predict the behavior of hollow slender reinforced concrete columns with variable slenderness ratios more and less than 80.5 under axial load and eccentric load.

2. Research into irregular reinforced concrete slender column with and without openings such as circular shape, T-shape, L- shape, I-shape, due to architectural works.
3. Studying the effects of dynamic loads on hollow slender reinforced concrete columns.
4. Study the behavior hollow slender reinforced concrete columns under bi-axial eccentric loaded.

REFERENCES

- ACI (2014). Building Code Requirements for Structural Concrete (ACI 318-19). American Concrete Institute.
- ACI Committee 211.1-91. Standard Practice for Selecting Proportions for Normal Heavyweight, and Mass Concrete (ACI 211.1- 91).
- Aleksandar K. (1997). Preliminary Design of Slender Reinforced Concrete Highway.
- ASTM (C496/C496M-2004). Standard Test Method for Splitting Tensile Strength of Cylindrical Concrete Specimens. 4.2, 1-5.
- ASTM C78 (1992). Standard Test Method for Flexural Strength of Concrete, American Society for Testing and Materials, (2002), (42) Env206, Concrete-part 1, Specification, performance, production and conformity, European Standard.
- Azizinamini, A., Darwin, D., Eligehausen, R., Pavel, R., & Ghosh, S. K. (1999). Proposed modifications to ACI 318-95 tension development and lap splice for high-strength concrete. *Structural Journal*, 96(6), 922-926.
- Bakhteri, J., and Iskandar, S. A. (2005). Experimental study of reinforced concrete columns concealing rain water pipe. *Jurnal Teknologi*, 43, 13-26.
- Bijan D., Lohrasb.F, Amin.A and Manouchehr.S. (2018). Investigating allowable distance between powerhouse and transformer caverns to prevent buckling phenomenon using numerical and analytical methods (case study: Bakhtiary dam and HPP. *Journal of Geophysics and Engineering*. 1984.
- Bill M., John B., and Ray H. (2007). Reinforced concrete design: to Eurocode 2 (7th ed). Palgrave Macmillan International Higher Education, New York.
- B.S. British Standard (Part 116: 1983). Methods for Determination of Compressive Strength of Concrete Cubes. 1-8.
- Campione, G., Colajanni, P., La Mendola, L., & Spinella, N. (2007). Ductility of reinforced concrete members externally wrapped with fiber-reinforced polymer sheets. *Journal of Composites for Construction*, 11(3), 279-290.

- Chanakya A. (2009). Design of structural elements: concrete, steelwork, masonry and timber designs to British standards and Eurocodes (3rd ed). 26.
- Cem Y. and Osman K. (2004). An Experimental Study on the Behavior of Reinforced Concrete Columns using FRP Material. Conference on Earthquake Engineering Vancouver, B.C., Canada, paper (No. 919).
- David D., Charles W. and Arthur H. (1997). Design of concrete structures. (5th ed), McGraw-Hill, New York.
- Elmihilmy, M. T. (2003). Experimental Investigation of Reinforced Concrete Slender Columns Under Axial Load and Flexure. JOURNAL OF ENGINEERING AND APPLIED SCIENCE-CAIRO, 50(3), 467-482.
- Falah A. J. (2015). Flexural Strengthening of RPC Beams with External CFRP (Doctoral dissertation, University of Baghdad). 67.
- Ferguson, P.M., Breen, J.E. and Jirsa, J.O., (1981). Reinforced concrete fundamentals (4th ed). John Wiley and Sons, New York, 694.
- Fiona C. (2004). Structural Engineer's Pocket Book (3rd ed). London, England, 239.
- Games D. and Musa H. (2016). Failure modes of RC columns under loading. International Journal of Scientific and Engineering Research, 7 (12), 1293.
- Hadi, M. N., Goaziz, H. A., and Yu, T. (2018). Experimental investigation of CFRP confined hollow core reactive powder concrete columns. Construction and Building Materials, 174, 343-355.
- Hamdy M. A., and El-Tony M. E. (2016). Simplified design procedure for reinforced concrete columns based on equivalent column concept. International Journal of Concrete Structures and Materials, 10(3), 393-406.
- Ihsan A. S., Mohammed J. H. and Emad A. A. (2018). Effect of Hollowing Ratio on the Behavior of Hollow Self-Compacting Reinforced Concrete Slender Column Under Eccentric Loading. 390-394.
- Iraqi Standard No. 5 for the aggregation of natural resources, 1984.

- Iraqi Standard No. (45) for the aggregation of natural resources, 1984. coarse aggregate.
- IQS 2091/1999. Carbon steel bars for the reinforcement of concrete. 1-11.
- Jabor, A. J. (2013). Behavior of Reinforced Concrete Hollow Circular Columns With Steel Fiber Inclusion Under Cyclic Bending. *Journal of University of Babylon*, 21(4),1138-1152.
- Katarina G. and Juraj B. (2013). Full-scale testing of CFRP-strengthened slender reinforced concrete columns. *Journal of composites for construction*, 17(2), 239-248.
- Lignola, G. P. (2006). RC hollow members confined with FRP: Experimental behavior and numerical modeling (Doctoral dissertation, Ph. D. Thesis, University of Naples, Italy). 29.
- Lignola, G. P., Prota, A., Manfredi, G., and Cosenza, E. (2007). Deformability of reinforced concrete hollow columns confined with CFRP. *ACI Structural Journal*, 104(5), 629-637.
- Lignola, G. P., Prota, A., Manfredi, G., and Cosenza, E. (2007). Experimental performance of RC hollow columns confined with CFRP. *Journal of Composites for Construction*, 11(1), 42-49.
- Mander, J. B., Priestley, M. J. N., and Park, R. (1988). Observed stress-strain behavior of confined concrete. *Journal of structural engineering*, 114(8), 1827-1849.
- Mohammed A.H and Ali A.L. Acceptance for published, (2019). Experimental Work to Study the Strengthening Effect of SFR and CFRP on a Part or Whole of the Length of Slender RC columns. *Civil and Environmental Engineering Journal*
- Mohammed H. H. (2020). Behavior of Hollow Core Reinforced Columns with Steel Tubes Using Self Compacted Nano Concrete. ph.D thesis, University of Baghdad.

- Mohammed, D. H. (2007). Behavior of Reinforced Concrete Beams Strengthened by CFRP in Flexure (Doctoral dissertation, Ph. D. Thesis, University of Technology, Iraq).2.
- Mustafa K. and Abd alridah S. (2018). Utilizing of Carbon Fiber Reinforced Polymer Sheets for Strengthening of Fire Exposed Reinforced Concrete Columns. International Journal of Civil Engineering and Technology (IJCIET),9 (10) ,3.
- Mrema, G. C., Gumbe, L. O., Chepete, H. J., and Agullo, J. O. (2011). Rural structures in the tropics: design and development. FAO. Rome, Italy, 127.
- Module 10 Compression Members (2017). Short Compression Members under Axial Load with Uniaxial Bending. Lesson 23, Version 2 CE IIT, Kharagpur.
- Mousavian, S. H. (2010). Experimental study of reinforced concrete columns with embedded pipe (Doctoral dissertation, M. Sc. Thesis, Universiti Teknologi Malaysia).
- Nadeem A., Yousef A., Rizwan A. and Husain A. (2014). Experimental investigation of slender circular RC columns strengthened with FRP composites. Construction and Building Materials, 69, 323-334.
- Nadim H. and Akthem A. (1976). Structural Concrete Theory and Design (4th ed). Wily and Sons, New Jersy, 395-396.
- Park, H., and Paulay, T. (1975). Reinforced concrete structures. New York, NY: Wiley.
- Pessiki, S., and Pieroni, A. (1997). Axial Load Behavior of Large Scale Spirally Reinforced High Strength Concrete Columns. Structural Journal, 94(3), 304-314.
- Richart, F. E., Draffin, J. O., & Olson, T. A. (1948). Effect of eccentric loading, protective shells, slenderness ratios, and other variables in reinforced concrete columns. University of Illinois at Urbana Champaign, College of Engineering. Engineering Experiment Station.

- Salonga, J. A. Innovative Systems for Arch Bridges using Ultra High-Performance Fibre-Reinforced Concrete. University of Toronto (Canada). 43-44.
- Standard, B. (1985). Structural use of concrete-Part 1 & 2 . BS8110.
- Sumajouw, D. M. J., Hardjito, D., Wallah, S. E., and Rangan, B. V. (2007). Fly ash-based geopolymer concrete: study of slender reinforced columns. *Journal of materials science*, 42(9), 3124-3130.
- Thomas, R. C., and Cooper, T. R. (1995). Displacement ductility capacity of reinforced concrete columns. *Concrete International*, 17(11), 61-65.
- Wang, C., Salmon, C.G., and Pincheira, J. A. (2007). *Reinforced Concrete Design* (7th ed). John Wiley & Sons, Inc., 948.
- Webber, A., Orr, J. J., Shepherd, P., and Crothers, K. (2015). The effective length of columns in multi-storey frames. *Engineering Structures*, 102, 132-143
- Yazici, V., and Hadi, M. N. (2009). Axial load-bending moment diagrams of carbon FRP wrapped hollow core reinforced concrete columns. *Journal of Composites for Construction*, 13(4), 262-268.
- Youcef S., Sofiane A. and Mohamed C. (2013). Effectiveness of strengthening by CFRP on behavior of reinforced concrete columns with respect to the buckling instability. *Materials and Structures*, 48(1-2), 35-51.
- Yousif, M. Z. (2012). RC Beams Strengthening by Carbon Fiber Reinforced Polymer Against Two Points Load Divergence. *Journal of Engineering and Sustainable Development*, 16 (2).
- Yuliartri, K. and Hadi, M.N.S. (2010). Comparative behaviour of hollow columns confined with FRP composites. *Composite Structures*, 93(1), 198-205.
- Zahn, F. A.; Park, R. and Priestly, M. J. N. (1990). Flexural strength and ductility of circular hollow reinforced concrete columns without confinement on inside face. *Structural Journal*, 87(2), 156-166.

الملخص

غالبًا ما يتم توفير الفتحات المستعرضة والثقوب الطولية في أعمدة خرسانية مسلحة للسماح بالوصول للخدمات مثل أنابيب السباكة والأسلاك الكهربائية، عندما تكون تكلفة الخرسانة مرتفعة نسبيًا، أو في الحالات التي يجب فيها الحفاظ على وزن الأعضاء الخرسانية عند الحد الأدنى. هدفت هذه الدراسة إلى إجراء تجريبي لسلوك الأعمدة الخرسانية المسلحة النحيفة المجوفة تحت الاحمال المركزية والاحمال اللامركزية. تضمن الجزء التجريبي من البحث اختبار خمسة عشر عموداً مجوفاً نحيفاً من الأعمدة RC بأبعاد (140×80×2000) مم وبنسبة نحافة (80.54). تم تقسيم الخمسة عشر عمود إلى تسع مجموعات لدراسة المتغيرات المهمة. كانت هذه المتغيرات تقوية عن طريق التسليح العرضي، والتقوية بواسطة ألياف الكربون البوليمرية، و اللامركزية و شكل التجويف. يتم عرض الملاحظات العامة المتعلقة بالحمل النهائي، الإزاحة الجانبية، العزم الأقصى، الليونة، امتصاص الطاقة و انماط الفشل في عينات العمود.

إن تقوية الأعمدة الخرسانية المسلحة من نهايات الأعمدة بواسطة التسليح العرضي و ألياف الكربون البوليمرية تجعل العمود يتصرف بكامل طاقته ويحدث الالتواء في الثلث الوسطي من العمود بدلاً من الفشل المبكر عند الحواف. أيضاً عند المقارنة أعطت التقوية بواسطة ألياف الكربون البوليمرية فقط او مع وجود التسليح العرضي أداءً أفضل من حيث الحمل النهائي، عزم الانحناء النهائي، الإزاحة الجانبية القصوى، الليونة و امتصاص الطاقة من التقوية بواسطة التسليح العرضي على نفس مسافة التقوية.

أشارت النتائج التجريبية إلى أن استخدام التقوية بواسطة التسليح العرضي بأطوال مختلفة عند طرفي الأعمدة أدى إلى زيادة الحمل النهائي بنسبة (2.7، 8.3، 61.1) عند تغيير مسافة التقوية بالتسليح العرضي من (140، 333) ملم إلى (500) ملم، على التوالي. أدى التقوية بواسطة لوح ألياف الكربون البوليمرية من نهاية التسليح العرضي حتى 50% عند طرفي العمود الذي له نفس شكل التجويف إلى زيادة في الحمل النهائي بحوالي (16.4-37.9)%.

إن اللامركزية أحد العوامل المهمة لمعرفة قدرة تحمل الأعمدة وخاصة الأعمدة النحيفة. زيادة الانحراف يعني أن عزم الانحناء يزداد. تسببت قيمتا اللامركزية (e = 20 mm) (e = 40 mm) في انخفاض الحمل النهائي للأعمدة النحيفة المجوفة. بالنسبة للامركزية 20 مم و 40 مم، وجد أن الأعمدة ذات التجويف المستطيل تؤدي إلى انخفاض في قدرة تحمل العمود بحوالي (2.8) و (11.11) مقارنة بالأعمدة النحيفة المعرضة للحمل المحوري.

تتمتع الأعمدة الخرسانية المسلحة ذات الفتحات الدائرية، سواء مع أو بدون ألياف الكربون البوليمرية، بأداء أفضل من حيث الحمل النهائي، عزم الانحناء النهائي، الإزاحة الجانبية القصوى، الليونة، و امتصاص الطاقة مقارنة بالأعمدة ذو الفتحات مستطيلة. أثبتت نتائج الاختبار أن الأعمدة ذات الفتحة الدائرية تتمتع بأداء جيد مقارنة بالأعمدة ذات الفتحة المستطيلة (مساحة الفتحة الدائرية

تعاذل مساحة الفتحة المستطيلة) ، تحت نفس الحمل واللامركزية تساوي 20 مم. كانت الزيادة في الحمل النهائي 14.29% في عمود ذو فتحة دائرية مقارنة بعمود ذو فتحة مستطيلة.

أيضًا ، تم فحص عمود تحت اللامركزية 120 مم ($e / h = 150\%$) وتم تقوية العمود بالكامل بواسطة ألياف الكربون البوليمرية. وجد أن الحمل النهائي قد انخفض مقارنة بالأعمدة الأخرى وسجل فشلًا مبكرًا.



جمهورية العراق
وزارة التعليم العالي والبحث العلمي
كلية الهندسة / جامعة ميسان
قسم الهندسة المدنية



دراسة عملية للاعمدة الخرسانية النخيفة المجوفة

أطروحة

مقدمة الى كلية الهندسة جامعة ميسان كجزء من متطلبات الحصول على درجة الماجستير في
علوم الهندسة المدنية / الانشاءات

من قبل

آلاء محمد ساهي

بكالوريوس هندسة مدنية 2017

بإشراف

اد.د محمد صالح عبد علي

رجب 1442

يناير 2021